12-2005

A Numerical Study of Curved Labyrinth Seals for Steam Turbines

Sricharan Kishore Ayyalasomayajula
University of Tennessee - Knoxville

To the Graduate Council:

I am submitting herewith a thesis written by Sricharan Kishore Ayyalasomayajula entitled "A Numerical Study of Curved Labyrinth Seals for Steam Turbines." I have examined the final electronic copy of this thesis for form and content and recommend that it be accepted in partial fulfillment of the requirements for the degree of Master of Science, with a major in Mechanical Engineering.

Ahmed D. Vakili, Major Professor

We have read this thesis and recommend its acceptance:

Basil Antar, Louis Deken

Accepted for the Council:
Carolyn R. Hodges

Vice Provost and Dean of the Graduate School

(Original signatures are on file with official student records.)

To the Graduate Council:

I am submitting herewith a thesis written by Sricharan Kishore Ayyalasomayajula entitled "A Numerical Study of Curved Labyrinth Seals for Steam Turbines." I have examined the final electronic copy of this thesis for form and content and recommend that it be accepted in partial fulfillment of the requirements for the degree of Master of Science, with a major in Mechanical Engineering.

Ahmad D. Vakili

Major Professor

We have read this thesis
and recommend its acceptance:

Basil Antar

Louis Deken

Accepted for the Council:

Anne Mayhew

Vice Chancellor and
Dean of the Graduate School

(Original signatures are on file with official student records.)

A NUMERICAL STUDY OF CURVED LABYRINTH SEALS FOR STEAM TURBINES

A Thesis
Presented for the
Master of Science
Degree
The University of Tennessee, Knoxville

Sricharan Kishore Ayyalasomayajula

December 2005

Acknowledgements

I sincerely thank the help and efforts of everyone that has directly or indirectly helped me complete this research work. My advisor and professor, Dr. Ahmad Vakili, has been the most influential personality during the entire period of my Master's study and the current project. It has been a wonderful experience working with him. His tutelage has taught me more than just the required academic coursework. His technical acuity, work culture and advice are best enjoyed first-hand than when heard from others. I am in debt to my co-advisor on this project, Dr. Louis Deken, who was always willing to help me and whose company has taught me the practical aspects of dealing with engineering problems which has markedly improved the quality of my work. My colleague and friend, Dr. Abraham Meganathan, has been an indispensable part of the many brainstorming sessions during my project. His keen perception of problems has more than once helped me understand some of the most critical elements of my work.

Though I have stayed away from my family and friends in India, it is only through their continuous support and encouragement did I accomplish task. I am grateful to them forever. A special mention has to be made about my cousin Srikanth Mudigonda, who is presently a Ph.D. student at the University of Missouri, St. Louis, Missouri. I appreciate his constant support and efforts at making me overcome the absence of my family.

I thank Dr. Basil Antar for consenting to be a member on my thesis examination committee. Last, but not the least, is the support of all my friends and colleagues at UTSI. But for them I would not have been able to overcome the absence of my family and complete my Master's study.

Abstract

A numerical experiment has been conducted to study and evaluate the structural behavior of newly designed labyrinth seals. Structural analysis was performed to understand, evaluate and compare new seals with a baseline straight seal that is typical of commonly used seals in steam turbines. New configurations of labyrinth seal knives were developed for use in steam turbines [17]. The main objective of this study is to develop a better understanding of selected various labyrinth seals that may be configured to minimize the steam leakage and reduce seal interactions with the shaft. Computational fluid dynamic modeling of the various configurations, from a related study, and preliminary structural analysis led new designs to incorporate curvature into knife geometries including a sharp flat free-edge. Two-dimensional linear elastic static structural analysis was performed on a baseline straight labyrinth seal knife and seven different new configurations incorporating flexible geometries like curved seals, using finite element analysis software ANSYS®. Structural behavior of all new seals was evaluated in comparison with the results obtained for the baseline straight seal knife. Results show that the new geometries are more flexible than the straight seal knife, within the elastic limit of the same material. Of the seven geometries of new curved knives, two (C4 and C5) had higher load bearing capacity than all the others and one of them exceeded the load bearing capacity of the straight knife. The two high performing configurations, CS1 and CS2, have very thin knives compared to the other configurations. These two were found to be the most flexible among all the seven new configurations, considered. The maximum deformation and load bearing capacity of all the seven knives were correlated against a single non-dimensional geometrical parameter that appears to govern such variations and, therefore, define the improved designs.

Table of Contents

List of Tables

List of Figures

Nomenclature

a	knife thickness at fixed ends (in.) (Figure 15 and 16)
A	cross-sectional area of the knife in a radial plane from the shaft axis (in.^{2})
Area	area of the knife (in.^{2}) (Figure 15 and 16)
b	knife thickness at mid-length section (in.)
c	knife thickness at free ends (in.)
c_e	distance of the extreme fiber from the neutral fiber for a beam (in.)
d	distance of representative curve from the right-most edge of fixed end (in.)
E	Young's modulus of material of knife
F	force applied on the free end of knife; force applied on a beam (lb.)
F_r	ratio of force capacity of curved knife to that of straight knife
h_k, L	knife length geometry in a radial direction from the shaft axis (in.) (Figure 15 and 16)
I, $I(x)$	area moment of inertia of cross-section of a beam (in.^{4})
l_o	offset distance between free and fixed ends parallel to the fixed end (in.) (Figure 43 and 44)
l_s	shoulder length or equivalent length (in.) (geometry specific) (Figure 43)
M	moment on a beam (lb-in.)
$r1$	radius of the inner curve of a curved knife (in.)
$r2$	radius of the outer curve of a curved knife (in.)
r	radius of representative curve of a curved knife (in.)
$xpos$	distance of the section first reaching elastic limit along length of knife from its fixed end (in.)
Δx	deformation of knife along x-axis (in.)
Δx_r	ratio of Δx of a curved knife to that of a straight knife
$ypos$	distance of the section first reaching elastic limit perpendicular to length of knife from its fixed end (in.)
Δy	deformation of knife along y-axis (in.)

α	knife taper angle at free end (geometry specific) (Figure 43)
β	knife shoulder taper angle (geometry specific) (Figure 43)
σ_b, σb	bending stress in a knife (psi)
σ_{ij}	stress along the direction j and acting on a plane perpendicular to i (psi)
σ_n, σn	normal tensile or compressive stress in a knife (psi)
σ_{tot}	total stress in a knife (psi)
σ_y, σy	yield strength of material of knife (psi)
θ	angle of contact in the transverse view for two surfaces in contact or intersection (Figure 12)
v_n	normal tensile or compressive strain in a knife
v_b	bending strain in a knife

1. Introduction

Steam and gas turbines are one of the primary means of producing electricity and power in the present day. But the energy efficiency of these turbines can be said to be an almost anti-thesis to the success with which they have been adopted to run the motor of the modern world. From day one of their inception for the production of electricity on a commercial basis, turbines have been posing an as yet unconquered challenge of achieving high efficiency. It has long been known that there exists a constant loss of working fluid from turbo-machinery. Stocker [1] estimated that every 1% decrease in leakage flow through a high-pressure turbine seal would result in a 0.4% decrease in the specific fuel consumption. Based on Stocker's methodology and the jet fuel consumption figures in the US for 1998, a fuel savings of approximately 16 million barrels a year of jet fuel alone can be achieved. And with the ever increasing demand for fossil fuels, these figures would translate into much higher values in the present day scenario.

In the present thesis only steam turbines have been considered. So the mention of turbines, hereafter, refers only to steam turbines. A score of factors comprising the design constraints and the inherent science involved in their working can be blamed for the low efficiency rates of steam turbines. Albeit, one parameter has been identified as a prospective start point to improve the efficiency – the leakage of steam before it has performed useful work in the turbine.

A number of solutions have been sought for and adopted to overcome the loss of steam, with turbine seals leading the effort. The whole range of seals employed to date can be classified broadly into two categories – contact and non-contact types. Labyrinth seals form the class of non-contact type seals. These have been well documented as being used in steam and gas turbines and other turbo-machinery applications where a robust yet relatively simple seal is required between two differentially separated pressure zones [1-5].

The labyrinth type seals boast of specific advantages like

- low maintenance
- simplicity of design
- negligible running torque
- lower wear of the shaft

One of the most important advantage of labyrinth seals is their long operational life. This is due to their non-contacting nature of operation. The labyrinth seals function by creating resistance in the flow of steam passing through the seal. This results in dissipation of the kinetic energy of steam in the form of turbulent vortices in the cavities of the turbine sections.

There are variations in the operation of the labyrinth seals by virtue of their geometry and construction. Based on the arrangement of the teeth they can be classified as teeth-on-rotor and teeth-on-stator type seals. There have also been models tested with teeth on both the rotor and the stator and have been termed as seals with interlocking teeth [6].

Based on the geometry of the steam flow passage, the seals can be convergent, divergent or straight-through labyrinth seals. Due to the possibility of variable cross-section for the flow passage, the teeth alignment can be either parallel to the rotor axis or straight-through or, can be stepped following the convergent or divergent nature of the flow.

There have also been models constructed with honeycomb stators and the teeth on the rotor [7].

Though there are various configurations of the labyrinth seal, both in industrial application and in the development, these seals suffer from relatively high steam losses compared to the contact-type seals. This can be attributed to the lack of a “mechanical seal” between the two pressure zones. Hence, any and all effort to enhance the performance of the labyrinth seal would have to be either on developing a new configuration or improving the existing designs. In either case the aim of the efforts would be to develop a seal that

- has good dynamic sealing properties,
- has higher compliance with the shaft,
- is simple in geometry for ease of manufacture and maintenance, and
- very long life cycle comparable to the existing seals.

2. Review of Literature

The successful use of labyrinth seals in commercial steam turbines dates back to the starting years of the twentieth century, accompanied by a score of problems encountered with their operation and performance. Hence, a significant amount of research has been performed on developing theories to predict the leakage characteristics and performance of various seals including labyrinth seals. A study of the existing literature on the labyrinth seal revealed the strides taken towards understanding the leakage mechanisms and also a number of other questions like how to increase the dynamic sealing of the seal and so on, that have yet to be answered.

The first significant analytical effort on the problem of labyrinth seal can be attributed to Adolf Egli [2] of the Westinghouse Electric Co. Egli made an attempt at formulating the problem by assuming the flow of steam through a labyrinth seal analogous to an orifice flow. He discussed the flow of steam through the labyrinth seal as the adiabatic expansion of steam through a series of throttlings.

The work of Bilgen and Akgungor [8] tried to enhance the existing theories on the leakage and frictional characteristics of the seal by experimental verification. But the theory proposed made the assumption that the flow of steam can be approximated to Poiseuille flow due to the low clearance to diameter ratio. This resulted in large differences between the results obtained from the theory and the experiments.

A significant amount of research effort has been dedicated to model and theorize the flow through the seal but Wright [9] has attempted at collecting the much needed data to understand the forces acting on the seal elements. Many parameters affecting the forces have been accounted for paving the way for developing theories to understand the forces acting on the seal. Subsequent research in this direction was done by Leong and Brown [10]. They documented the lateral forces acting on the seal elements and

attempted to develop a mathematical model describing the influence of the different aspects of the flow like the eccentricity in the rotation of the shaft, seal size and rotor speed on the total lateral forces.

A comprehensive effort to catalog the rotordynamic coefficients of forces on the seal has been made by Childs and Scharrer [11, 12]. Though this is predominantly an experimental effort, it gave important insights into the flow patterns within the seal cavities influenced by such factors like pressure gradients, rotor speed and seal clearance.

The existent literature may broadly be classified into one half dedicated to minimizing the leakage flow in current designs of the seal and, the second half trying to improve the baseline seal configuration and alignment inside the turbines. While a lot of effort has been devoted to the first half, the second category, nevertheless, had some very promising prospects.

In the study undertaken by Michaud *et al* and Vakili *et al* [13-16] new configurations for teeth-on-stator type seals have been evaluated. A study of the flow characteristics suggested improvements in the seal performance and as such new configurations have been studied.

The work of Michaud *et al* and Vakili *et al* has been based on the idea that the leakage of steam through the seal can be minimized by understanding the interaction of its flow path with seal elements. The agreement between experimental data and computational results supported this idea. The analysis of the performance of the new configurations has been mainly dedicated to the flow of steam by means of computational fluid dynamics software. But to conduct a thorough evaluation of the performance of the new configurations, in addition to the fluid dynamic analysis a structural analysis of the configurations had to be undertaken. This forms the main body of the present work, and any mention of a labyrinth seal, henceforth, refers to a teeth-on-stator type of labyrinth seal.

3. Need for New Labyrinth Seals

The application of labyrinth seals in the industry has a long track record owing to the various advantages of these seals over the continuously popular brush and other types of seals. The contact type sealing properties of the other seals is the main contributing factor for their popularity over the labyrinth seals. Due to a mechanical contact between the seal elements and the shaft, the leakage of steam can almost completely be eliminated. But the contact type seals have their set of disadvantages like:

- due to the constant rubbing between the seal elements and the shaft, the wear on both is higher,

- the higher wear results in shorter operating life of the seal elements and hence, their frequent replacement and the associated costs and,

- the most important disadvantage being the wear of the turbine shaft which is most undesirable for the operation of a turbine.

Labyrinth seals, on the contrary, mitigate or totally overcome these disadvantages due to the absence of contact or rub between the seal elements and the turbine components. As a result, from this perspective, they are superior to the contact type seals. But as has already been stated, the labyrinth seals are not as effective in their sealing properties as the contact type seals.

Sealing mechanism in a labyrinth seal:

The labyrinth seals operate by making use of the flow characteristics of the steam through the seal cavities. Flow visualization study and measurements in a baseline labyrinth seal indicated the following as the major mechanisms for energy loss [13]:

- viscous dissipation losses in the turbulent jet during throttling between the seal elements and the shaft

- viscous losses in the form of turbulent vortices in the cavity chambers

- viscous losses at flow stagnation areas and,

- losses incurred due to the sharp changes in the direction of flow around the edges of the steps on the shaft and the edges of the seal elements.

Loss mechanisms in a labyrinth seal are depicted in Figure 1.

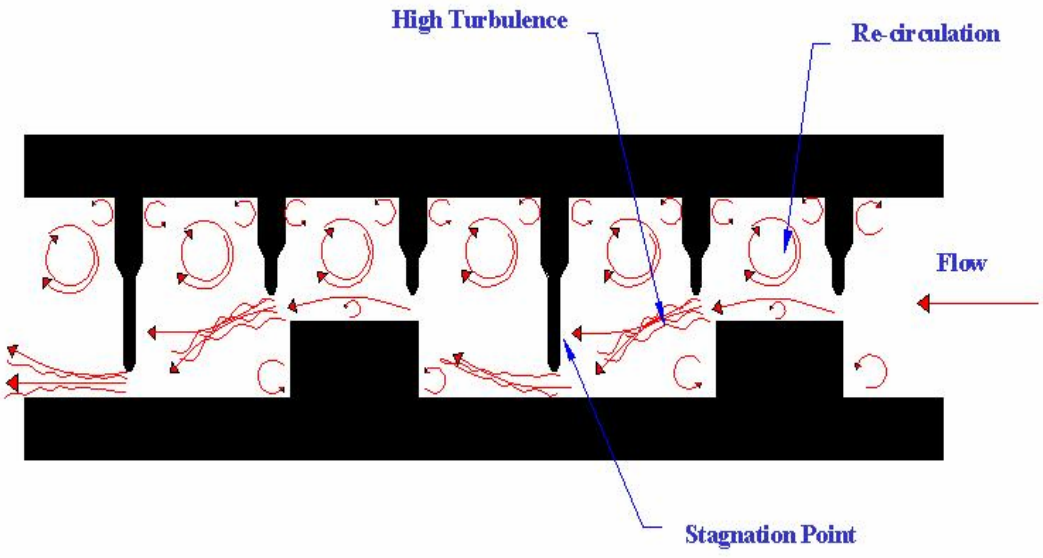

Figure 1. Schematic of flow in a labyrinth seal [13]

The leakage of steam can be reduced by increasing the amount of energy lost through the various mechanisms of energy dissipation in the seal cavities – turbulence, circulation, flow-stagnation etc. The investigations of Michaud [13, 14] and Vakili *et al* [15] led to the development of new configurations for the labyrinth seal. These new configurations were studied for their flow characteristics [15 – 17], and the results suggest that for improved sealing characteristics a good configuration for the seal should be able to dissipate the kinetic energy of the steam flow in the seal to the maximum by using many or all of the mechanisms cited above.

The shaft of a turbine is known to exhibit vibrations about its axis. As a result, there are documented instances of the impingement of the shaft on the labyrinth seal elements, thus permanently deforming them. The seal elements are designed to perform for maximum efficiency in their non-deformed condition. Hence, in addition to the lack of a mechanical sealing, the labyrinth seals also have to overcome the problem of lower performance due to permanent deformation upon impingement with the shaft. Thus, the main challenges associated with designing a labyrinth seal are:

- improving the sealing characteristics even though there is no mechanical seal

- designing the seal elements to exhibit high efficiency even in the case of large or permanent deformation upon impingement with the turbine shaft

- designing the seal elements such that they have high structural flexibility resulting in no or very small permanent deformation upon impingement with the turbine shaft at the same time not compromising the sealing efficiency at any instance of operation of the turbine.

An ideal geometry of the seal element would not only cause the dissipation of the steam energy, thereby decreasing the leakage, but also perform at close-to-maximum design efficiency with or without deformation. Efforts have been made to achieve such a

seal configuration. The practical difficulties in conceiving such a seal-geometry translated the efforts into striking a balance between the performance on the flow-containment front and mechanical strength front, consequently imposing a practical limit on the maximum efficiency possible to date.

4. New Configurations of Labyrinth Seal

As discussed in the previous chapter, improved sealing characteristics may be achieved by creating as many sources of energy losses as possible in the flow of steam though the labyrinth seal. The leakage of steam through the seal has been found to be influenced by the following mechanisms [16]:

- Stagnation of the flow on the knives and other solid boundaries.

- Generation and sustenance of highly turbulent vortices and other non-isentropic energy conversion processes.

- Curvature of the path taken by the leakage flow.

A study of the flow characteristics of steam through the vertical seal against the other configurations as discussed by Michaud [13] produced the following as the strategies to improve the seal design:

- The leakage jet was found to be extending from one orifice of the seal assembly to the next orifice with minimal loss in its kinetic energy. To improve the sealing efficiency, the design should be able to direct the velocity vectors into either the rotor or the walls of the knives or the casing where flow stagnation would be facilitated.

- The kinetic energy of the steam can also be attenuated by the creation of highly turbulent vortices in the cavity between adjacent knives of the seal. Hence the labyrinth design should be able to create such vortices in the seal cavities.

It is known that the steam flowing across the knives exerts a pressure on them. This was more pronounced in the case of the seal with slant knives wherein the steam impinged on the slant surface of the knives pressing them towards the shaft. Added to this is the fact that the shaft experiences vibrations about its axis thereby impinging on the seal knives and deforming them. Therefore, the knives are under the influence of two mutually opposing forces – steam pressure pressing them towards the shaft and the shaft forces forcing them towards the stator. As a result, the knives should be designed to be flexible and experience minimal deformation and/or damage due to these two forces.

Hence, a new configuration for the labyrinth seal should satisfy the following criteria to maintain a high sealing efficiency:

- The seal knives should have good flexibility to minimize permanent deformation due to the shaft motion.

- As was stated above, the knives are under the action of two mutually opposing forces. Hence, the configuration is not only designed to withstand the shaft forces alone but also to withstand the resultant of the two forces.

- In the event of the impingement of the knives with the shaft there is every possibility of scouring of the shaft. In such a scenario, there should be the least amount of wear on the shaft. Therefore, the geometry, material and design of the knives have to be such that the shaft is left unharmed.

- The knives may have to comply with the current operational constraints of maintaining the minimum required clearances and tolerances yet never compromising their operational efficiency.

- Last but not the least is the long operational life and, the ease of maintenance of the seal and its components. Labyrinth seals are renowned for their simplicity and

the ease of handling and assembling. Hence, the new configuration should possess similar features.

These criteria led to the design and study of the following new geometries for the seal knives [16]:

- Combination of C-shape and straight knives (Figure 2)
- Z-shape with flat edge knives (Figure 3)
- C-shape with sharp edge knives (Figures 4 and 5)
- C-shape with flat edge knives (Figures 6 – 9)

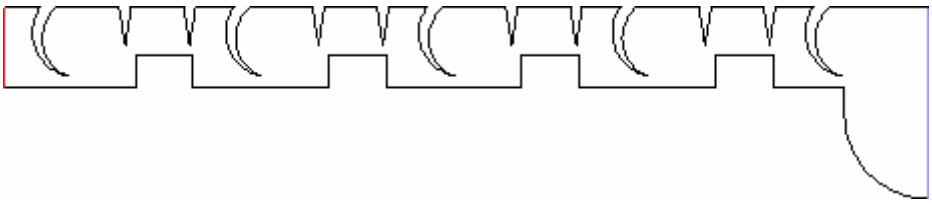

Figure 2. C-Shaped Tall Knife (Sharp Edged) and 2 Vertical Short Knives

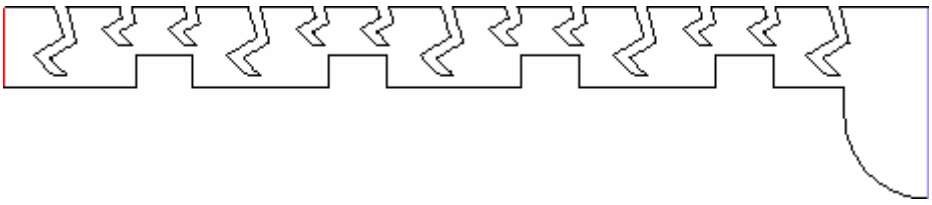

Figure 3. Z-Shaped Knives, 1 Tall + 2 Short Knives

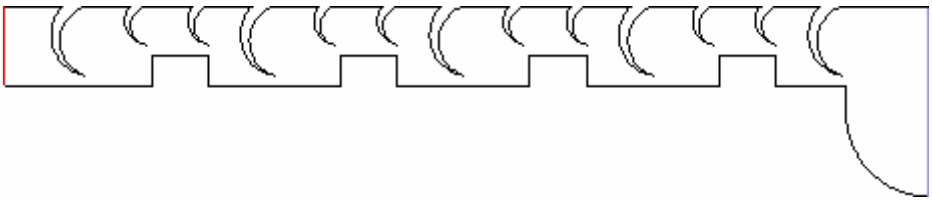

Figure 4. C-Shaped Sharp Edged Knives, 1 Tall + 2 Short Knives

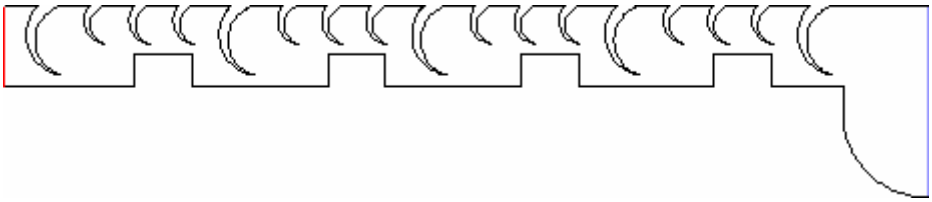

Figure 5. C-Shaped Sharp Edged Knives, 1 Tall + 3 Short Knives

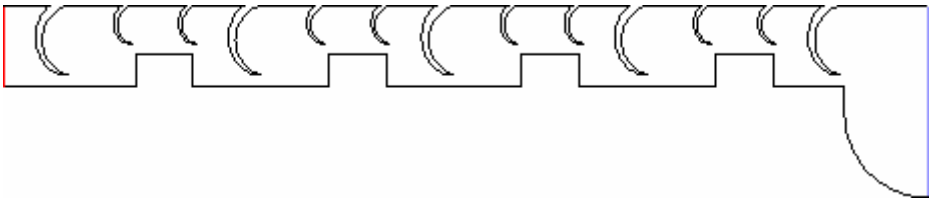

Figure 6. C-Shaped Flat Edged Knives, 1 Tall + 2 Short Knives

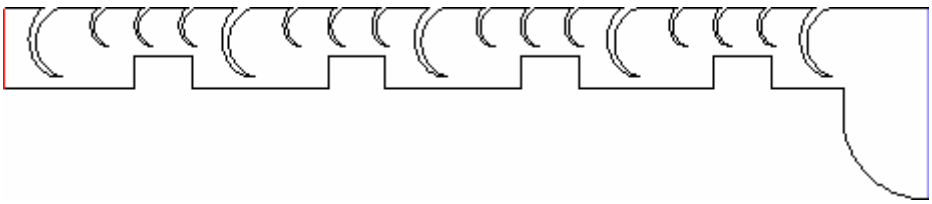

Figure 7. C-Shaped Flat Edged Knives, 1 Tall + 3 Short Knives

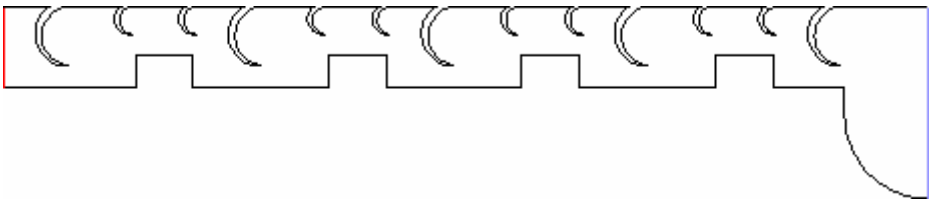

Figure 8. C-Shaped Flat Edged Bent Knives, 1 Tall + 2 Short Knives

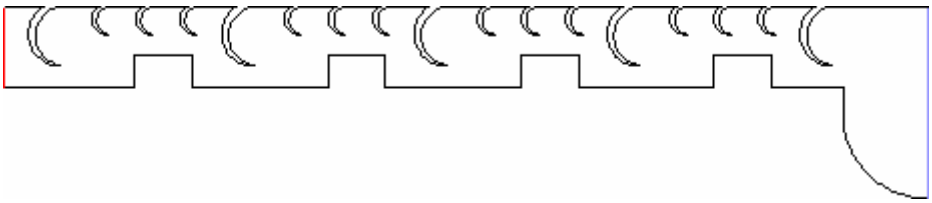

Figure 9. C-Shaped Flat Edged Bent Knives, 1 Tall + 3 Short Knives

All these configurations have the same clearance between the knife edge and the shaft. The Computational Fluid Dynamic (CFD) studies on these configurations revealed that the C-shaped geometry is better suited to directing the flow onto the walls of the turbine and /or the knives of the seal compared to either the baseline seal or the other configurations considered above, thus causing more energy dissipation in the curved shaped seal. Also, the CFD studies showed that the curved seals with three short knives prevented more leakage than the ones with two short knives [16].

This result satisfies only one-half of the objectives of conceiving the seal that can reduce the leakage of steam better than the existing designs. The other half comprises the structural analysis of the geometry. The seal geometry should:

- undergo least amount of deformation due to shaft and steam loads and,

- maintain the same or almost the same leakage characteristics as that of the undeformed geometry.

Thus the main objective of the structural analysis would be to define geometry for the seal such that it deforms the lowest under the shaft and steam loads. In the most efficient framework of analysis, the structural and the CFD analysis form a closed feed-back loop; the CFD analysis produces the geometry with improved leakage characteristics while the structural analysis refines this geometry for better strength and resistance to the loads, thus providing the CFD analysis with new input for improvement.

In the present thesis, work has been presented related only to the latter part of the total effort described above, that of using structural analysis software to refine a geometry found to exhibit better leakage characteristics than the others as suggested by the CFD study. The start point for the structural analysis is the baseline seal moving on to the C-shaped seal. A special mention pertaining to the two different kinds of the C-shapes is that one has a sharp free edge while the other has a flat one parallel to the turbine axis. As can be expected, the C-shape with the flat edge was found to exhibit higher load bearing capacity compared to the sharp-edged one.

5. Theoretical Background

The interaction between the shaft of the turbine and the seal elements, hereafter called knives, comprises a combination of forces normal and tangential to the surface of contact between the two. On the global scale, these result in 3-dimensional stresses in the knives due to the impingement of the shaft. But very close to the region of impingement the stresses are predominantly due to contact-forces which are localized to the contact region. Thus, to understand the forces and stresses developed in the knives, both normal and tangential stresses and, contact stresses are to be taken into account.

To understand the nature of the interactions between the shaft and the seal, it is necessary to first know the arrangement of the seals around the shaft in a turbine. Figure 10 shows the longitudinal cross-section of a typical seal segment arranged inside a housing built into the stator and around the shaft.

As can be seen from Figure 10, there are shock-absorbing springs in the housing to protect the seal segments from impact loads of the shaft. Hence, net forces leading to deformation of the knives can be approximately expressed in the vectorial form as:

$$\boldsymbol{\Delta F} = \boldsymbol{F}_{shaft} + \boldsymbol{F}_{d} + k\boldsymbol{\delta}$$

where,

$\boldsymbol{\Delta F}$ = net forces on the knives,

$\boldsymbol{F}_{shaft}$ = shaft forces,

$\boldsymbol{F}_{d}$ = resultant of all damping forces,

k = spring coefficient and,

$\boldsymbol{\delta}$ = deflection of the springs

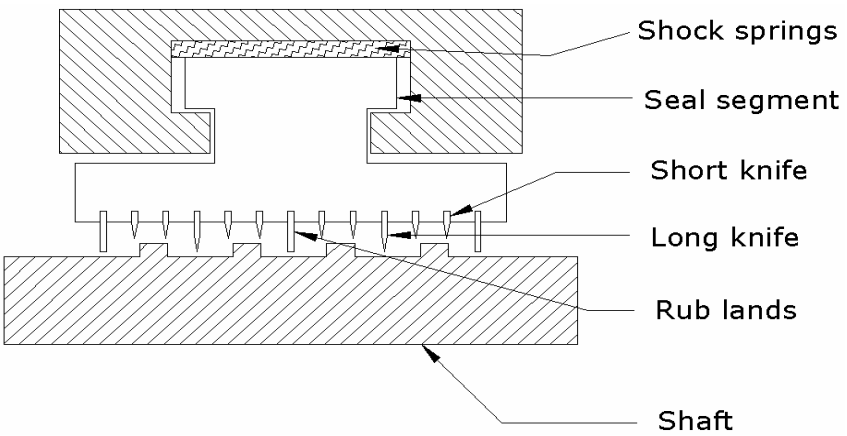

Figure 10. Typical arrangement of a seal around the shaft of a turbine

This is an approximate equation and represents only the static form of the forces not considering the presence of many other forces like the vibrations, friction between the knives and the shaft etc. Nevertheless, it is a good approximation to the actual values if other forces can be neglected.

Along with the shock-absorbing springs, rub-lands are provided for each segment minimizing the rubbing of the shaft on the knives. Such segments of seals are arranged in the form of sectors of a circle around the shaft. This sectored arrangement is done to facilitate maintenance and replacement of the seals and the shaft.

As mentioned in the previous chapter and shown in Figure 1, the knives also experience steam forces. Thus, the equation describing the deformation of the knives can be approximated as:

$$\boldsymbol{\Delta F} = \boldsymbol{F}_{shaft} + \boldsymbol{F}_{steam} + \boldsymbol{F}_{d} + k\boldsymbol{\delta}$$

where, $\boldsymbol{F}_{steam}$ is the vector denoting the steam force on the knives.

Normal loads and stresses in the knives are governed by the standard equations for determining 3-dimensional stresses. In the Cartesian form, these equations are :

$$\frac{\partial \sigma_{xx}}{\partial x} + \frac{\partial \sigma_{yx}}{\partial y} + \frac{\partial \sigma_{zx}}{\partial z} = 0$$
$$\frac{\partial \sigma_{xy}}{\partial x} + \frac{\partial \sigma_{yy}}{\partial y} + \frac{\partial \sigma_{zy}}{\partial z} = 0$$
$$\frac{\partial \sigma_{xz}}{\partial x} + \frac{\partial \sigma_{yz}}{\partial y} + \frac{\partial \sigma_{zz}}{\partial z} = 0$$

Body forces like centrifugal forces, weight of the knives etc. have been neglected in these equations. These equations are based on the assumption that the knives deform within the elastic limit of the material.

Before delving into the discussions about the nature and type of stresses developed in the knives, it is necessary to establish the coordinate system being used. Taking advantage of the axial symmetry of a steam turbine shaft and the arrangement of the seal segments, the cylindrical system of coordinates is best suited for stress analysis. Since the primary concern of the present study is stress analysis of the seal knives, a 2-dimensional Cartesian coordinate system was placed at the fixed end or the root of the knife. Hence, the direction of the shaft loads is in the radial direction while the thickness of the knife and the axis of the turbine are along the z-axis in the 2-dimensional description. In the 3-dimensional case, the circumference of the seal segment and the shaft follow the azimuthal axis.

A point of mention would be that for the 2-dimensional stress analysis, the coordinate system has been chosen as the rectangular Cartesian system with the x and y axes lying along the radial and the z axes of the cylindrical coordinate system, respectively. This change in the coordinate system does not affect the 2-dimensional analysis, because all stresses have been considered to follow the plane-strain condition.

Hence, the direction of impingement of the shaft onto the knives will be in the radial direction while, in the 2-dimensional case this would be along the positive y-axis.

Contact-stresses:

In addition to the ordinary stresses, the knives also experience what are known as contact stresses. All real-life materials deform when their surfaces are brought into contact by means of external forces; the deformation occurs at the surface in the region of contact.

As can be seen from the geometry of the knives and the shaft (Figure 11), the shorter knives interact in the same way with the steps on the shaft just as the longer ones with the shaft.

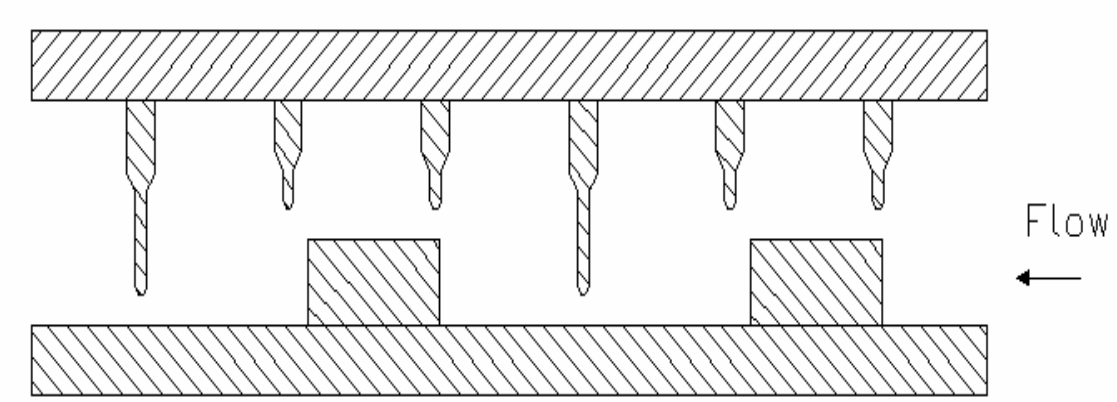

Figure 11. Configuration of the baseline seal [13]

During the operation of the turbine, the shaft does not always rotate about its geometric axis. There is a small vibratory motion about its geometric axis that can be attributed to many reasons like,

- Irregularities in the design and construction of the shaft, thus leading to an eccentricity of its axis.

- Defects in the positioning of the shaft bearings.

- The inertia of the shaft when the turbine is first started from rest.

- Irregularities in the geometry of the different turbine components like the diffusers, vanes etc. contributing to asymmetry.

- Irregularities in the mechanism used to start the turbine from rest, causing an unforeseen vibration in the shaft rotation.

- A change in the power required from the turbine causes an imbalance in the forces on the shaft, this being mainly dependent on the way the power from the turbine is finally utilized.

There can be many more than those stated above but all lead to rotational vibrations of the shaft. At the start of the turbine, the shaft rotates from a standstill to the operational speed. During this period, the rotational speeds of the shaft may match its natural frequencies leading to large amplitudes of vibration of the shaft. But this phase of vibration is very brief and the shaft finally stabilizes at its operational speeds since the operational speeds are designed not to coincide with shaft natural frequencies. Though the amplification is for a brief period, it can cause the shaft to impinge on the knives. The same occurs even during the shut-down of the turbine when the shaft speeds transit through the resonance phase and reduce to zero. Hence, the seal knives are to be designed

to overcome the loads due to these amplified vibrations in addition to the more uniform and predictable vibrations at the steady state condition. Whenever the shaft impinges on the knives, the shaft and the knife come into contact and both deform locally under the loads. These contact stresses differ from the ordinary loads in that they are highly localized and their affect subsides rapidly with distance from the contact region [18, 19].

Each knife forms a cylindrical surface around the shaft. As explained by Boresi and Schmidt [18], the region of contact between two coaxial cylindrical surfaces is a rectangle with the longer side of the rectangle along the cylinder axis. In the present case, the length of the seal segment is its thickness at its free end which is along the axis of the turbine shaft. But the thickness of the seal segment is very small compared to the length of the shaft. As a result, the rectangle now is of a length equal to the thickness of the free end of the knife which is in contact with the shaft.

The width of the rectangle depends on the degree of deformation of the seal's inner diameter and the extent of penetration of the shaft into this inner diameter. An approximate value of the width can be obtained from the principles of simple geometry. Considering two partially intersecting circles, the angle θ subtended by the intersection region at the center of the larger circle is given by:

$$Cos\theta = \frac{\delta r^2 + 2*(ri - rs)*(ri - \delta r)}{2*ri*(ri - rs + \delta r)}$$

These two circles in Figure 12 represent the transverse cross-sections of the seal and the shaft when the shaft has impinged into the seal.

$\therefore$ Width of the rectangle, AC = $2*ri*Sin\theta$

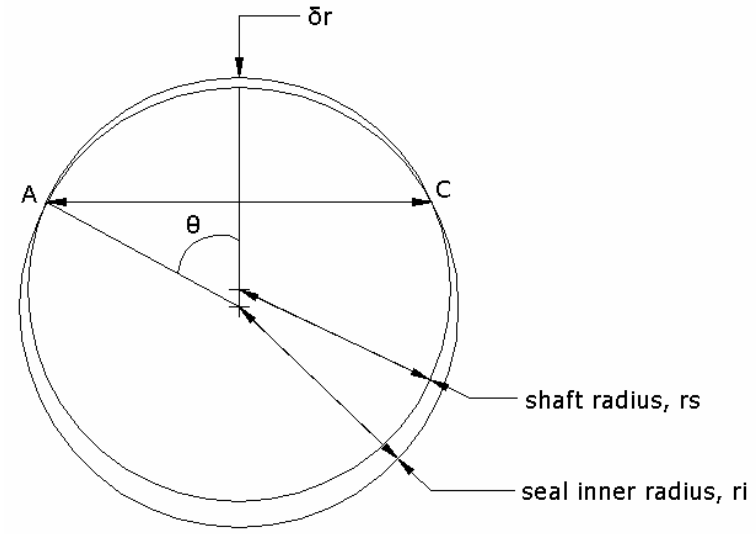

Figure 12. Two intersecting circles of almost equal radii

But the expression presented above for θ is based on the discussions for two interesting circles in plain geometry. Hence, they do not account for the elasticity of the seal inner diameter in both radial and circumferential direction. This is quite evident from Figure 12, where the points A and C are clearly defined while it does not occur in such a clear-cut way in nature. In fact, the surface defining the seal inner diameter deforms according the principles of strength of materials continuously maintaining a continuous curvature. The points A and C of Figure 12 are called points of singularity and occur only at the time of failure of the seal. As a result, the actual value of θ differs from that obtained by the above expression. In addition, for the case of real world materials, the value of δr becomes zero during the period of contact. Nevertheless, the value of θ found from the earlier expression gives an estimation of the width of the rectangle and hence an approximation for the magnitude of contact stresses.

For all practical considerations, the shaft can be treated to be rigid relative to the knives and hence, the smaller circle in Figure 13 has been depicted to be intact.

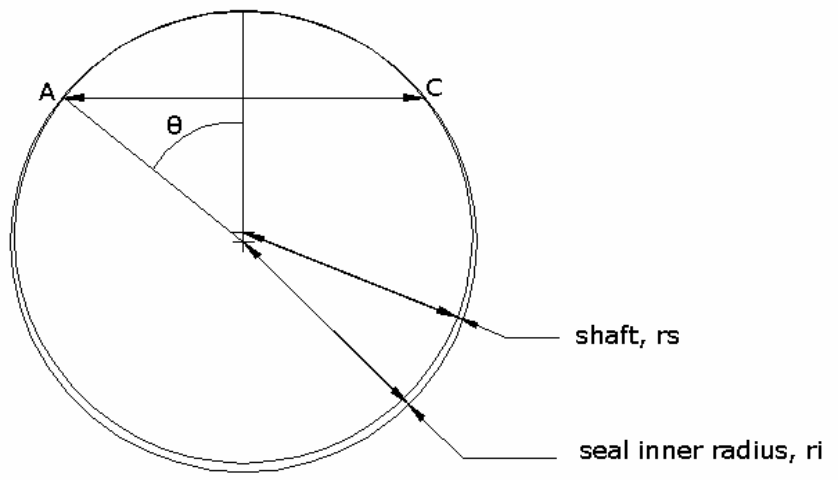

Figure 13. Distortion in the outer circle at the region of contact with the inner circle

In addition to the ordinary loads, frictional forces between the surfaces of the shaft and the knife also prevail. These forces are dependent on the radial shaft forces and the nature of the shaft surface and the free-edge surface of the knife.

The presence of friction causes the total stresses in the contact region to be very high compared to the case of normal loads acting alone [18].

But, in the present case the analysis is limited to only the contact loads and normal operational loads at the knife-shaft interface. Hence, the effect of friction is neglected.

In a steam turbine, the seal segments are arranged around the shaft not in one single circle but of many equal sectors finally completing the circle (Figure 14). This is done for ease of maintenance and other practical reasons.

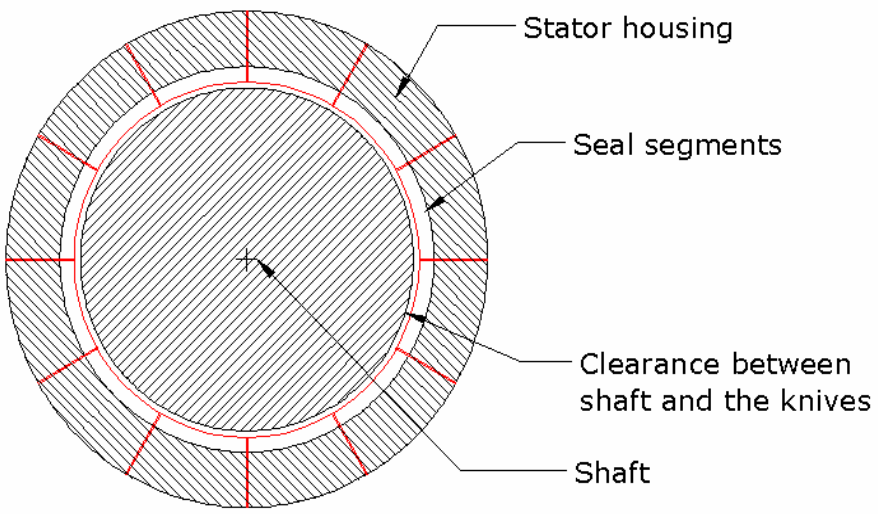

Figure 14. Typical sectored arrangement of the labyrinth seal around the turbine shaft

2-Dimensional stress analysis:

To understand the nature and variation of normal operational stresses internal to the knife, a good approximation is the study of the 2-dimensional distribution of stresses within the longitudinal cross-section of the seal segment. The stress distribution in the longitudinal cross-section of the seal, which resembles a knife, can be treated as a 2-dimensional cantilever beam (Figures 15 and 16). The knife behaves as a cantilever beam of unit thickness perpendicular to the plane of the section with a compressive load applied along its free end. For the case of the baseline seal, the only stresses developed in the cross-section are due to normal forces in the radial direction of shaft rotation. The stresses thus developed are normal radial stresses. All reference to normal radial stresses hereafter will be made as normal stresses. But, if the cross-section is in the shape of 'C', in addition to the normal stresses, there are bending stresses (Figure 16).

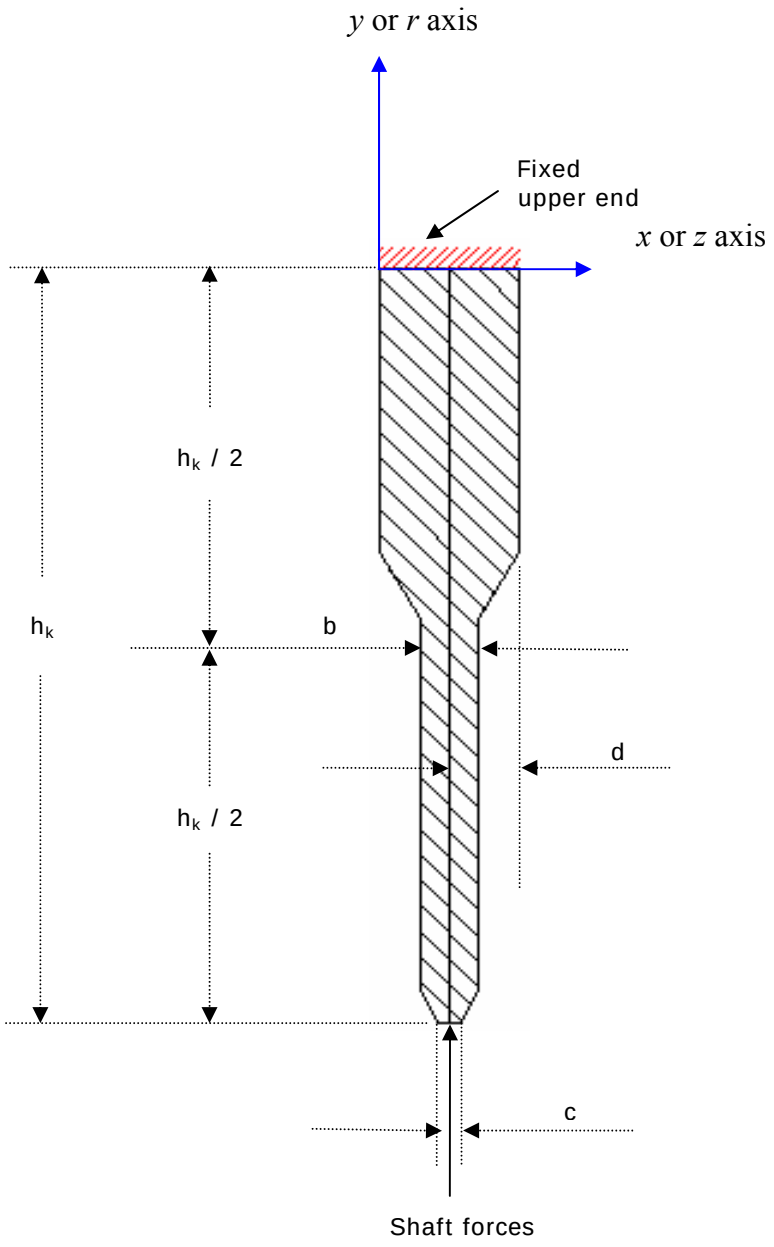

Figure 15. Schematic of the baseline knife with geometric parameters, constraints and load

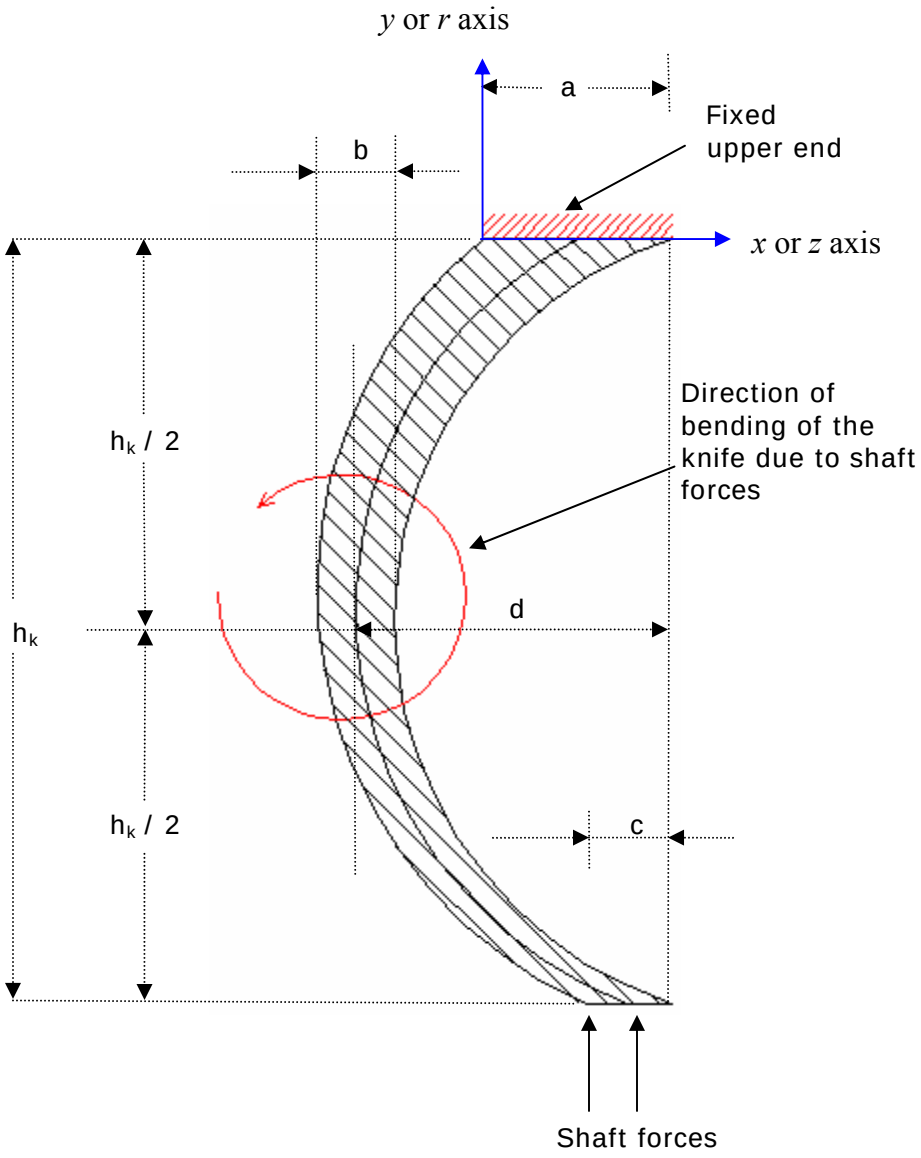

Figure 16. Schematic of the C-flat knife with geometric parameters, constraints and loads

The total stress at a particular cross-section of a straight prismatic beam is given by,

$$\sigma_{tot} = \frac{F}{A} + \frac{Mc_e}{I}$$

where,

σ_{tot} = total stress at a particular section, *psi*

F = load applied on the beam, *lb.*

A = area of the section where the stresses are to be determined, $in.^2$

M = the bending moment due to the load, *lb-in.*

c_e = distance of the extreme fiber of the section with maximum compressive stresses from the neutral axis, *in.*

I = area moment of inertia of the section, $in.^4$

Due to the bending moments and the associated bending stresses, the maximum load that the curved knife can withstand before undergoing a plastic deformation would be smaller than that of the 'straight' knife. But the curved shape has the advantage of higher flexibility over the straight knife. This particular property of the curved shape offers the possibility of designing the seal geometry that is more flexible within the elastic limit of the material of the seal. Complementary to this feature are the studies which show the superior performance of the curved shape over the straight shape with regards to flow-direction, thus improving the sealing efficiency [16].

The deflection of a uniform beam with an initial curvature y_0 as a function of its length is given by [19],

$$\frac{d^2y}{dx^2} = -\frac{F*(y(x)+y_0)}{E*I(x)}$$

In this equation, the moment of inertia is constant. If the beam is of non-uniform thickness, the moment of inertia is a function of the position of the particular section along the length of the beam. Hence, the equation now becomes,

$$\frac{d^2y}{dx^2} = -\frac{F*(y(x)+y_0)}{E*I(x)}$$

Thus, the equation has now assumed a non-linear behavior becoming all the more difficult to solve analytically. Numerical methods are implemented to such equations.

6. Structural Analysis

The main objective of this research is to study the structural design and conduct the stress analysis of new labyrinth seal configurations.

The simulation studies of the steam flow through the seal have suggested that the new seal configurations have better sealing characteristics than the baseline seal [16]. A structural analysis study was performed to study the behavior of the baseline seal (Figure 17) and the new configurations. The baseline seal was chosen as the start point for the structural analysis. The experimental setup for testing the flow characteristics of this configuration was discussed in detail by Michaud *et al* [13]. The data obtained from the experiment and a computational fluid dynamics simulation of the same setup suggested the conception of alternate designs to the seal element. The seal elements will henceforth be addressed as knives (Figure 10).

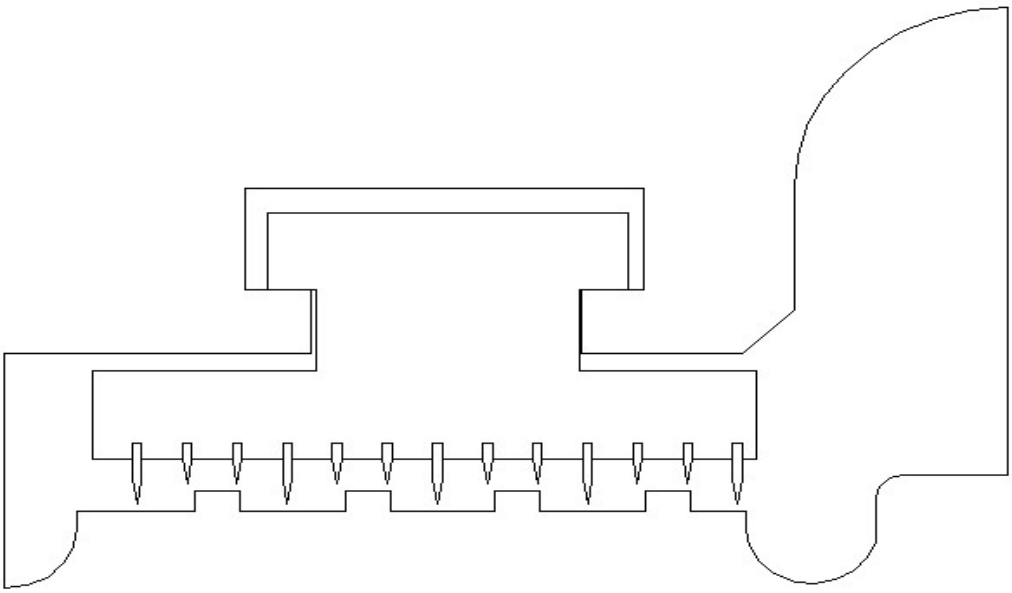

Figure 17. Baseline Seal Configuration

The different seal configurations discussed by Michaud [13] were subjected to a limited structural analysis for the case of static loading. The following are the salient features of the structural analysis:

- The analysis was based on finite element method.
- The analysis was performed using the commercially available finite element structural analysis software ANSYS®.
- The knife in a seal behaves like a cantilever beam. Hence the broader edge or the root end of it was fixed.
- Maximum number of key-points and lines used : 100 each
- Maximum number of grid nodes used : 1000
- Static compressive load was applied on the free end.
- The loading on the knives was treated to be a case of plane-strain.
- The load is static and within the elastic limits of the material.
- The knives were treated to be made of carbon steel.

The compressive force required to cause failure of the knife was found by applying loads iteratively in an incremental order. The maximum load is that which causes a maximum total stress just lower than or equal to the yield strength of the material.

Material properties of the seal: cf. *Appendix A*

Description of the load setup:

The main loads on the knife are of two categories: structural and fluid generated.

The fluid generated loads are exerted by the steam flowing through the seal. These forces and moments are dependent on the flow path taken by steam, and the pressure and velocity of steam.

The structural loads on the seal are due to the impingement of the rotor on the free edge of the seal. In the ideal case of operation of the turbine, the shaft rotates without any eccentricity or vibration about its geometric axis. But due to the many inconsistencies in the dynamic balance of the rotor, pressure of steam, the inherent design defects and etc., the rotor experiences vibratory motion about the original axis. These vibrations are very high during the start of the turbine from a position of stand still and dampen as time progresses. Though the modern steam turbines are designed to minimize the vibrations of the shaft, they nevertheless exhibit them. As a result, even before the motion of the shaft becomes regular, there is every possibility of impingement of the shaft on the seal elements.

Only structural loads were considered in this analysis. These loads on the seal were treated to be two-dimensional and static in nature and acting on the free edge of the knives. The loads were always within the elastic limit of the knives.

The clearance between the knife's edge and the shaft is 0.04 in. which is also the distance the shaft has to move before impinging on the knives. In the current analysis, motion of the shaft was exaggerated to be more than 0.04 in. to study the scenario where the shaft motion becomes too large. But, as mentioned in the previous chapter, the net forces acting on the knives are a resultant of the shaft and steam loads in addition to the

damping effect of the shock-absorbing springs. As a result, the present approach can be viewed as a study of the effect of the resultant of the shaft, steam and other forces on the knives than the shaft forces alone.

Structural analysis of the different seal configurations:

As has been stated earlier, the knife was assumed to be in a plane-strain condition and the loads were within the elastic limits of the material of the seal. The knives were assumed to behave as cantilever beams to approximate the actual case inside a turbine wherein the seal is secured in the stator casing. The labyrinth seal is composed of both long and short knives. A preliminary analysis of the long and short knives showed that the shorter knife can bear more load than the longer knife before reaching the elastic limit. As a result, the longer knife was made the focus of study and all results presented are for behavior of the longer knife.

Choice of elements used for modeling:

The analysis was performed using the area element Plane2 available in the structural analysis software ANSYS®. The Plane2 type of element is a 2-dimensional area element which can accommodate the conditions for plane-strain and was well suited for the present analysis. A triangular area element was found to be able to conform more satisfactorily to the curvature of the C-shaped knife than a quad-type area element. Hence a triangular elemental grid was used.

As has been discussed in the earlier chapters, the total stresses developed at any particular cross-section of a beam is given by,

$$\sigma_{tot} = \frac{F}{A} + \frac{Mc_e}{I}$$

In the present case of a 2-dimensional model, the thickness of the model perpendicular to its plane was taken as unity. Hence, the term ‘cross-section’ refers to a particular section along the length of the knife with unit thickness perpendicular to the plane of the knife. Proceeding with this expression, the total stress at a particular section of the C-shaped knife can be computed using the above equation.

As has already been stated in the previous chapter, the maximum load on the knife is that which causes the maximum total stress to be equal to or just less than the yield strength of the material of the knife. In other words, the maximum load is that load which the material can withstand and still remain within its elastic limit. Thus, the maximum value of the load was computed iteratively by maintaining the total stress within the elastic limit of the material.

This maximum load and the area of the section reaching the elastic limit can then be substituted in the above equation to analytically calculate the total stress. Since the geometry of the knife is known exactly, the various parameters in the equation like the area of the cross-section of a particular section of the knife, the maximum distance of the extreme fiber from the neutral fiber etc. are known and this gives the maximum value of the total stress.

The assumption that the knife behaves similar to a beam led to the use of beam type elements. Also, when a calculation was performed using the above equation, a significant difference in the maximum value of the total stress was found between the computational result and the analytical result for the same value of the load applied on the free end of the knife. This showed that the area elements were not able to give an exact account of the behavior of a beam. On the other hand, they were able to provide with an order of magnitude comparison of the results between the different configurations. Also, the amount of time taken to setup the finite element model using area elements was very small that that for beam elements.

The thickness of the knives varied along the length of the knife from its fixed to free end. This in turn results in variation in the area of cross-section and the moment of area of the sections and, the distance of the neutral fiber from the extreme fibers of the section. As a result, the beam element chosen has to take into account this variation in the different properties of the geometry. The beam element Beam54 in ANSYS® is suited for the analysis of a beam of non-uniform thickness. The geometries considered in the present study have circular shapes on the inner and the outer edges of the C-shape. Also, it was assumed that the neutral fiber of the geometry is situated midway between the inner and the outer curves of the C-shaped knife. As a result, the entire knife was considered as a single circular curve with its properties taken into consideration in its real constants.

The analytical and computational values obtained by using this new element were in very good agreement with each other. This successful agreement between the analytical and computational values resulted in the reconstruction of the analysis model using beam elements.

Coordinate system for the analysis with beam type elements:

When using the area elements, the models were constructed as shown in their load setup diagrams (Figures 15 and 16). But, for the beam elements the knife geometries were rotated by 90º for the sake of convenience and ease of input of data. The fixed end of the knife formed the origin of the Cartesian coordinate system with its length stretching along the positive x-axis. Since the effect of body forces like gravity was neglected, this change in the orientation of the knife does not affect the final result.

With the use of beam type elements, the geometries now resembled only a representative straight line in the case of the straight seal and a circular curve for the C-shaped seal (Figures 18 and 19).

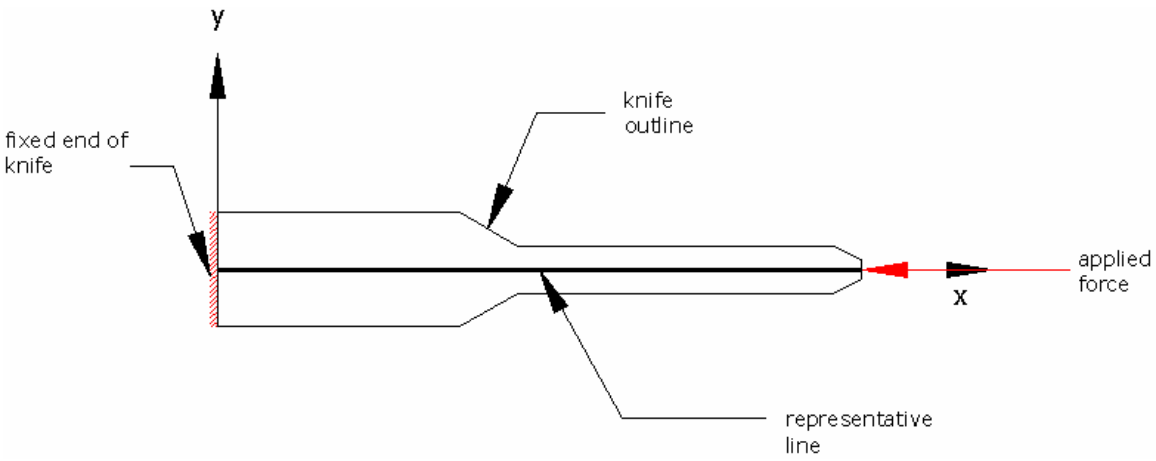

Figure 18. Representative line of the straight knife

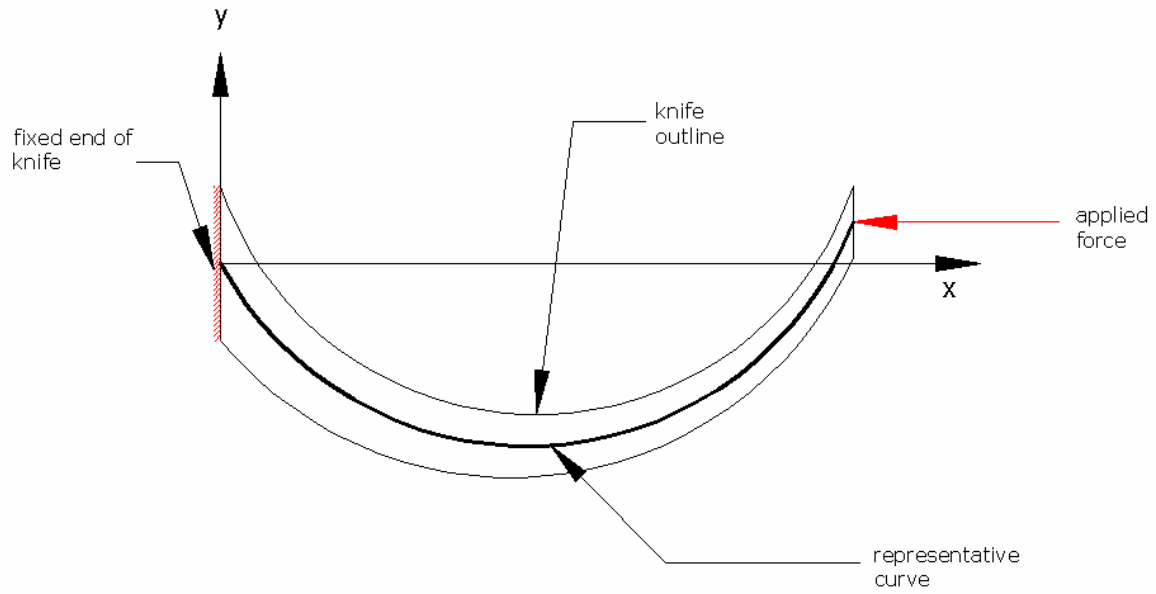

Figure 19. Representative curve of the C-flat knife

Straight Seal:

The baseline seal will henceforth be addressed as the straight seal and its knife the straight knife. The geometry of the straight knife has both uniform thickness and uniform taper along its length. Hence, two types of beam elements were used to simulate this variation in the thickness – Beam2 for the portion of the knife with uniform thickness and Beam54 for the portion with the taper. The element Beam2 treats the geometry to be of constant thickness.

New configurations:

The new configurations can broadly be divided into three categories based on the geometry of the knives: Z-shaped, C-shaped with sharp edge and C-shaped with flat edge.

The computational fluid dynamics simulation of the flow has shown that the leakage reduction in any of the C-shaped seals is superior to the Z-shaped seal [16]. Hence, the structural analysis of the new geometries was preferentially performed excluding the Z-shaped seal. The load setup for the C-shaped seal is the same as the straight seal. The C-shaped seal with the sharp and the flat edges will hereafter be addressed as C-sharp and C-flat seals, respectively and their knives C-sharp and C-flat knives, in that order.

Since the thickness of the C-shaped knives varies non-uniformly along their length, the beam element type Beam54 was used to construct the model. This element allows for the non-uniformities and asymmetries in the thickness relative to the neutral fiber. But there exists a constraint on the use of this element. The element assumes that the thickness varies linearly along its length. Hence, the ‘representative curve’ of the C-shaped knife now becomes a composite curve made of small straight lines with the

'thickness' of the curve varying linearly across each of these small straight lines (Figures 20 and 21). Added to this was the limitation on the number of 'keypoints' and lines available to generate the model. This limits the accuracy of the final model. In order not to compromise the accuracy of the model, the size for each of the lines was chosen to reflect the variation in the values of thickness and corresponding area moment-of-inertia along the length of the knife at the same time not exceeding the limit on the number of lines.

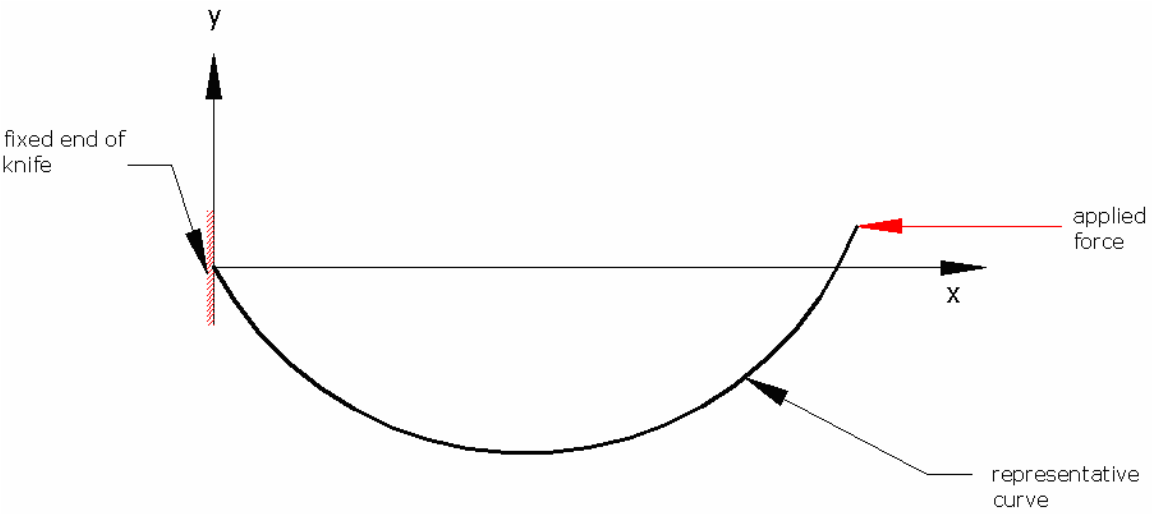

Figure 20. Representative curve of a C-flat seal

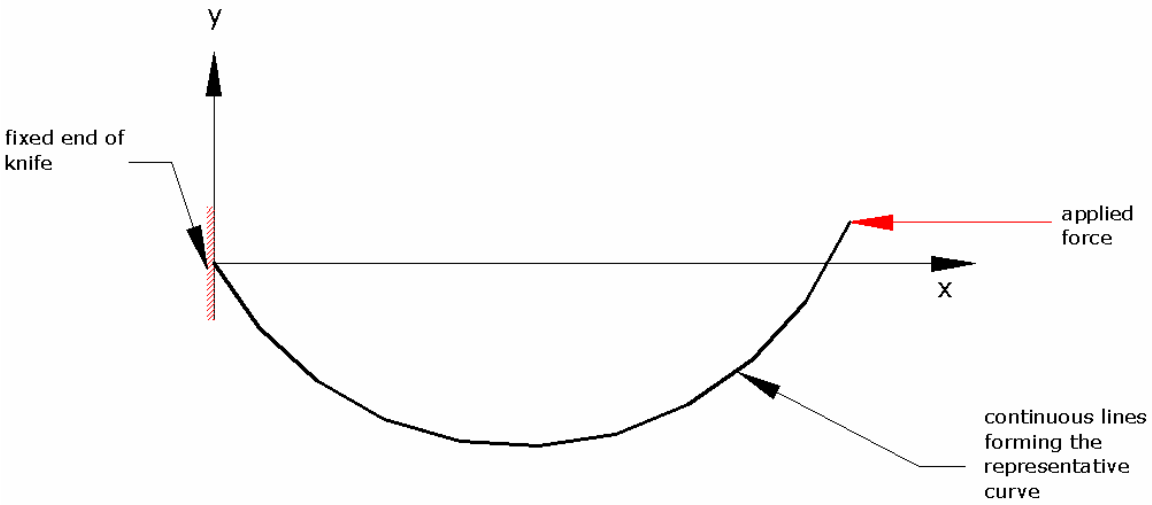

Figure 21. Finite element model of the representative curve of Figure 20

7. Results and Discussion

The structural analysis of the labyrinth seal geometry is a formidable task and demands huge amounts of data both from experiments and computational studies. But, in the present study the analysis has been simplified due to the limit on the data available and the computational resources. A balance had to be struck between the simplicity of the model used for the analysis and its representation of the real world operation of the seal. This process was all the more difficult because of the complexity of the problem, which is highly non-linear and 3-dimensional in behavior.

The following are the assumptions used to obtain the results presented in the earlier chapters and the associated conclusions.

- The structural analyses were 2-dimensional, static, steady and linear in nature and within the elastic limits of the material.

- Material properties used for the analysis were those of carbon steel and were assumed to be isotropic (*Appendix A*).

- The analysis carried out was purely structural. The knives were assumed to be at thermal equilibrium with the steam flow.

- The models were assumed to be in a plane-strain condition.

- The case of a cantilever beam under axial compressive loads was used to analyze the models. As a result, the root or broader ends of the knives were fixed for all degrees of freedom of translation and rotation.

- It was assumed that the shaft causes only compressive loads in the knives. All loads parallel to the shaft of the turbine and perpendicular to the knives at their free ends were not considered.

- Contact stresses were not analyzed since they exist in a direction normal to the plane of present analysis; contact stresses modify the analysis into 3-dimensions.

- The beam elements used for constructing the models interpolate the real constants for each element linearly between its nodes. Though the variation of the thickness is not linear, due to the small size of the elements used, this linear interpolation was deemed accurate for the final results.

- The accuracy of the dimensions of the geometries used was 10e-05 in.

  The numerical values of the forces were rounded for second decimal accuracy.

Preliminary analysis using area elements:

Though the use of area elements to perform the structural analysis was not as accurate as the use of beam elements, it nevertheless provided certain insight into the performance of the various geometries. It also has the advantage of ease of construction of the model. On the other hand, the beam type elements require large amount of data to be input based on the complexity of the geometry and the accuracy of the final model. As a result, the area elements were used as a start point for the comparison of the performance of the straight and the C-sharp seal knives.

The results of this preliminary analysis are as follows (Figures 22 – 29).

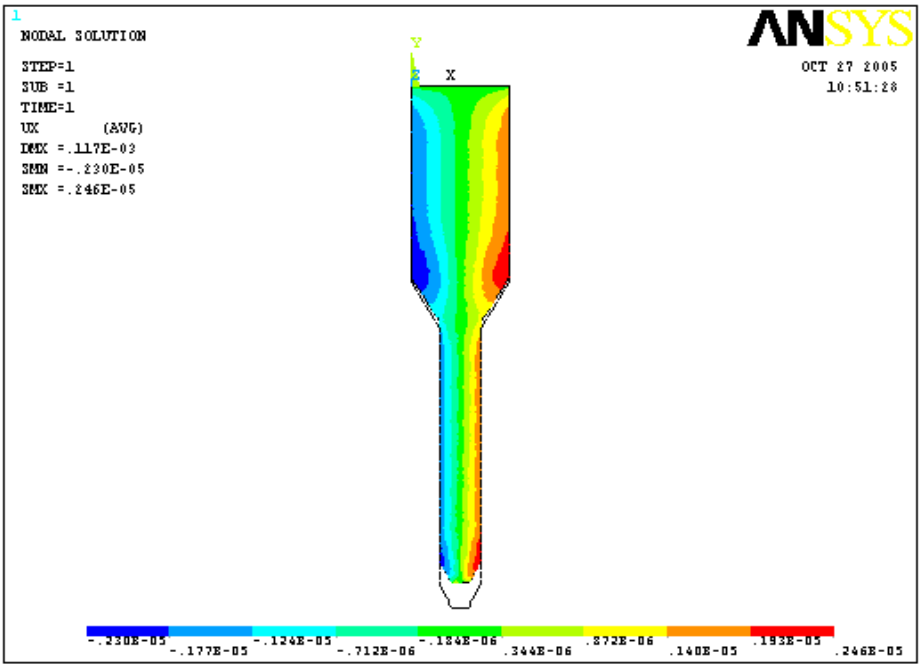

Figure 22. Straight knife - Deformation along x-axis

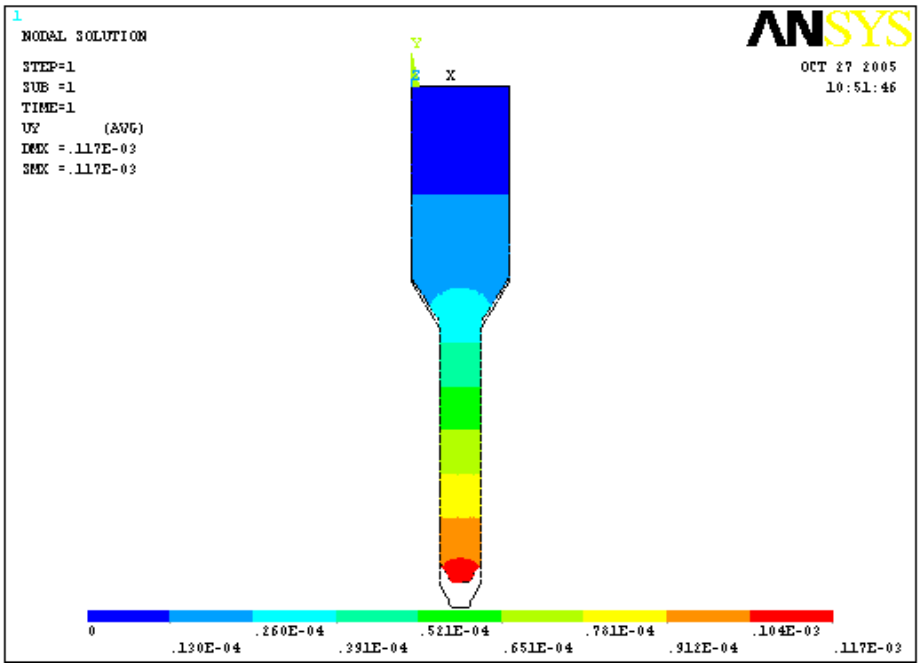

Figure 23. Straight knife - Deformation along the y-axis or along its length

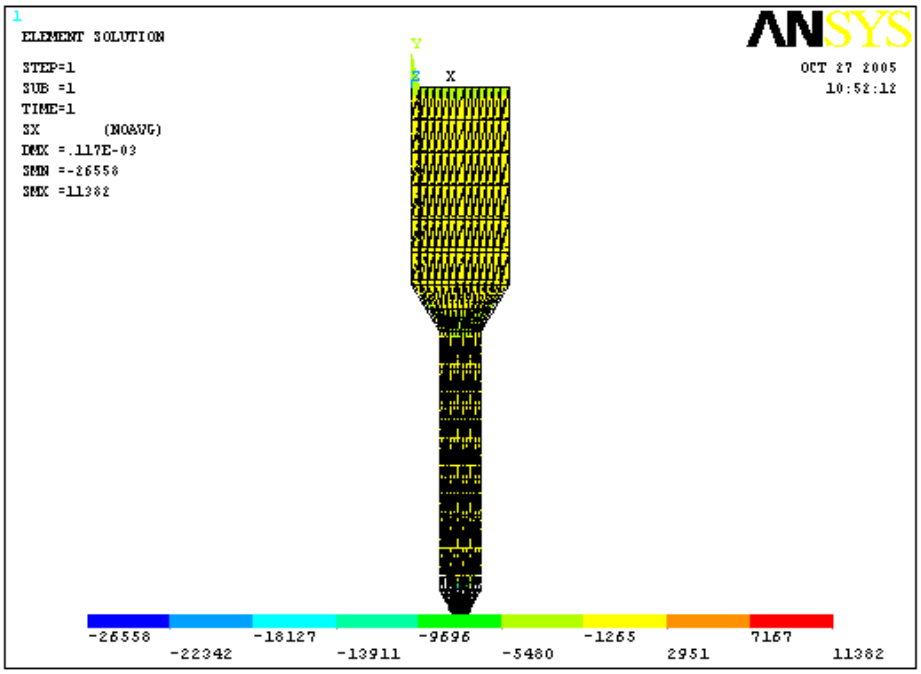

Figure 24. Straight knife - Stress along x-axis

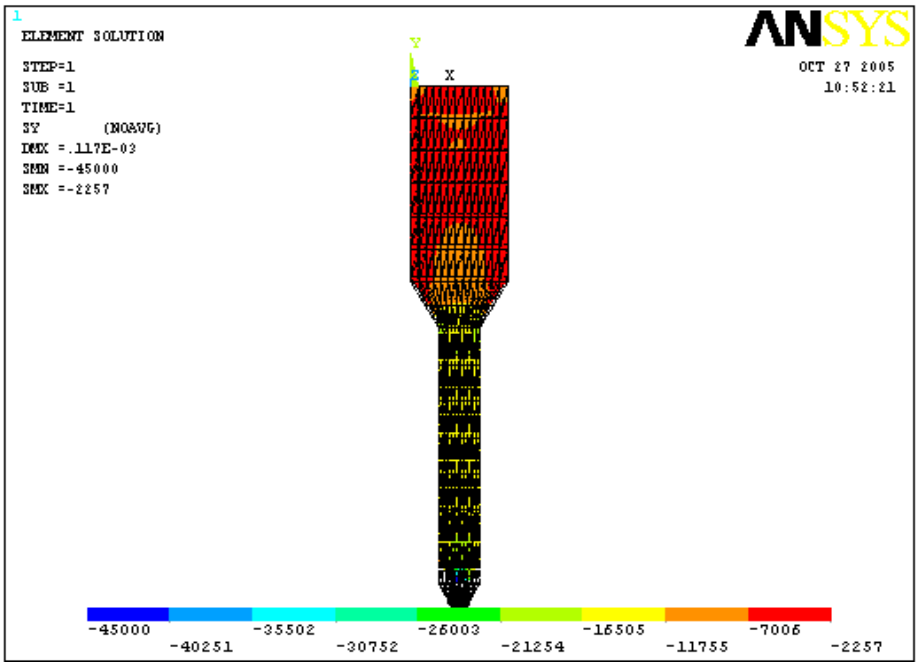

Figure 25. Straight knife – Stress along y-axis

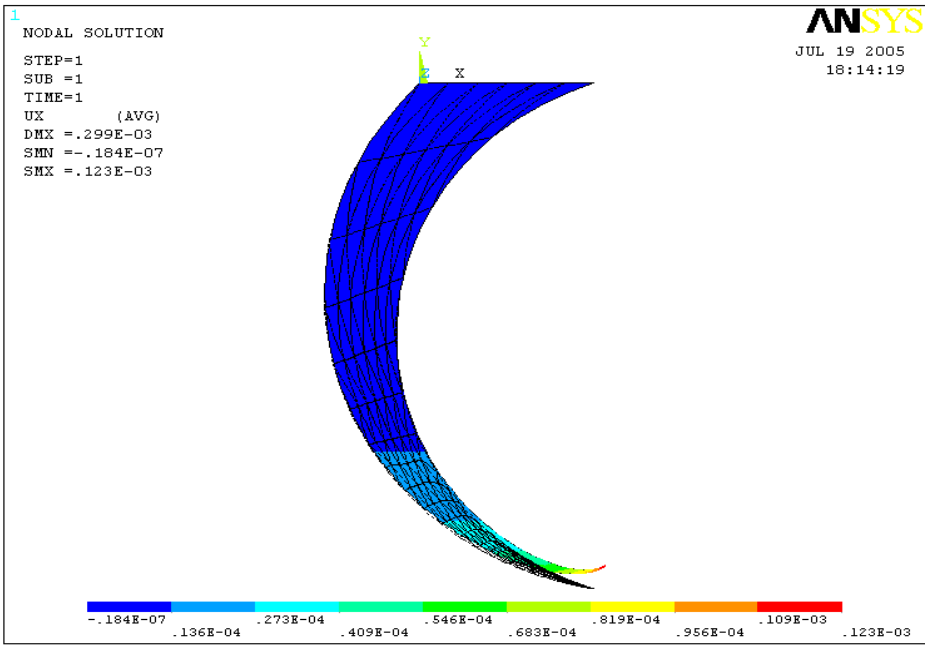

Figure 26. C-sharp knife – Deformation along x-axis

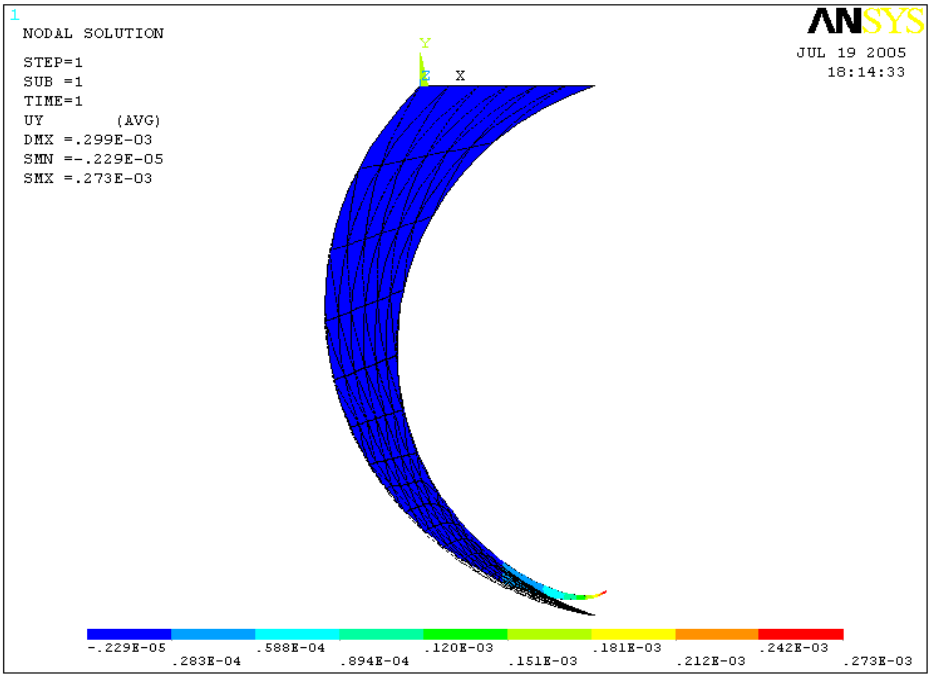

Figure 27. C-sharp knife – Deformation along y-axis

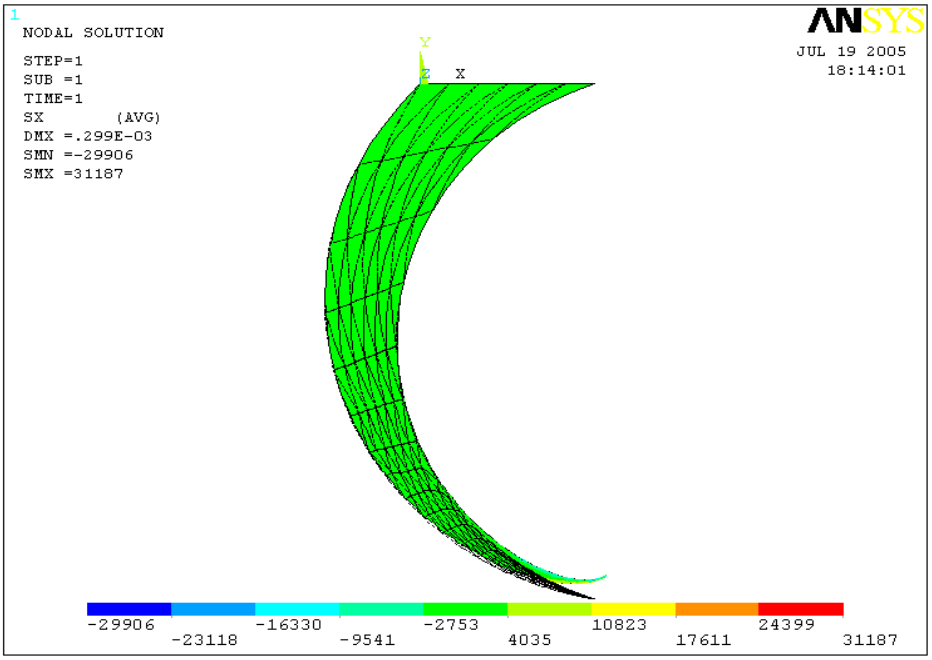

Figure 28. C-sharp knife – Stress along x-axis

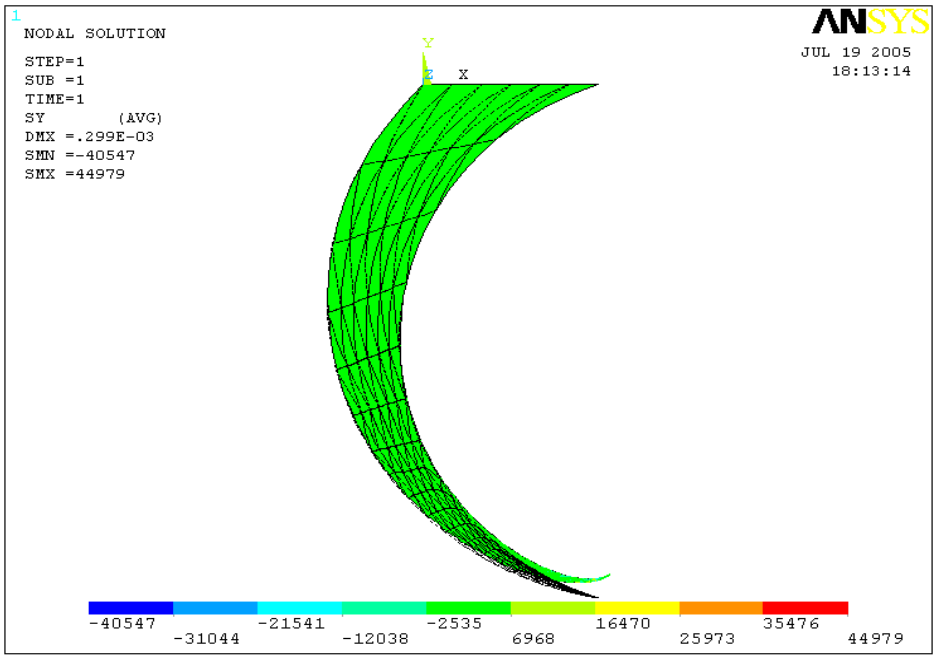

Figure 29. C -sharp Knife – Stress along y-axis

As seen from the above results, the straight seal knife has a very small deformation along its length under the influence of compressive loads. In other words, the straight knife is very stiff along the y-axis. This leads to the following conclusions:

- The straight knife has high resistance to the shaft motion which can scour the shaft.

- The proposed new seal geometry for the seal knife is less stiff and has higher flexibility along the x-axis.

The obvious reason for the high stiffness of the straight knife is lack of any 'freedom' to deform along axis of displacement. Hence the C-shaped configurations appeared a natural choice for improvement.

Based on these results the performance of the C-sharp knife was determined to be superior to that of the straight seal in terms of flexibility along its length. This is clearly evident from the magnitude of deformation of the shape along its length (along the y-axis) until the stresses developed reach the yield strength of the material. The value of its y-deformation is more than twice that of the straight knife.

The C-sharp configuration suffered from high local stresses at its free end in both the x and y directions. This can be expected due to the small thickness of the geometry at the free end. In addition, an analysis of this shape and the stresses developed in it brought forth the following problems:

- The thickness of the seal becomes very small at the free end, thus posing difficulties in both manufacturing and operation.

- Due to the very small thickness of the free edge, any rubbing of the seal with the shaft may rip the tip off posing a potential hazard to the safety of the internal components of the turbine.

- The ability of the C-sharp seal to minimize the leakage of steam is heavily dependent on the shape of the inner curvature and the free end of the 'C' shape. But the small thickness makes the edge very weak and may result in an unexpected behavior under the influence of loads, thereby affecting the flow of steam and thus the performance of the seal.

- The weakness of the edge drastically lowers the life of the seal defying one of the criteria for designing new configurations, namely creating a design that has long operational life and low maintenance similar to the straight seal.

All these shortcomings of the C-sharp knife make the C-flat knife a better choice to replace the straight knife.

Analysis using beam type elements:

Using the conclusions from the preliminary analysis and the fact that the beam elements are more accurate than the area elements, both the straight knife and C-flat knife configurations were analyzed using beam elements. The higher thickness of the free edge of the C-flat knife, compared to the C-sharp knife, makes the free edge more resistant to plastic deformation. Tables 1 and 2 give the geometric details of the different C-flat knife configurations considered and the results obtained from the structural analysis, respectively. Subsequent figures are results of analysis for the straight knife and one of the C-flat knives (Figures 30 – 40). Analysis results for the other C-flat knives are provided in *Appendix B*.

Table 1. Geometric parameters of the Straight and C-flat knives considered for structural analysis

Sl. No.	a (in.)	b (in.)	c (in.)	d (in.)	Area (sq.in.)	r1 (in.)	r2 (in.)	r (in.)
Straight	0.045944	0.019267	0.007410	0.022972	8.70E-03	N/A	N/A	N/A
**C1	0.0633	0.025621	0.0294	0.106788	0.0077	0.1370	0.1546	0.1434
**C2	0.0633	0.025304	0.0317	0.094939	0.0079	0.1439	0.1733	0.1549
**C3	0.0633	0.026000	0.0317	0.093753	0.0080	0.1449	0.1745	0.1563
**C4	0.0633	0.025945	0.0317	0.038247	0.0083	0.2027	0.3577	0.5917
**C5	0.0633	0.026569	0.0317	0.045000	0.0084	0.2822	0.8041	0.4107
***CS1	0.0451	0.011713	0.0050	0.099784	0.0037	0.1370	0.1482	0.1412
***CS2	0.0451	0.007389	0.0112	0.097507	0.0029	0.1370	0.1546	0.1435

1. Length of the different knives = 0.2601”
2. Line joining the right most edges of the fixed and free ends of all C-flat knives is perpendicular to both the ends
3. ** C1 through C5 denotes the C-flat knife.
4. *** CS1 and CS2 denote C-flat knives of thickness smaller than any of the knives from C1 to C2.

Table 2. Results of structural analysis

Seal Type	Force (lb.)	Δy (in.)	Δx (in.)	σ_n (psi.)	σ_b (psi.)	σ_{tot} (psi.)	ν_n	ν_b	xpos (in.)	ypos (in.)
Straight	360.45	0.00E+00	-1.30E-03	-45000	0	-45000	-1.55E-03	0.00E+00	0.260100	0.000000
C1	46.07	2.16E-03	-1.60E-03	-1884	±43108	-44992	-6.50E-05	±1.49E-03	0.164666	-0.069538
C2	51.6	2.00E-03	-1.27E-03	-2160	±42834	-44994	-7.45E-05	±1.48E-03	0.164666	-0.058016
C3	55.04	1.96E-03	-1.23E-03	-2243.5	±42750	-44994	-7.74E-05	±1.47E-03	0.164666	-0.025438
C4	639.54	8.64E-04	-1.96E-04	-15043	±29957	-45000	-5.19E-04	±1.03E-03	0.131333	-0.014193
C5	141.07	1.54E-03	-3.84E-04	-5930	±39166	-44999	-2.05E-04	±1.35E-03	0.156667	-0.010937
CS1	5.05	3.50E-03	-3.73E-03	-586.49	±44337	-44922	-2.02E-05	±1.53E-03	0.220663	-0.040297
CS2	1.91	4.94E-03	-4.85E-03	-384.15	±44560	-44944	-1.32E-05	±1.54e-3	0.196665	-0.033633

1. The beam extends along the positive x-axis with the fixed end at the origin of the Cartesian coordinate system.
2. x and y positions are with respect to the origin of the coordinate system.
3. Force applied is along negative x-axis.
4. All stresses are maximum computed stresses.
5. All deformations are maximum computed values.

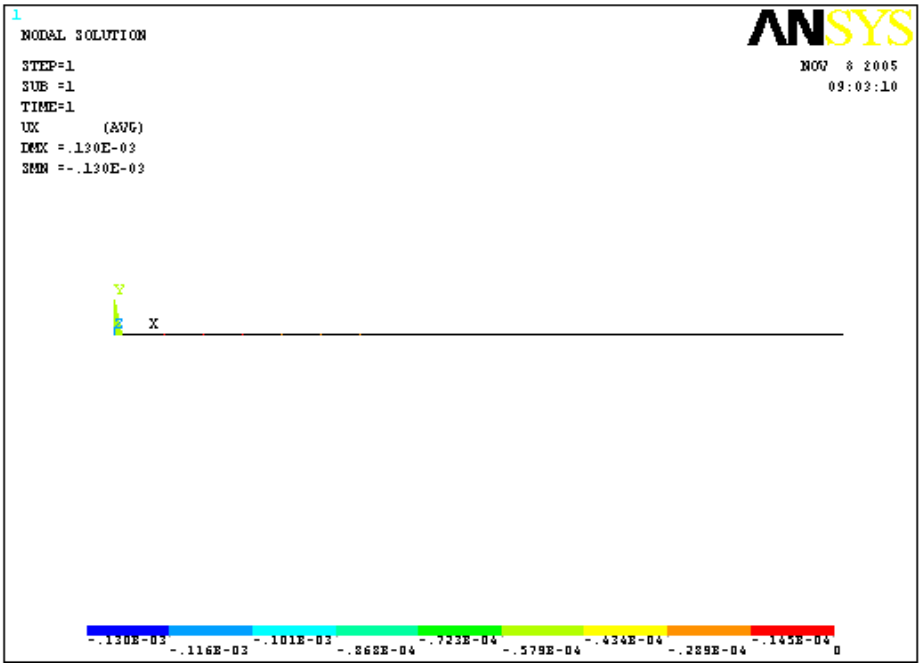

Figure 30. Straight knife - Deformation along x-axis

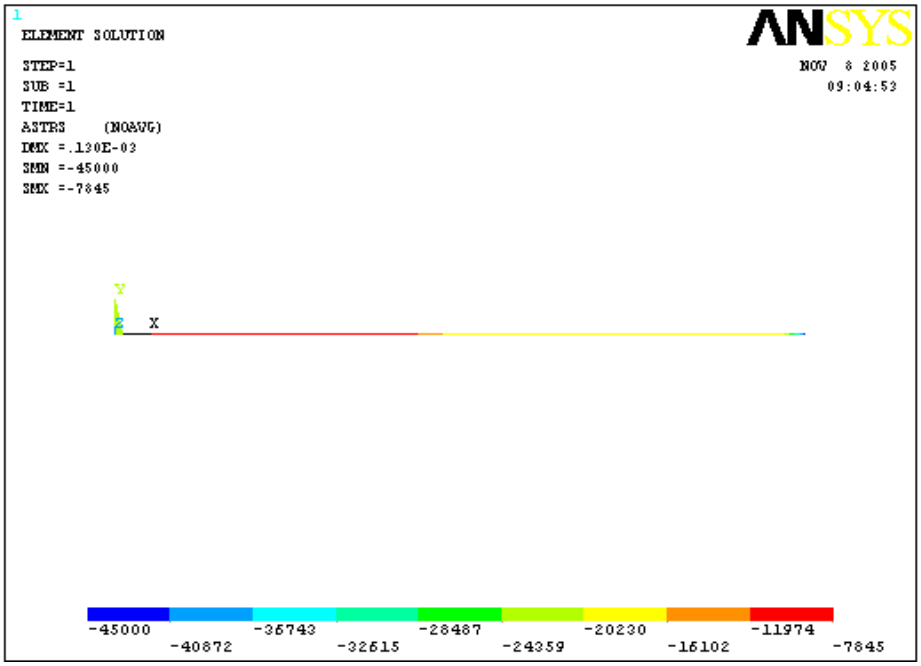

Figure 31. Straight knife – Normal stress

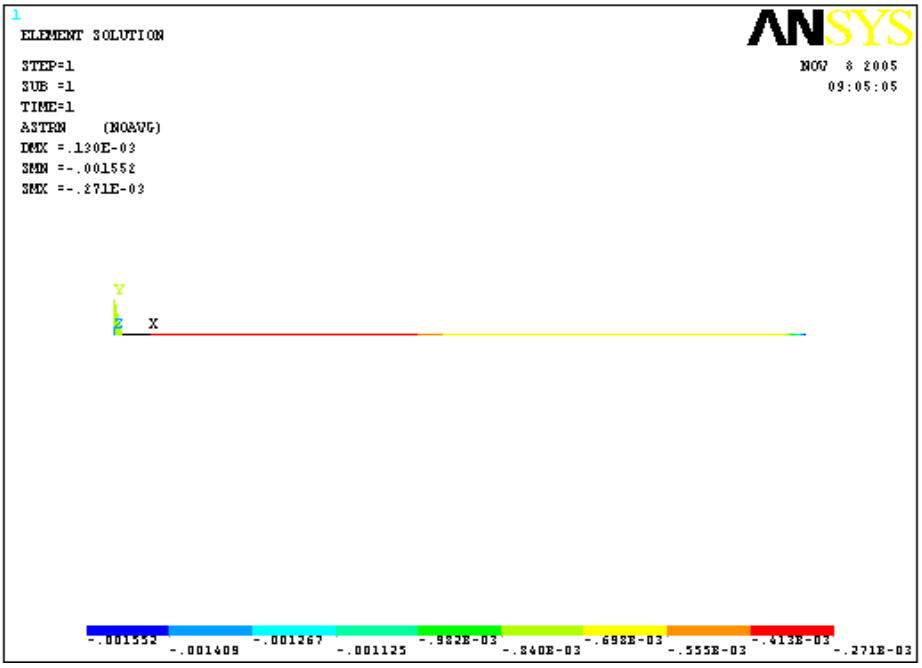

Figure 32. Straight knife - Normal strain

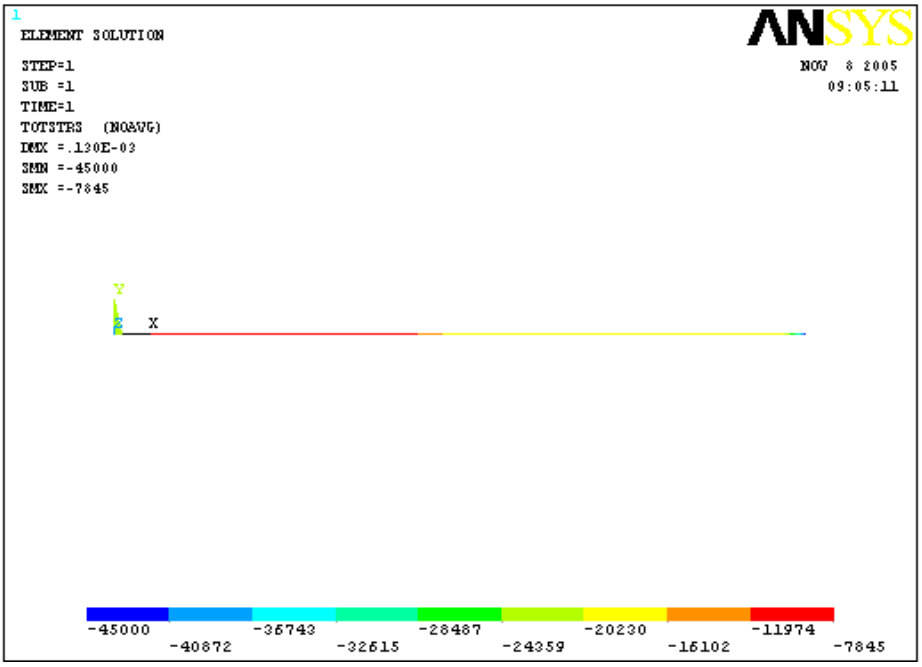

Figure 33. Straight knife - Total Stress

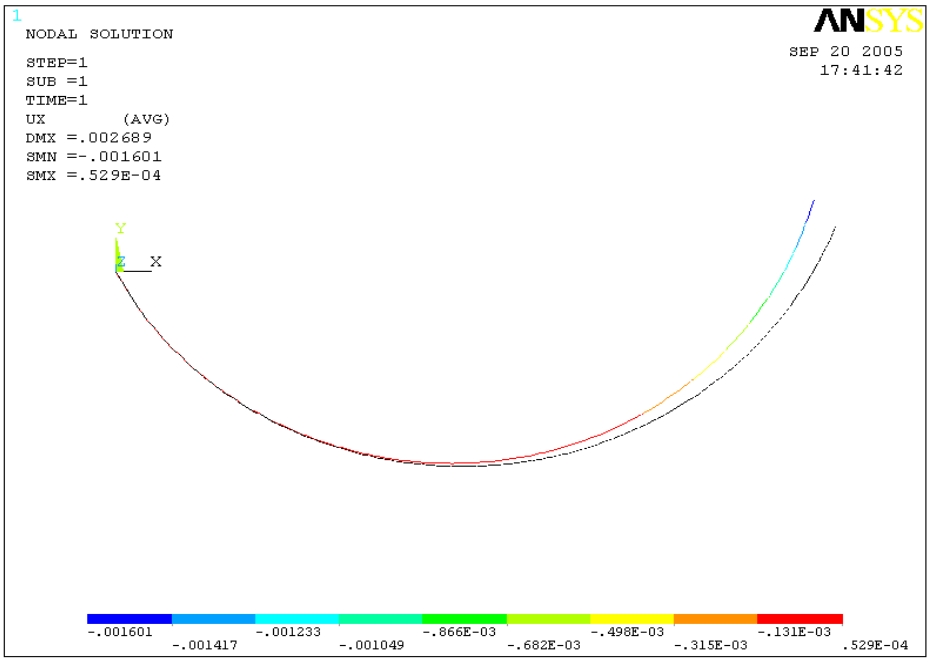

Figure 34. C1 knife - Deformation along x-axis

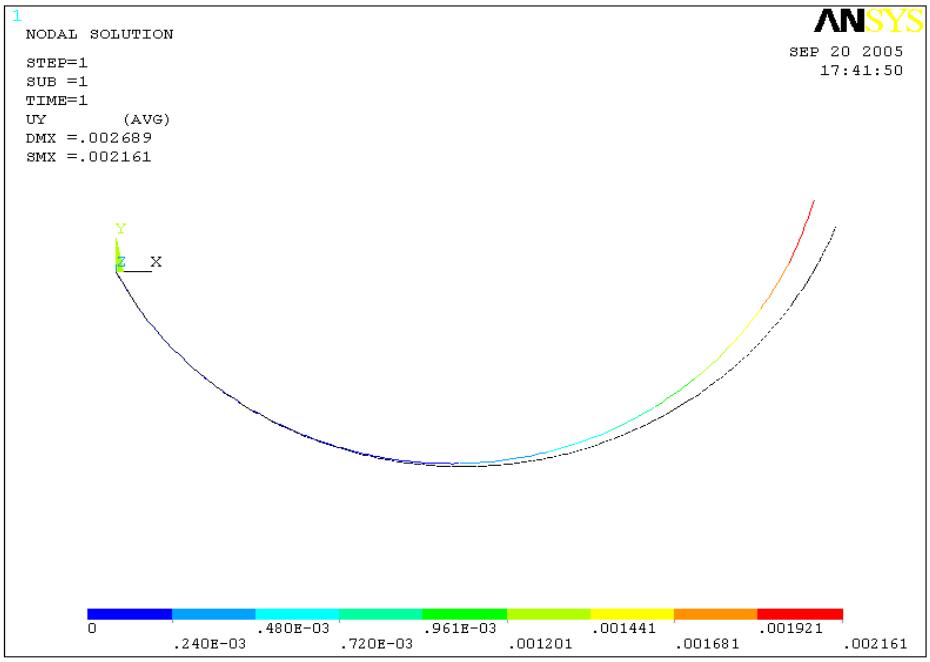

Figure 35. C1 knife - Deformation along y-axis

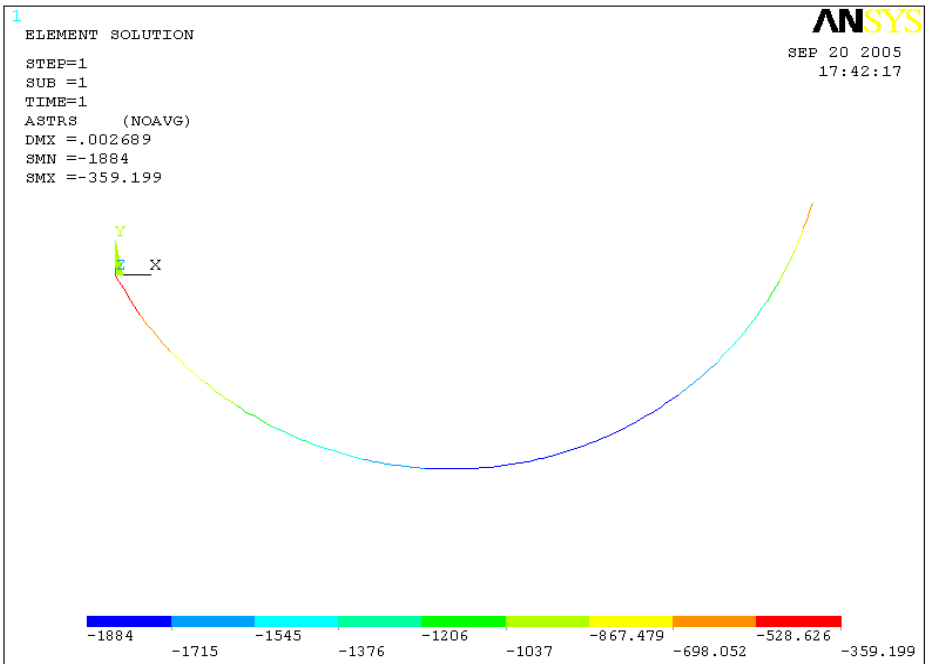

Figure 36. C1 knife – Normal stress

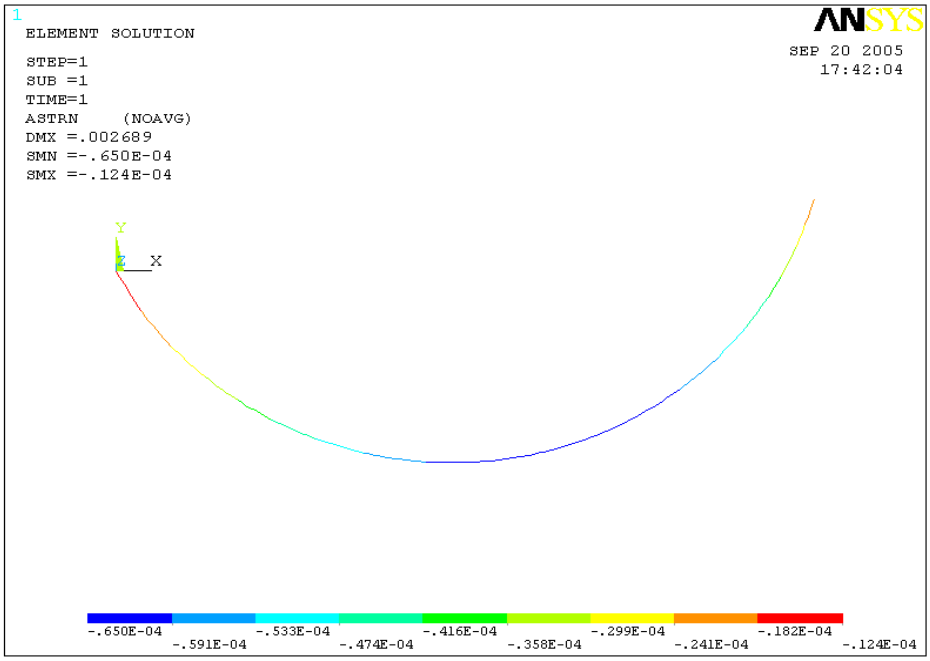

Figure 37. C1 knife – Normal strain

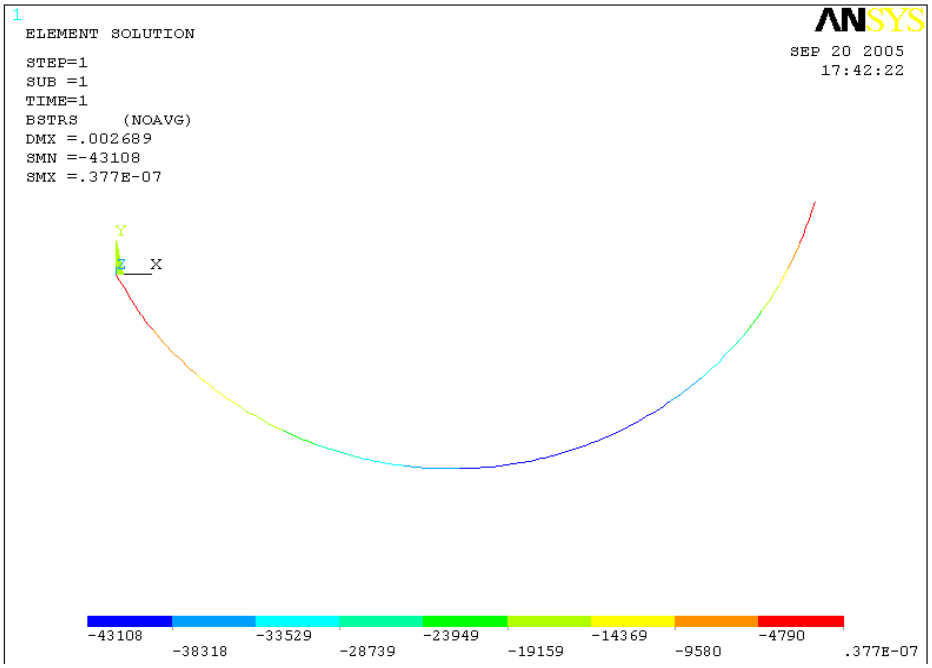

Figure 38. C1 knife – Bending stress

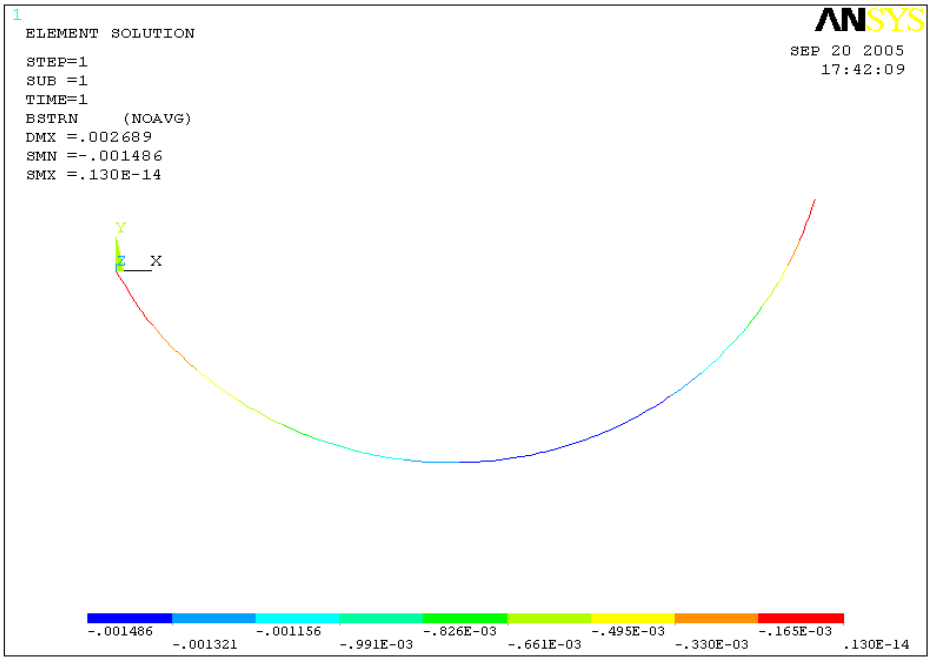

Figure 39. C1 knife – Bending strain

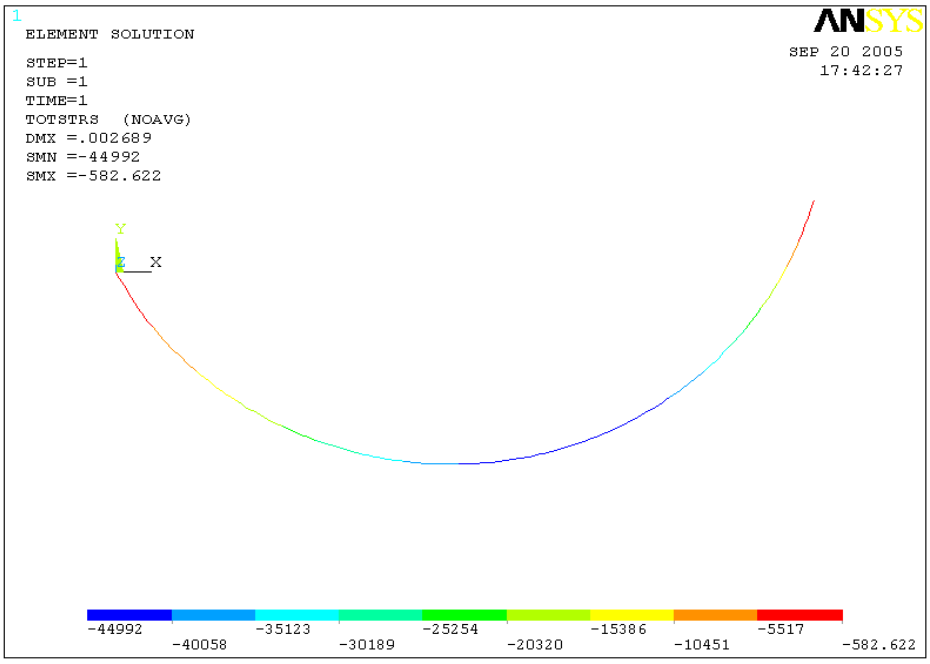

Figure 40. C1 knife – Total stress

It should again be noted that the values of the stresses and deformations are the maximum for the material used before reaching its elastic limit. Hence, if we consider the entries for the seal type C1 (Table 2), the maximum force shown to be 46.07 lb. results in a total stress equal to about 44992 psi which is almost equal to the elastic limit of the material (*Appendix A*). The loads considered were rounded off to the second decimal place as only a small variation in the third decimal place caused the maximum total stress in the material to be exactly equal to its yield strength.

Discussion of results:

The main emphasis of the present study was to develop new seal geometries or configurations that perform as well or better compared to the straight knife seal, with improved flexural behavior. Therefore, the results obtained from the analysis of the different C-flat knife configurations considered and documented in Tables 1 and 2 have been compared against the straight knife seal. Table 3 shows the comparison between the straight knife seal and the different C-flat knife seals. For the straight knife, the section with maximum total stress was found to be at the free end of the knife. As a result, the *xpos/L* value is unity for the straight knife. Also, as the straight knife does not experience any bending moments or stresses the value of σ_b/σ_y is zero for it and, its maximum axial stress, maximum total stress and yield strength are equal in value. Figures 41 and 42 show the variation of the different parameters of Table 3 for the different configurations.

Table 3. Comparison of results between Straight and C-flat knives

Sl. No.	Seal Type	F_r	Δx_r	σ_n ratio	σ_b / σ_y	$\Delta x / h_k$ (%)	$xpos / L$	$b / (b+d)$
1	Straight	1.000	1.000	1.000	0.000	0.500	1.000	0.4561
2	C1	0.128	1.232	0.042	0.958	0.616	0.633	0.1935
3	C2	0.143	0.979	0.048	0.952	0.489	0.633	0.2104
4	C3	0.153	0.942	0.050	0.950	0.471	0.633	0.2171
5	C4	1.774	0.151	0.334	0.666	0.075	0.505	0.4042
6	C5	0.391	0.295	0.132	0.870	0.148	0.602	0.3712
7	CS1	0.014	2.869	0.013	0.985	1.434	0.848	0.1051
8	CS2	0.005	3.734	0.009	0.990	1.866	0.756	0.0704

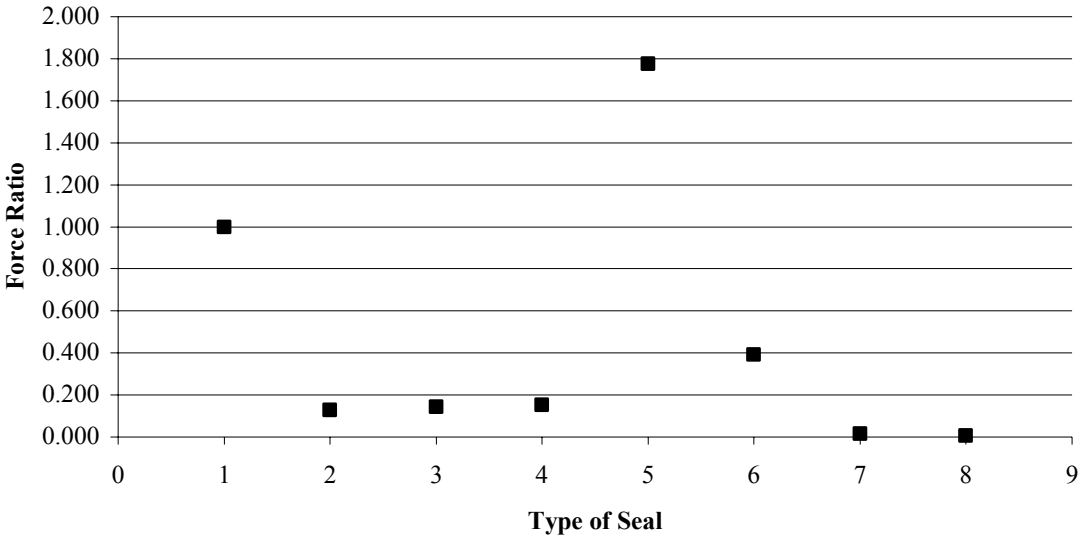

Figure 41. Force ratios of the different configurations of knives

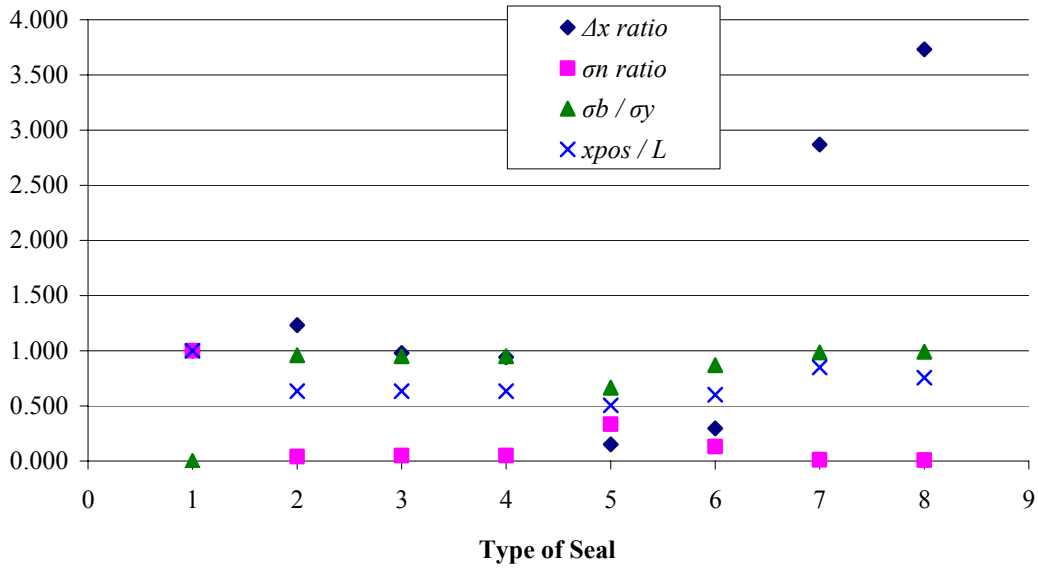

Figure 42. Variation of the different structural analysis parameters of C-flat knives with respect to Straight knife

In Figure 42, the ratio of strains has not been considered. This is because stresses are proportional to strains within the elastic limit of the material which implies that the ratio of strains is equivalent to the ratio of stresses.

The straight knife has its smallest cross-section at the free end. Since it suffers only axial stresses, the maximum total stresses are developed at the free end where the material of the knife reaches its elastic limit. As noted earlier, the maximum load bearing capacity of all the geometries was calculated against the yield strength of the material. On the other hand, the other configurations reach elastic limit at different sections away from their free ends.

Figure 41 shows that the configuration C4 has the highest load bearing capacity among all the configurations considered. Also, from Figure 42 it is clearly evident that C4 can withstand higher normal forces than the other curved knives. This implies that C4 has higher resistance to normal stresses than the other curved knives and can resist higher radial forces of the shaft than the other curved knives. Hence, if the goal of this study were to design a configuration that can withstand high radial forces of the shaft and still remain within the elastic limit, C4 would be an ideal starting point. Rather our goal in the present study is to design a configuration which has high flexibility under the influence of shaft forces. From this perspective, C4 is not suited for the job as shown by its high σ_n ratio. This means that in the event of impingement of the shaft on the knives, C4 does not conform to the shaft motion but resists a longer range of forces than the other configurations that may lead to scouring of the shaft. This is supported by the dip in the Δx ratio and σ_b ratio values at C4. The low Δx ratio shows that C4 has high resistance to the shaft forces and in turn to radial shaft motion. Hence, the configuration C4 may introduce some long term rubbing and excessive wear on the shaft. The low σ_b ratio of about 0.666 or 67% implies that the fraction of the total stress experienced by C4 due to normal stresses is 0.334 or 33% which is higher than the other curved knives. This is a direct indication of the rigidity of C4 along its length. The σ_b ratio is a direct measure of the fraction of the total stress contributed by the normal and bending stresses because, as

has been mentioned earlier, the maximum total stress, maximum normal stress and the yield strength are equal for the straight knife under the present load conditions.

The tips of the knives play an important role in containing the leakage of steam through the turbine. But the structural analysis results (Table 2) clearly show that the tip of the straight knife is the section first reaching the elastic limit, making it all the more imperative to look for alternative geometries and configurations for the knife that can accommodate shaft deformation.

Configurations C1, C2 and C3 (Table 2) behave almost identically to one another in terms of deformation and the stresses developed. They exhibit higher σ_b ratio and Δx ratio than C4 or C5 (Table 3). This implies that the flexibility of these configurations along their length is higher than both C4 and C5, and the straight knife.

The configurations from C1 through C5 have the same 'root' or fixed end thickness and a similar free end or tip thickness. But unlike these, the configurations CS1 and CS2 are much thinner at both the fixed and the free ends. The results of their structural analysis suggest far higher flexibility than any of the configurations C1 through C5. This can directly be attributed to the fact that thinner geometries are always more flexible than the thicker ones. As a result, under the objectives of the current study they would be the most suitable candidates for a labyrinth seal. Higher flexibility has the added potential for installing seals with a smaller clearance distance from the shaft than the straight seal. This is because of the fact that clearance employed between the seal and shaft in a turbine minimizes any damage to the shaft due to rubbing and scouring. But, if the seal has a higher flexibility it deforms more easily under the shaft loads. As a result, the amount of clearance can be reduced to a lesser value while maintaining the same degree of safety for the shaft.

An important feature of the results presented in Table 3 is the large forces that the configuration C4 can withstand before reaching its elastic limit compared to all the other

geometries presented in the table. This can be attributed to the geometric features of C4. A study of its geometry (Table 1) shows that the radius of curvature of the representative curve of C4 is much higher than C1, C2, C3, Cs1 and CS2. Such a high radius has made C4 behave like a straight knife with a thicker free end. This particular behavior of C4 made its load bearing capacity far superior to any other C-flat configuration (Table 2). The tendency to behave like a straight knife than a curved knife is also the reason for high normal stresses similar to the straight knife. Similarly, the load capacity of C5 is higher. Though the mid-length thickness of both C4 and C5 is the same, the difference in the radius of curvature of their representative curves makes C4 more rigid along its length. The high rigidity of C4 and C5, as compared to the other geometries, is not a desirable feature because higher rigidity translates into higher resistance to deformation which in turn implies more resistance to the motion of the shaft and possible damage to the shaft in the form of scouring or chipping.

The difference in the behavior of the configurations studied can directly be attributed to the different geometric dimensions like a, b, c, d, l_o, l_r, α and β (Figures 43 and 44). The dimension d determines the position of the 'representative curve/line' (Figures 18 and 19) with respect to the right most edge of the knife, while the dimension b helps to account for the thickness in the case of the straight knife and the radii of curvature with respect to the 'representative curve' in the case of the curved seal. In all the curved seal configurations that have been analyzed, the right most edges of the fixed and free ends were considered to be on a straight line that is perpendicular to both the fixed and free ends (Figure 16). But it may not be necessary and/or beneficial to meet or incorporate this feature always. In such an event, wherein the right edge of the free end is offset with respect to the fixed end, the dimension l_o becomes important. This is true of even the straight knife. In addition, the length of the root part l_r and the wedge angles α and β assume importance for the straight knife. Thus, the behavior of the different geometric configurations for the seal may be explained in terms of a mathematical relation incorporating these and various other dimensions.

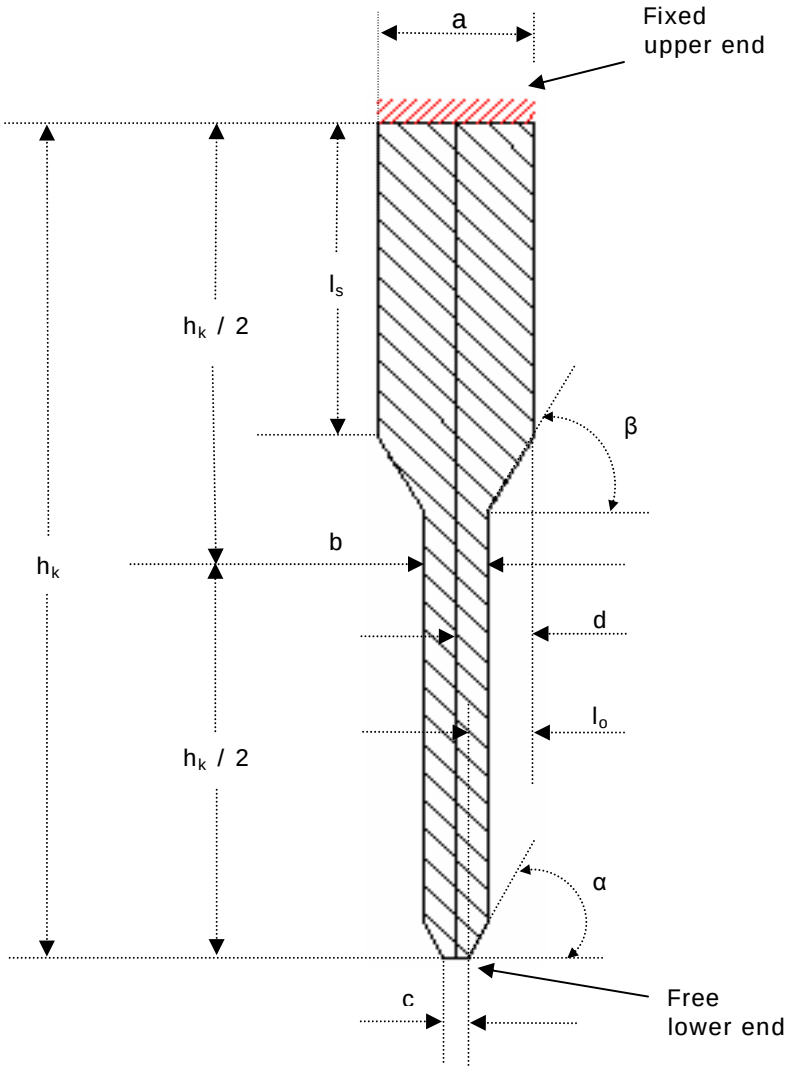

Figure 43. Schematic of the geometry of Straight knife with the different geometric parameters (compare with Figure 15)

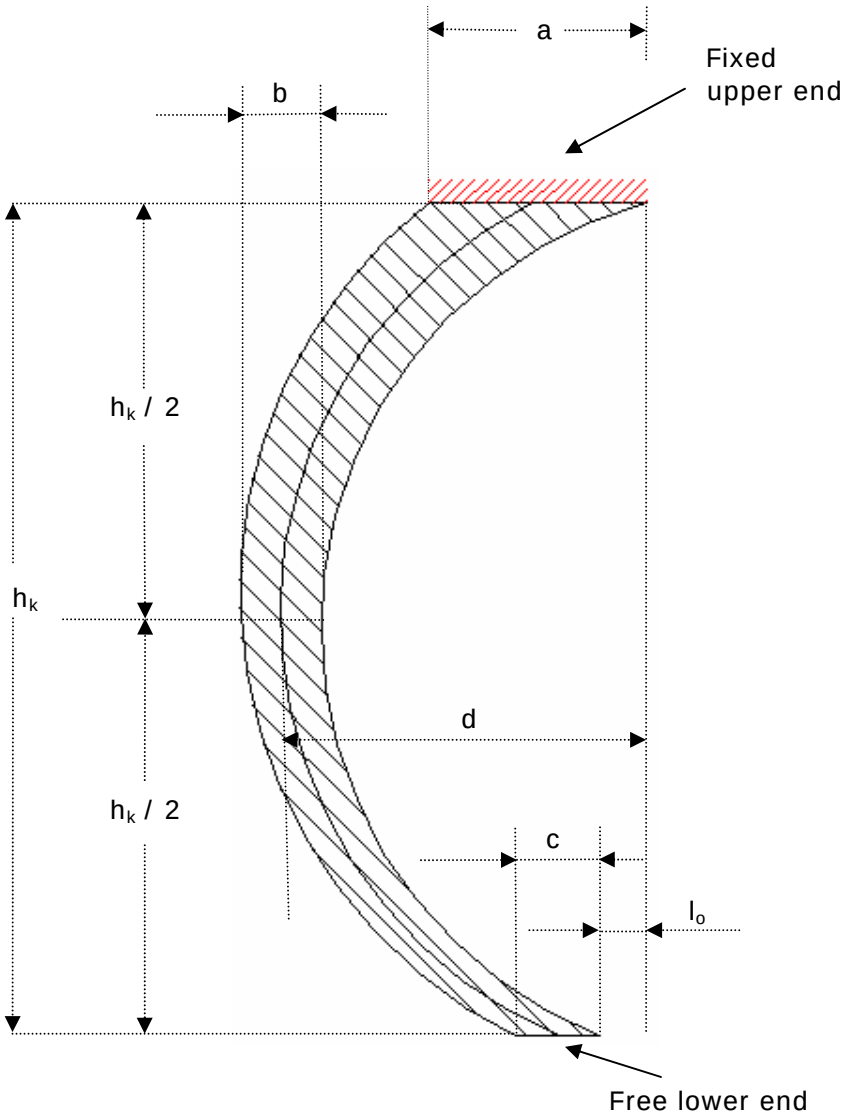

Figure 44. Schematic of the geometry of a C-flat knife with the different geometric parameters (compare with Figure 16)

Due to the lack of sufficient data, such a relation could not be formulated in the present study. Nevertheless, it was found that the behavior of the configurations analyzed depended on the radius of the 'representative curve' and the thickness of the knives at half their length. The non-dimensional geometric ratio *b/(b+d)* was found to be able to predict the variations in the flexibility of the different configurations. The plots in Figures 45 and 46 show F_r and Δx_r and, F_r and $\Delta x\%$ plotted against *b/(b+d)* for the C-flat knives. The two plots clearly reflect the trend in Figures 41 and 42. The straight knife was not considered for this plot because it was deemed that the straight knife is also influenced by the dimensions l_o, l_s, α and β. Since there was not sufficient data to study the behavior of these dimensions, the straight knife was not included in the plots of Figures 45 and 46.

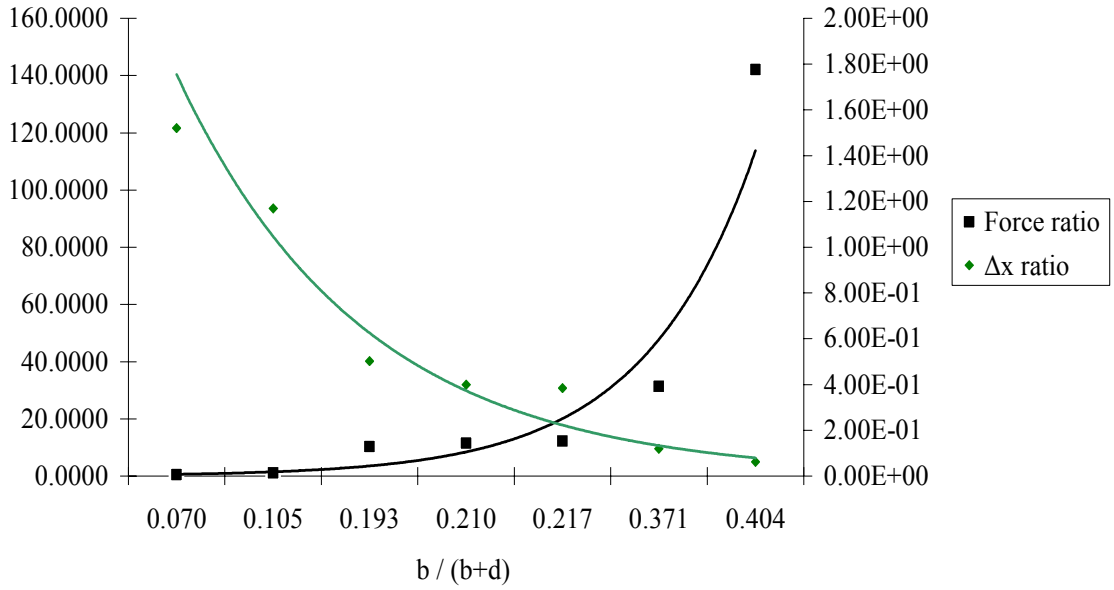

Figure 45. Variation of F_r and Δx_r with respect to b/(b+d)

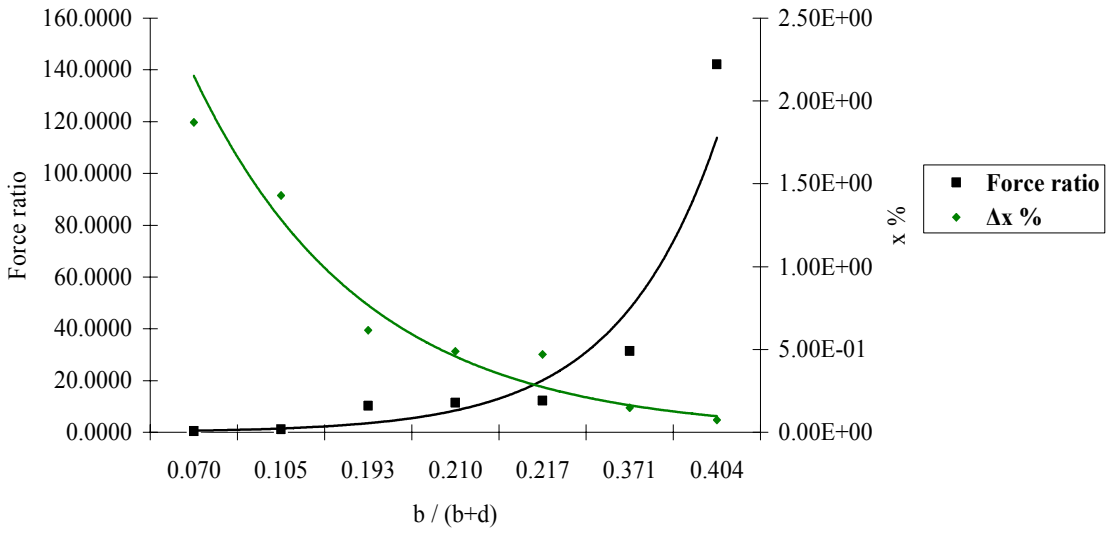

Figure 46. Variation of F_r and Δx % with respect to b/(b+d)

The plots based on the parameter *b/(b+d)* presented in Figures 45 and 46 are not exhaustive in the sense that only seven configurations for the C-flat knife were analyzed. A more detailed study might produce not just one plot for F_r or Δx_r or Δx % but a 'family' of plots based either on the variation of b or d or both. As a result the non-dimensional parameter may also include the dimension l_o. In a more generic configuration for the seal, there may be other geometric dimensions and parameters appearing in the non-dimensional parameter.

8. Conclusions and Recommendations

Conclusions:

The main objective of this study was to conduct the structural analysis of new configurations of labyrinth seals and compare them against a baseline labyrinth seal for structural viability purposes. To this end a static, steady 2-dimensional finite element structural analysis was performed on a baseline straight labyrinth seal, commonly in use in steam turbines, (referred to as the straight seal) within the elastic limit of its material. The material of the seal was common engineering steel (*Appendix A*). The results of the straight seal analysis show the need for new and improved seal configurations. The improved sealing of the new designs was supported by computational fluid dynamic studies of the straight seal and the new seals [13-17].

Comparison of the results of structural analysis between the straight seal and the new configurations indicated that three of the five C-flat seal configurations (C1, C2 and C3) exhibit higher flexibility than the straight seal. The higher flexibility has the added potential for installing seals with a smaller clearance distance from the shaft than the straight seal. Reduced clearance has the added advantage of reduced area of flow for steam, thus minimizing its leakage. Further, since the flexibility of the new seal is higher, the wear on it is expected to be minimal.

Two new seal configurations, C4 and C5, had very high load bearing capacity before reaching their elastic limits.

Two other configurations (CS1 and CS2) have more flexibility, making them a good choice for developing labyrinth seals with better sealing and contact performance.

A non-dimensional geometrical ratio was found to uniquely correlate flexibility of the different configurations. Though the data available was not exhaustive, this parameter appears to be a good indicator of the underlying relationship between the geometric variables of the knives and their flexibility.

Recommendations:

The problem of the labyrinth seal belongs to the class of multi-physics encompassing the fields of fluid dynamics, heat transfer, structural and thermal stress analysis and material science leaving aside the study of the functioning of the turbine itself. The present study was a simplification of the actual problem. As a result, there are many areas for improvement and further research to gain a deeper understanding of the behavior of a labyrinth seal in operation.

- The loads on the knives are time-dependent and not always within their elastic limit. Hence the foremost area of improvement would be to perform a non-linear dynamic analysis.

- The seal knives are subjected to vibrations due to the fluctuations in the operation of the turbine. Hence, a modal or vibration analysis would increase the understanding knife behavior.

- Since the present study was a 2-dimensional analysis, a 3-dimensional analysis would be a giant leap in understanding the problem because of the fact that the shaft and steam forces are not always radial or tangential to the knives.

- In a 3-dimensional analysis, the problem of contact stress gains significant importance. A study in this direction would be highly recommended. Also of

importance are the frictional effects of the rubbing of the knife free ends on the turbine shaft.

- The fluid dynamic effects of the flow of steam on the seals were not studied. This belongs to a class of problems called fluid-structure interactions. Such a study presents a holistic perspective of the problem from the fluid as well the structural side.

- The CS1 and CS2 configurations exhibited more flexibility than the C1 through C5 configurations. A further research into this particular type of geometry would be valuable.

- One of the most important recommendations would be the construction of a prototype for the ratification of the results obtained and to improve upon the fallacies and loop holes of the present study.

- Contact stress analysis would present deeper insights into the interactions between the shaft and the seal elements.

- Also, failure or fracture analysis would help to predict the operating life of the knives.

- The seal elements are constantly subjected to elongation and compression under the influence of steam and shaft forces. This can induce fatigue in the seal elements and eventually their failure. Fatigue analysis would provide grounds for better prediction of failure of the seal elements.

- Numerical simulation of the leakage of steam showed that the C-sharp seal performed better compared to the C-flat seal [16, 17]. But structural analysis showed that the C-sharp seal fails at its sharp end at a much lower load than the

C-flat seal. If the sharp end of the C-sharp seal can be made stronger, it could be a better choice over the C-flat seal.

- Use of non-metallic materials to construct or reinforce the sharp end might be a good option to improve the strength of the C-sharp seal. Investigation into the use of such materials in the design of seal elements is recommended.

References

References

1. Stocker, H.L., “Determining and Improving Labyrinth Seal Performance in Current and Advanced High Performance Gas Turbines,” AGARD Conference proceeding no. 237, “Seal Technology in Gas Turbine Engines,” April, 1978.

2. Egli, A., “Leakage of Steam Through Labyrinth Seals,” ASME Transactions vol. 57, 1935.

3. Morrison, G.L., and Chi, D., “Incompressible Flow in Stepped Labyrinth Seals,” ASME Paper 85-FE-4, Joint ASME/ACSE Applied Mechanics, Bioengineering and Fluids Engineering Conference, Albuquerque, NM, June 24-26, 1985.

4. Wyler, J.S., “Design and Testing of a New Double Labyrinth Seal,” ASME Paper 81-Lub-58, ASME Winter Annual Meeting, Washington D.C., Nov. 15-20, 1981.

5. Stocker, H.L., “Advanced Labyrinth Seal Design Performance for High Pressure Ratio Gas Turbines,” ASME Paper 75-WA/GT-22, ASME Winter Annual Meeting, Houston, Texas, Nov. 3 – Dec. 4, 1975.

6. Wachter, J., and Benckert, H., "Flow Induced Spring Coefficients of Labyrinth Seals for Applications in Rotor Dynamics," NASA CP 2133, Proceedings of Workshop on Rotordynamic Instability Problems in High Performance Turbomachinery, May 12-14, 1980.

7. Hawkins, L., Childs, D., and Hale, K., “Experimental Results for Labyrinth Gas Seals With Honeycomb Stators: Comparisons to Smooth-Stator Seals and Theoretical Predictions,” Journal of Tribology, vol. 111, Jan., 1989.

8. Bilgen, E., and Akgungor, A.C., "Leakage and Frictional Characteristics of Large Diameter Labyrinth Seals," National Conference on Fluid Power, 1972.

9. Wright, D.V., "Labyrinth Seal Forces on a Whirling Rotor," Rotordynamic Instability, ASME, NY, 1983.

10. Leong, Y.M.M.S., and Brown, R.D., "Experimental investigations of Lateral Forces induced by Flow Through Model Labyrinth Glands," NASA CP 2338, Proceedings of a Workshop on Rotordynamic Instability Problems in High Performance Turbomachinery, Texas A&M University, TX, May 28 – 30, 1984.

11. Childs, D.W., and Scharrer, J.K., "Experimental Rotordynamic Coefficient Results for Teeth-on-Rotor and Teeth-on-Stator Labyrinth Gas Seals," Journal of Engineering for Gas Turbines and Power, vol. 108, Oct., 1986.

12. Childs, D.W., and Scharrer, J.K., "Theory Versus Experiment for the Rotordynamic Coefficient of Labyrinth Gas Seals: Part II – A Comparison to Experiment," Journal of Vibration, Acoustics, Stress, and Reliability in Design, vol. 110, July, 1988.

13. Michaud, M. A., "An Experimental Study of Labyrinth Seal Flow," MS Thesis, University of Tennessee, August, 2002.

14. Michaud, M., Vakili, A.D., and Meganathan, A.J., "An Experimental Study of Labyrinth Seal Flow," Proceedings of IJPGC 2003 International Joint Power Conference, Atlanta, GA, June 16 – 19, 2003.

15. Vakili, A.D., Meganathan, A.J., Michaud, M.A. and Radhakrishnan, S., "An Experimental and Numerical Study of Labyrinth Seal Flow," Proceedings of

GT2005: ASME Turbo Expo 2005: Power for Land, Sea and Air, Reno-Tahoe, NV, June 6 – 9, 2005.

16. "Advanced Steam Labyrinth Seal Design – Phase 1 Initial Concept Evaluation," EPRI Report 1011932, Final Report, May, 2005.

17. Vakili, A.D., Meganathan, A.J., and Ayyalasomayajula, S., "Advanced Labyrinth Seals for Steam Turbine Generators," Proceedings of GT2006: ASME Turbo Expo 2006: Power for Land, Sea and Air, Barcelona, Spain, May 8 – 11, 2006.

18. Boresi, A., and Schmidt, R.J., "Advanced Mechanics of Materials," John Wiley & Sons, Inc., 6th ed.

19. Timoshenko, S.P., and Goodier, J.N., "Theory of Elasticity," McGraw-Hill Book Company, 3rd ed.

20. Fenner, R.T., "Mechanics of Solids," Blackwell Scientific Publications, 1989.

21. Beer, F.P., and Jonhston, Jr., E.R., "Mechanics of Materials," McGraw-Hill Book Company, 2nd ed.

22. US Patent no. 5244216

23. US Patent no. 5639095

24. US Patent no. 4420161

25. US Patent no. 5224713

26. US Patent no. 6394459

27. US Patent no. 6644667

28. US Patent no. 6435513

29. US Patent no. 6257586

30. US Patent no. 6131910

31. US Patent no. 6131911

32. US Patent no. 6105967

33. US Patent no. 6045134

34. US Patent no. 6027121

35. US Patent no. 5749584

Appendices

Appendix A

Properties of Carbon Steel Used in the Analysis

- Elasticity modulus : 29e+06 psi
- Poisson's ratio : 0.33
- Yield strength in tension : 45e+03 psi
- Tensile strength : 66e+03 psi
- Elongation or strain before plastic deformation : 25 – 30% of original length

Appendix B

Structural Analysis Results

Configuration C2:

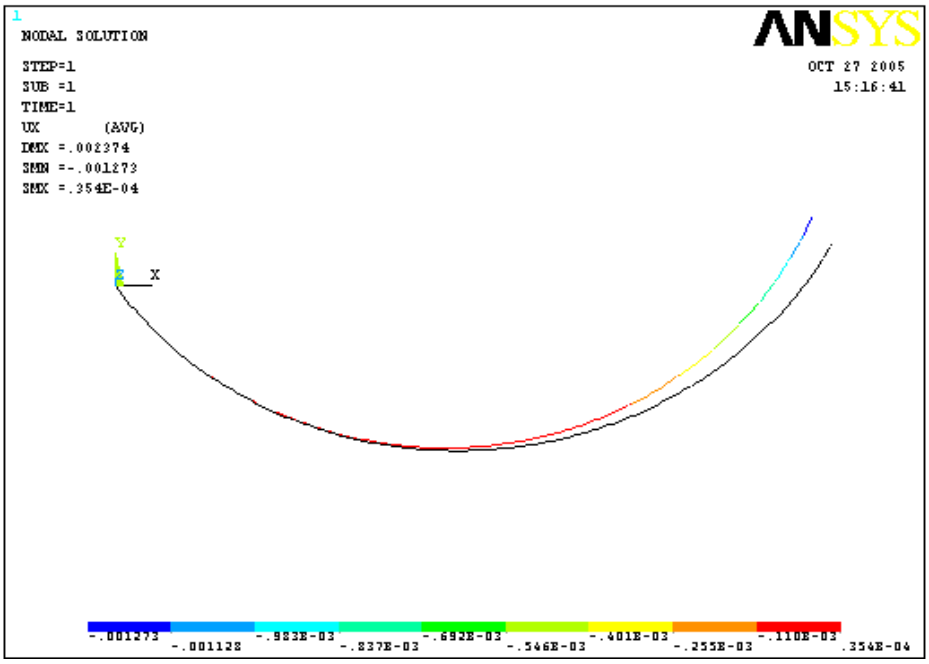

Figure 47. C2 knife - Deformation along x-axis

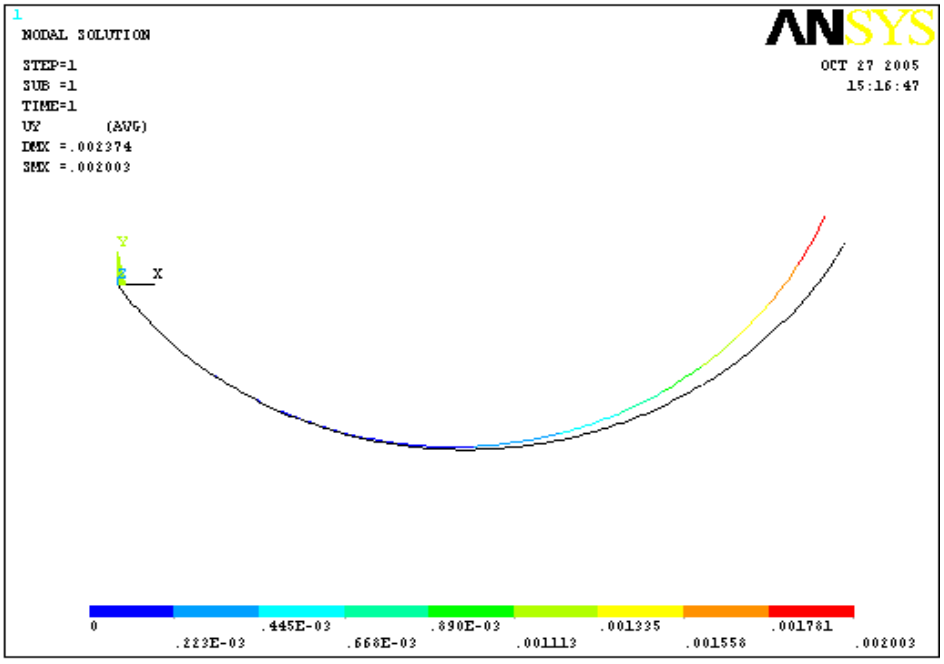

Figure 48. C2 knife - Deformation along y-axis

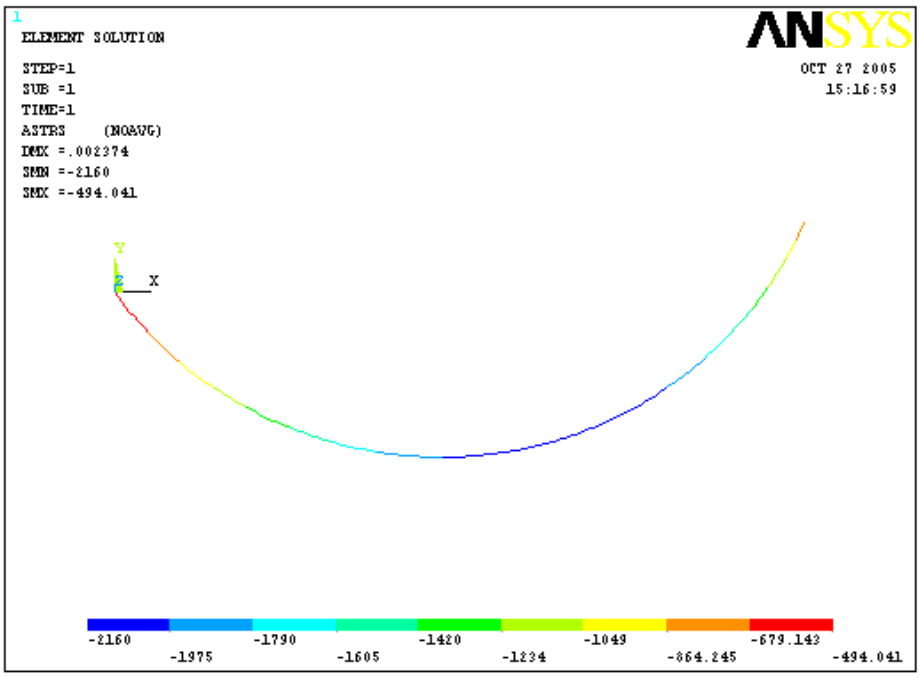

Figure 49. C2 knife - Normal stress

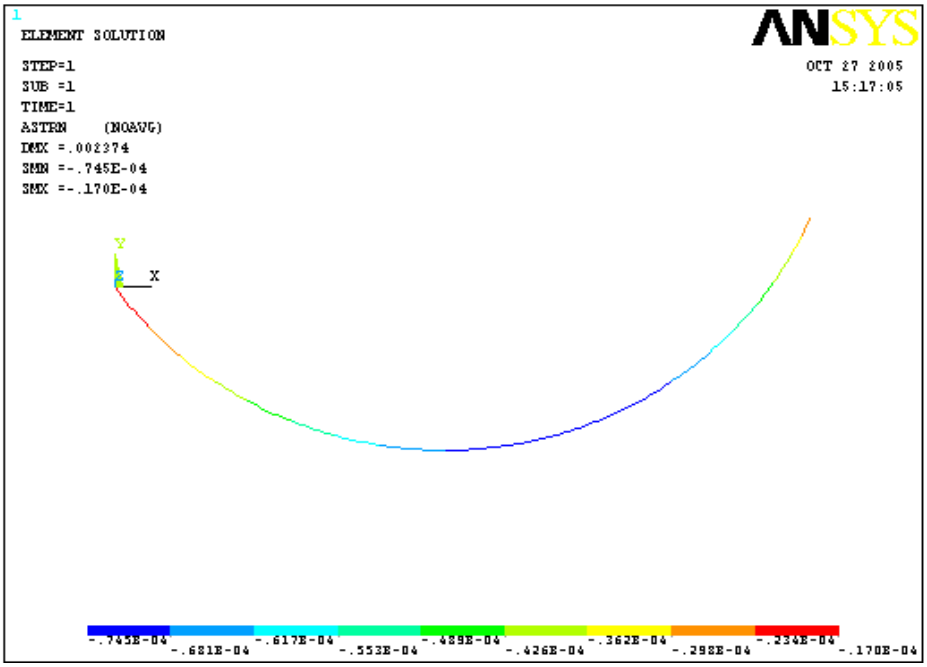

Figure 50. C2 knife - Normal strain

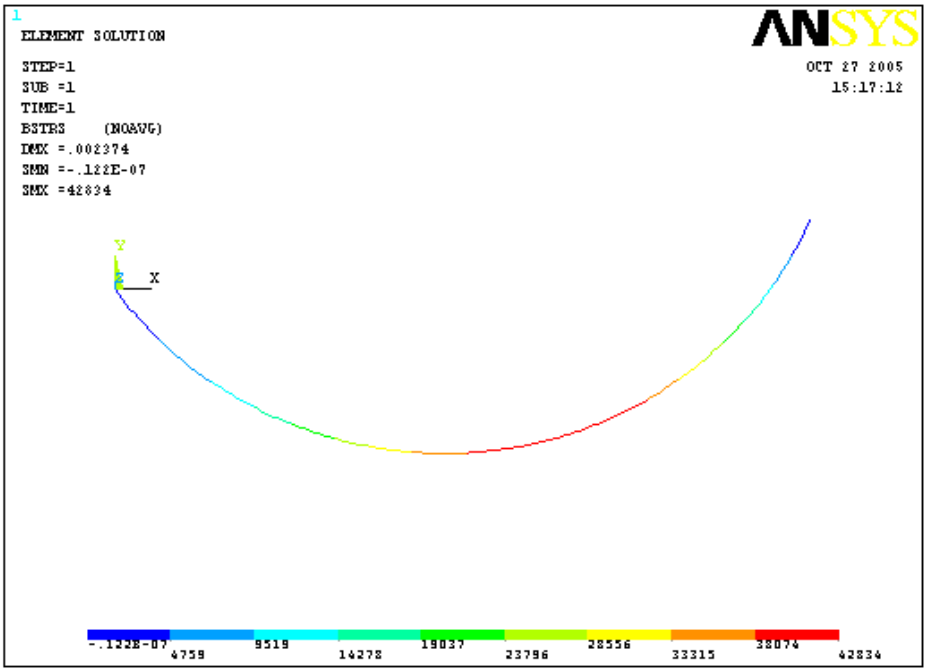

Figure 51. C2 knife - Bending stress

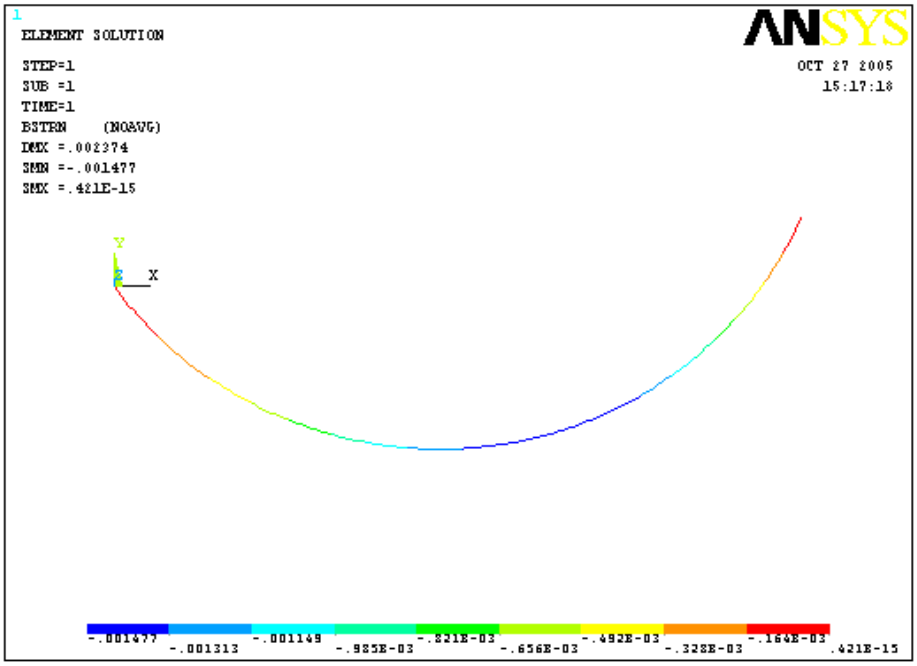

Figure 52. C2 knife - Bending strain

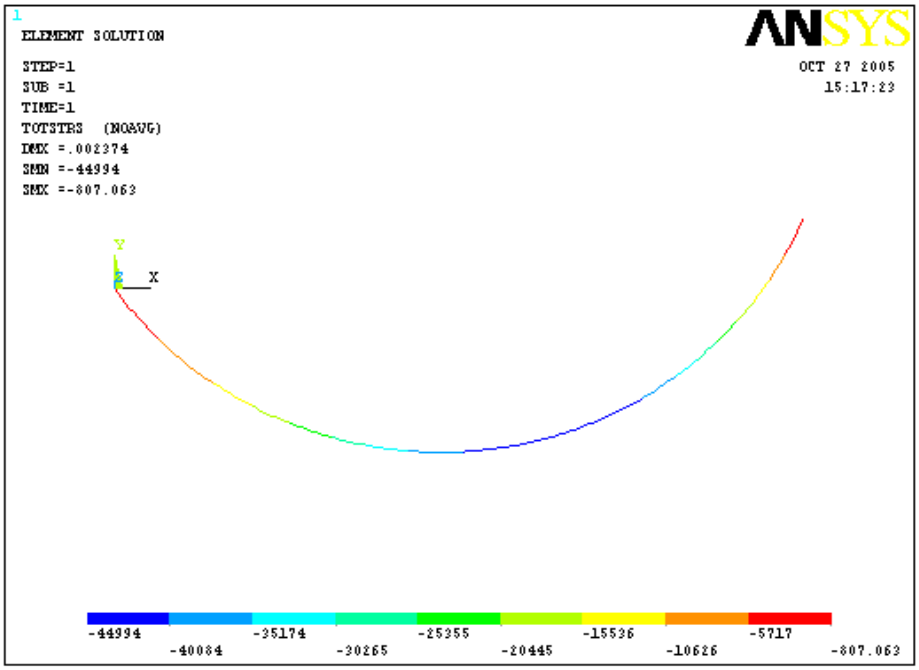

Figure 53. C2 knife - Total stress

Configuration C3:

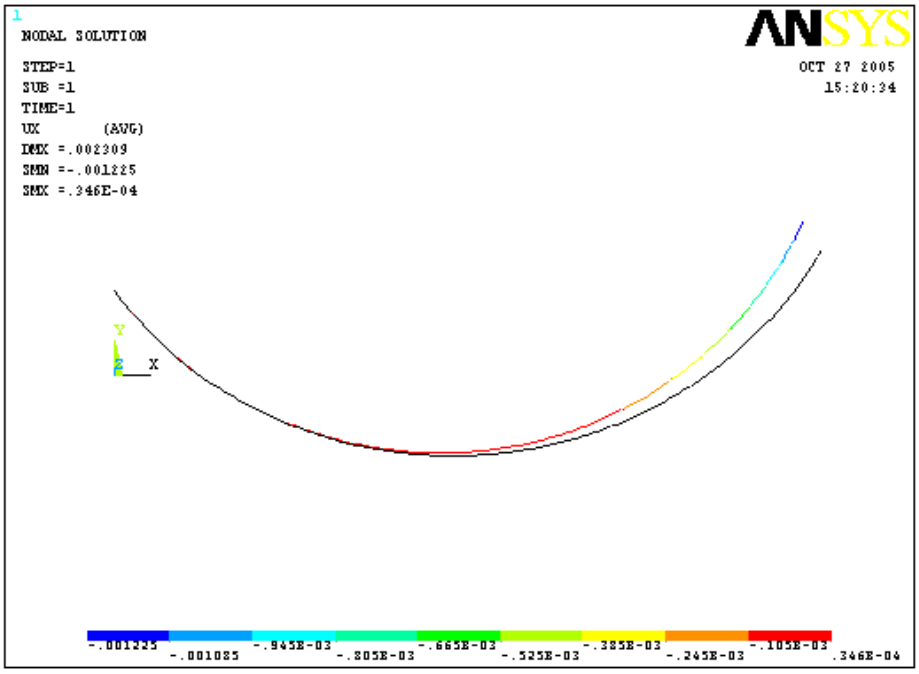

Figure 54. C3 knife - Deformation along x-axis

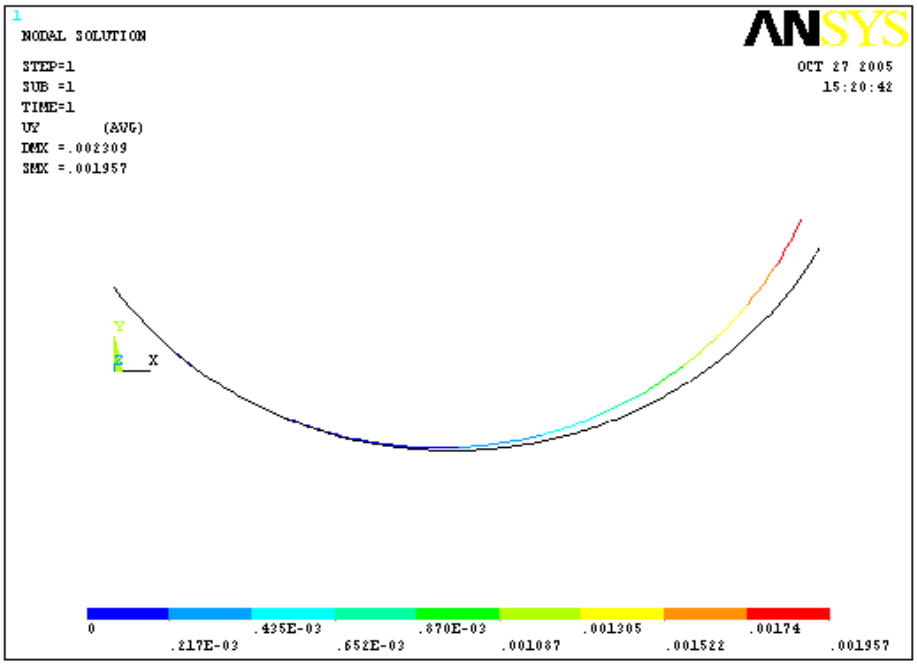

Figure 55. C3 knife - Deformation along y-axis

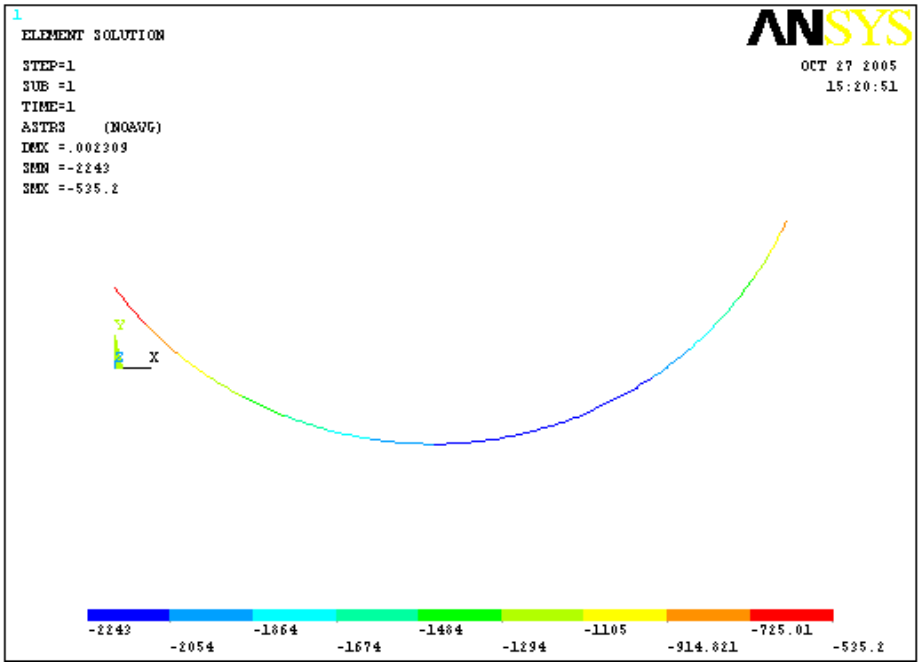

Figure 56. C3 knife - Normal stress

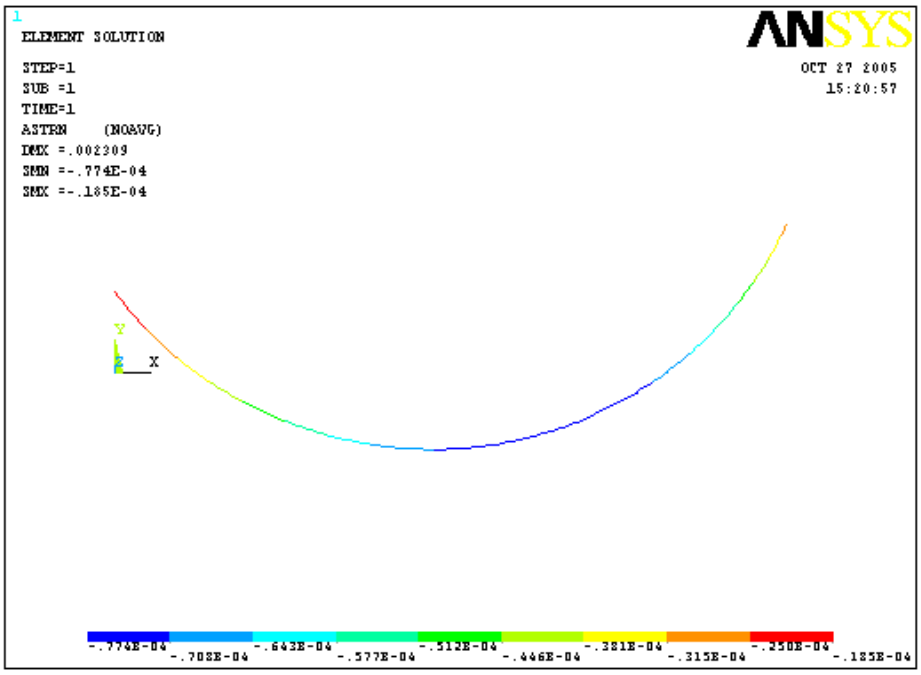

Figure 57. C3 knife - Normal strain

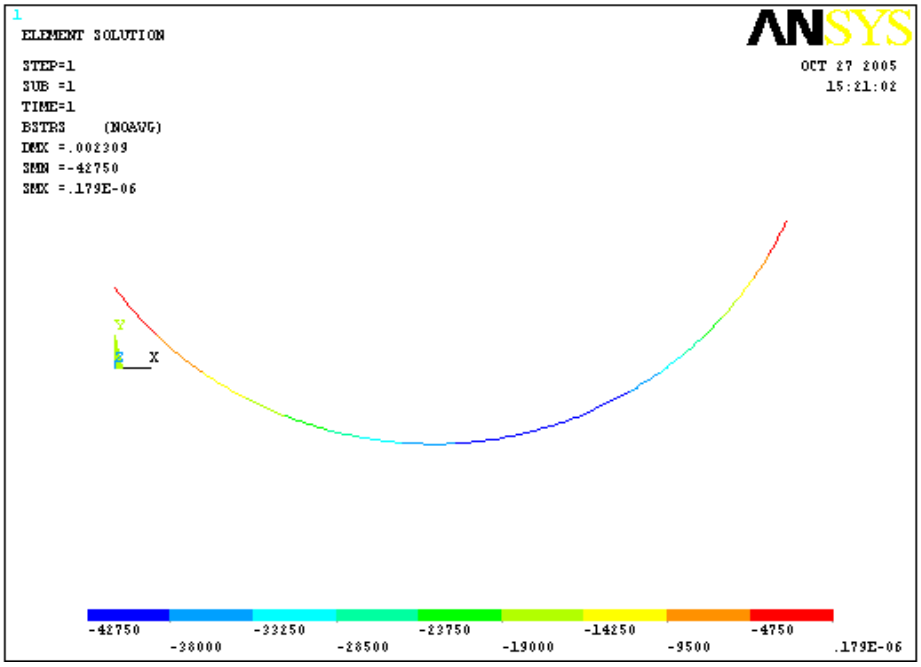

Figure 58. C3 knife - Bending stress

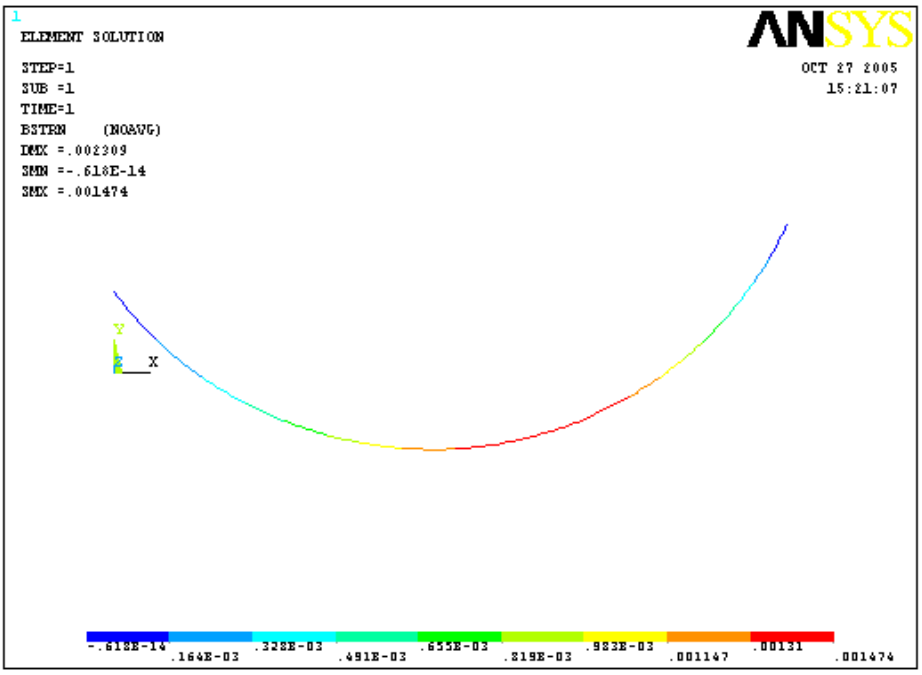

Figure 59. C3 knife - Bending strain

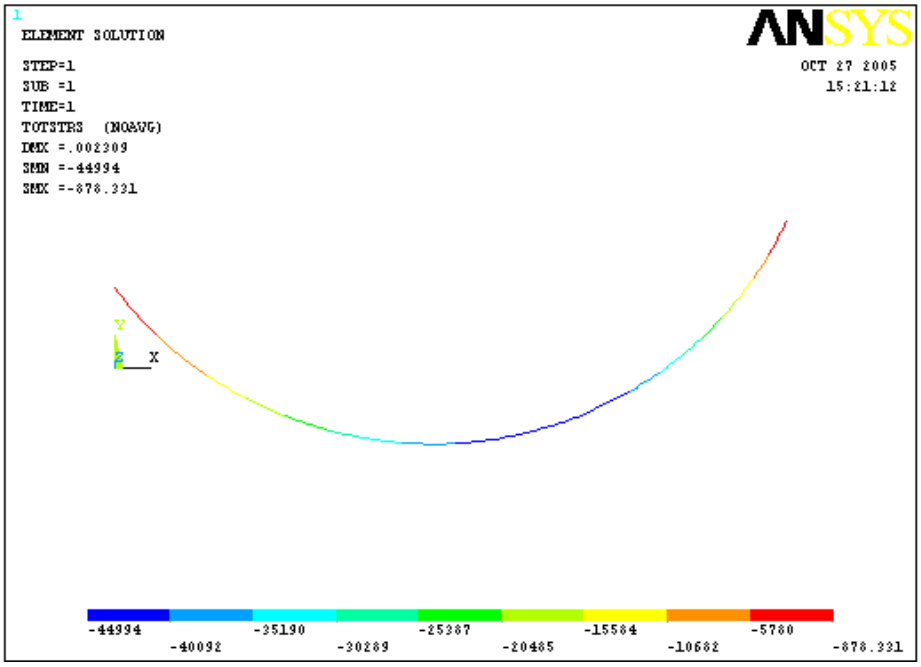

Figure 60. C3 knife - Total stress

Configuration C4:

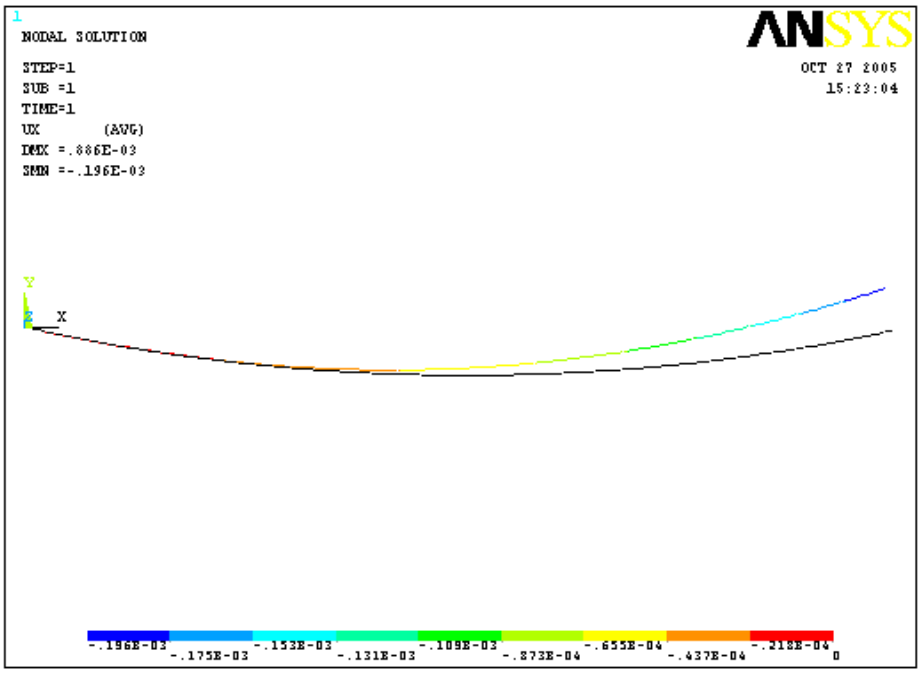

Figure 61. C4 knife - Deformation along x-axis

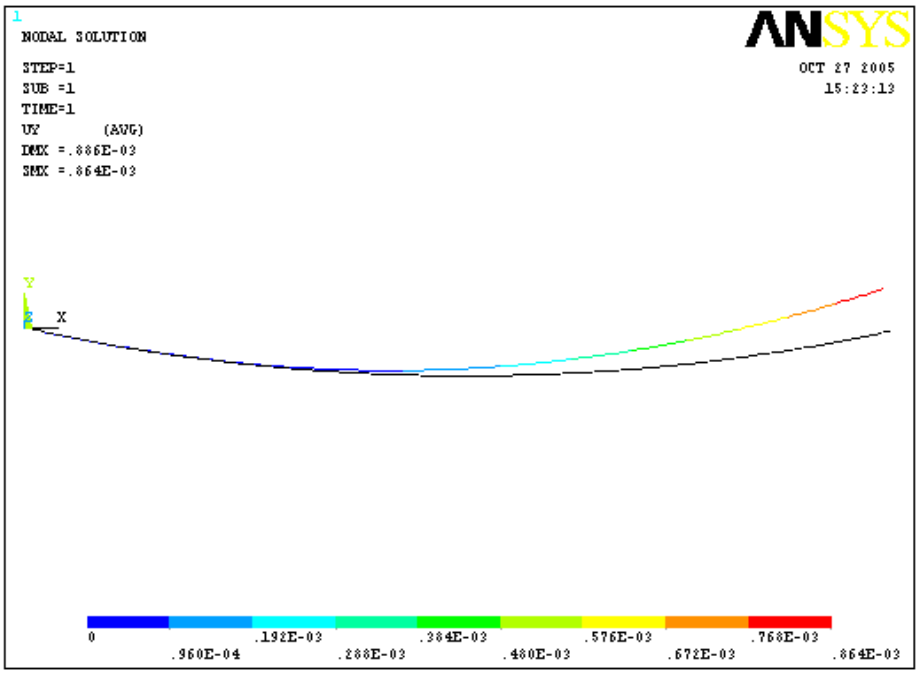

Figure 62. C4 knife - Deformation along y-axis

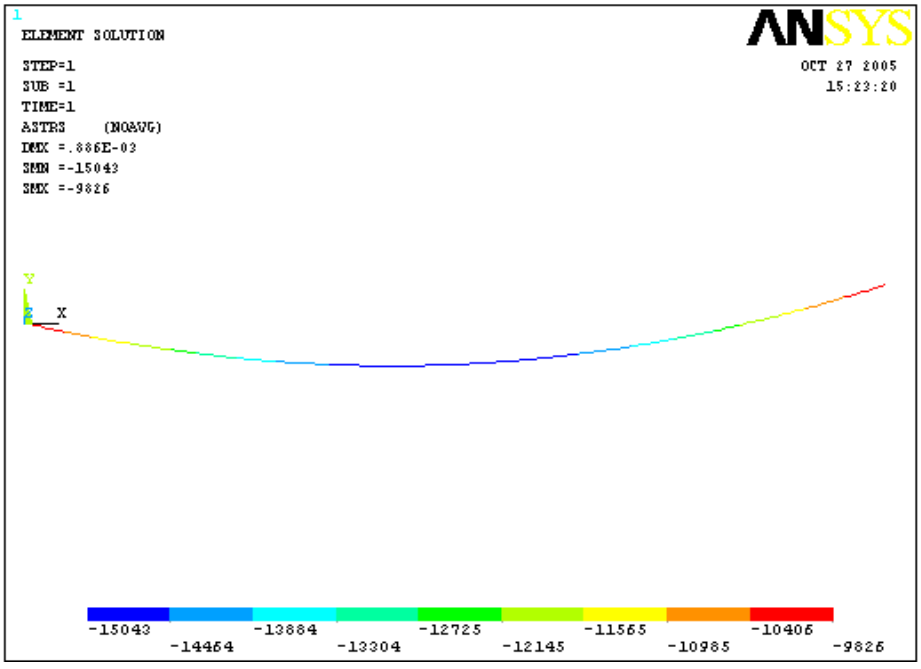

Figure 63. C4 knife - Normal stress

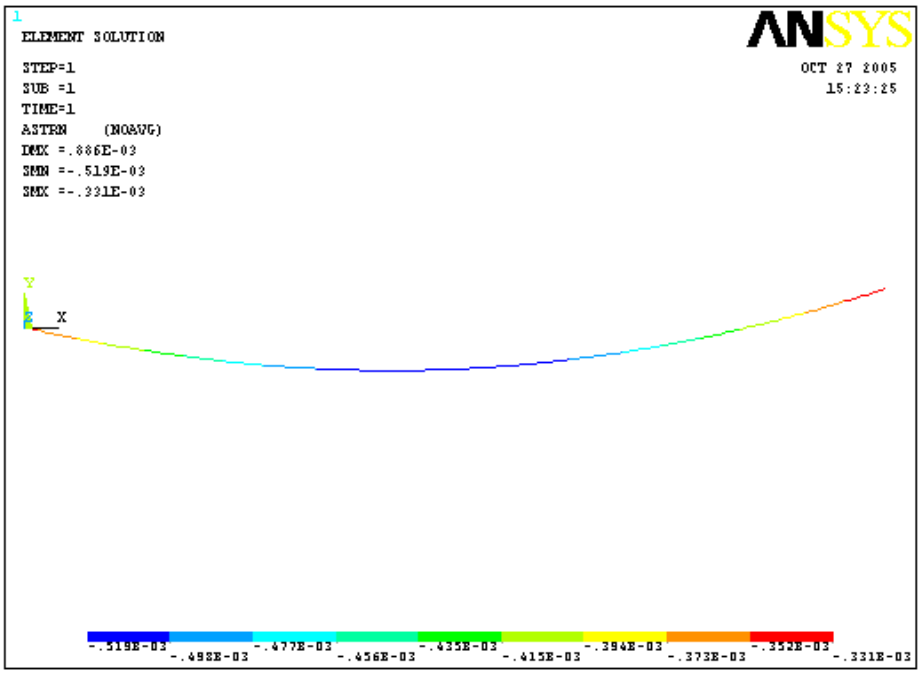

Figure 64. C4 knife - Normal strain

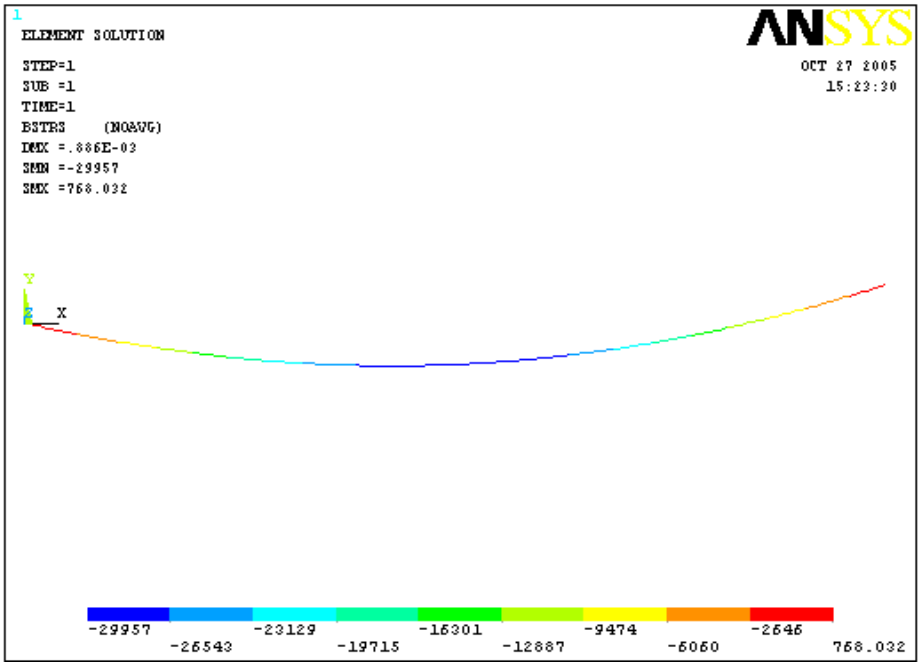

Figure 65. C4 knife - Bending stress

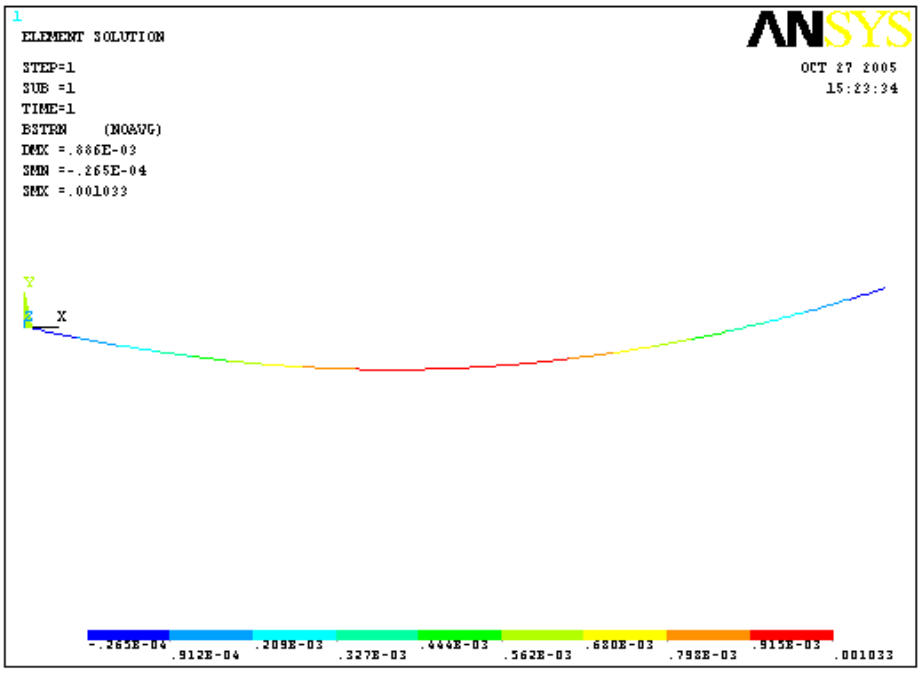

Figure 66. C4 knife - Bending strain

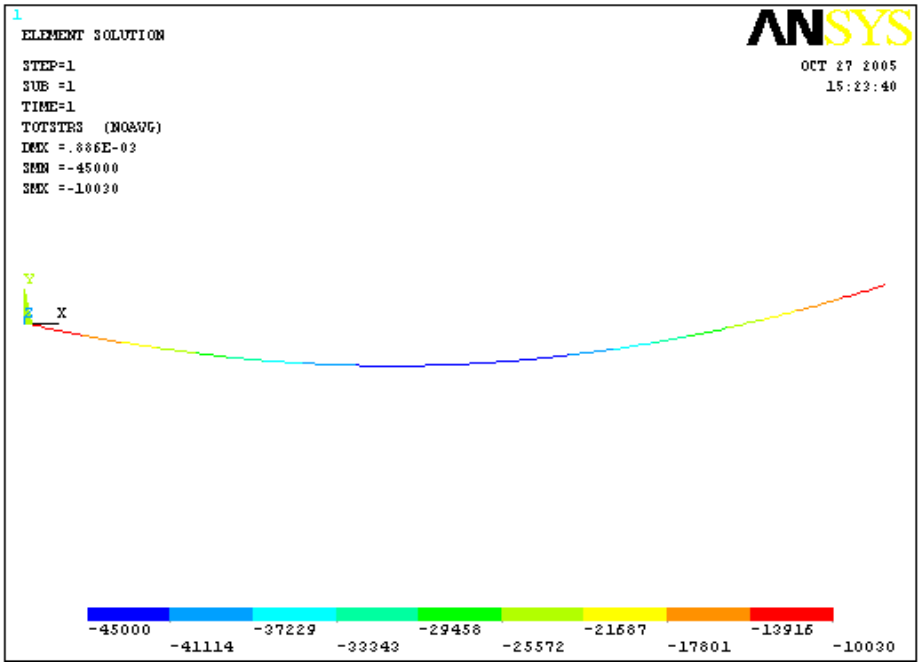

Figure 67. C4 knife - Total stress

Configuration C5:

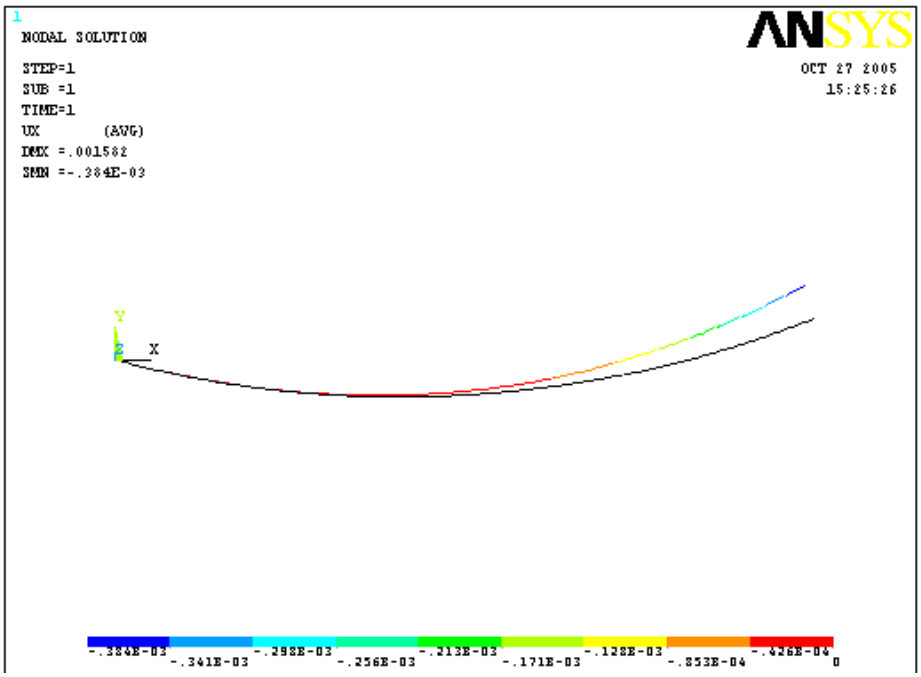

Figure 68. C5 knife - Deformation along x-axis

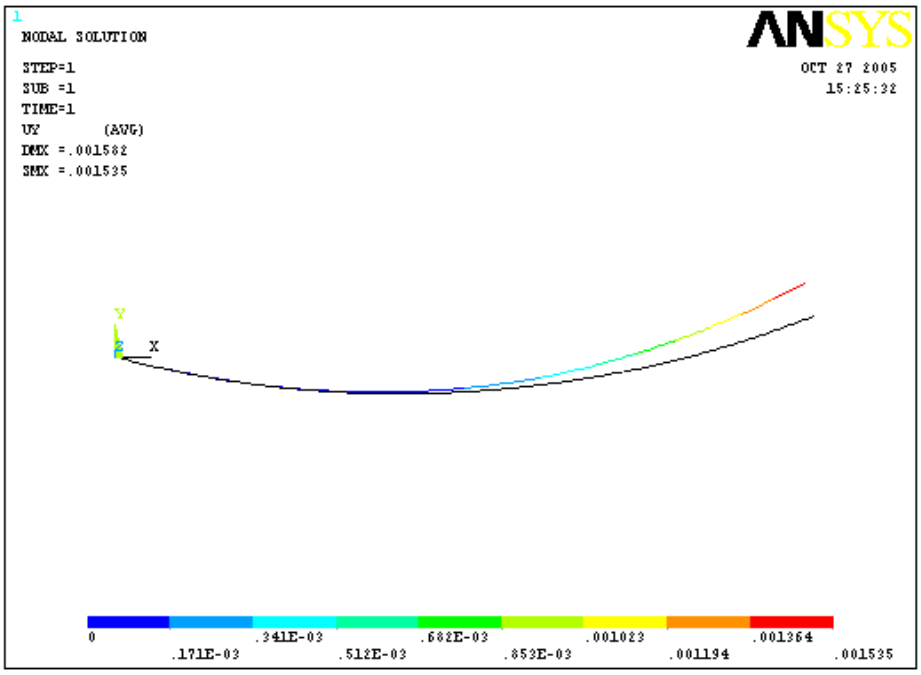

Figure 69. C5 knife - Deformation along y-axis

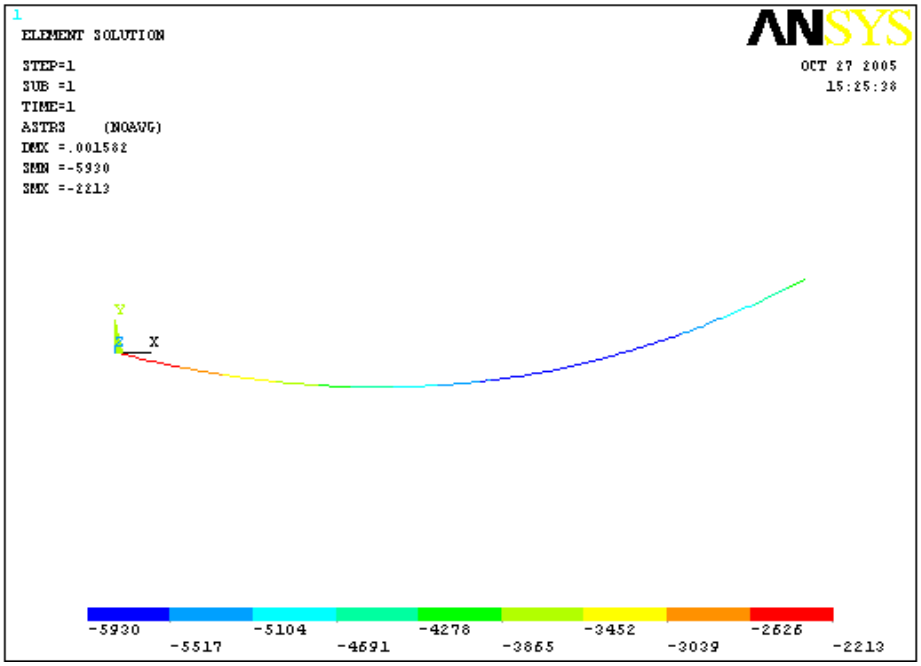

Figure 70. C5 knife - Normal stress

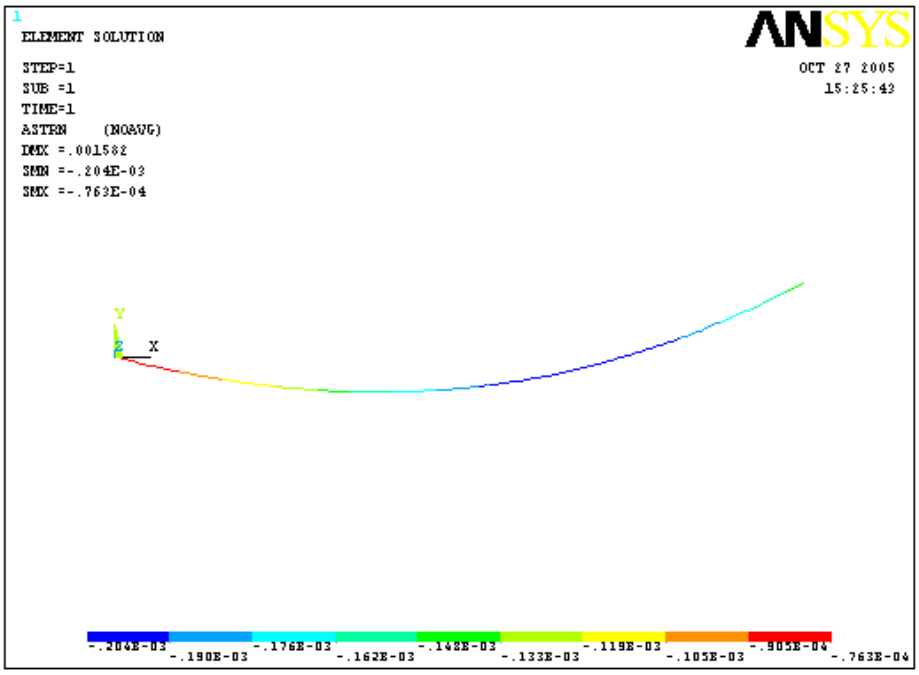

Figure 71. C5 knife - Normal strain

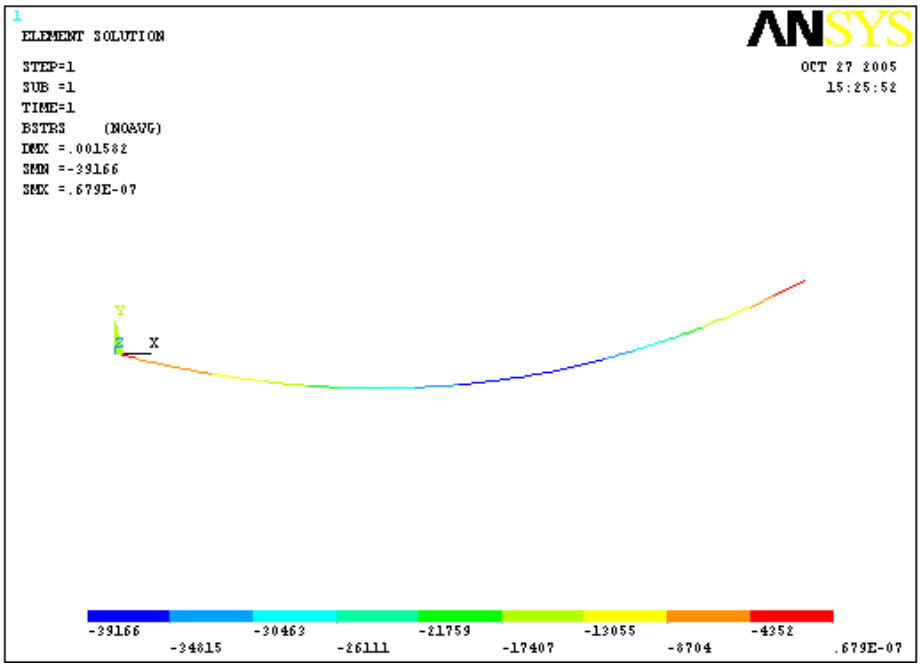

Figure 72. C5 knife - Bending stress

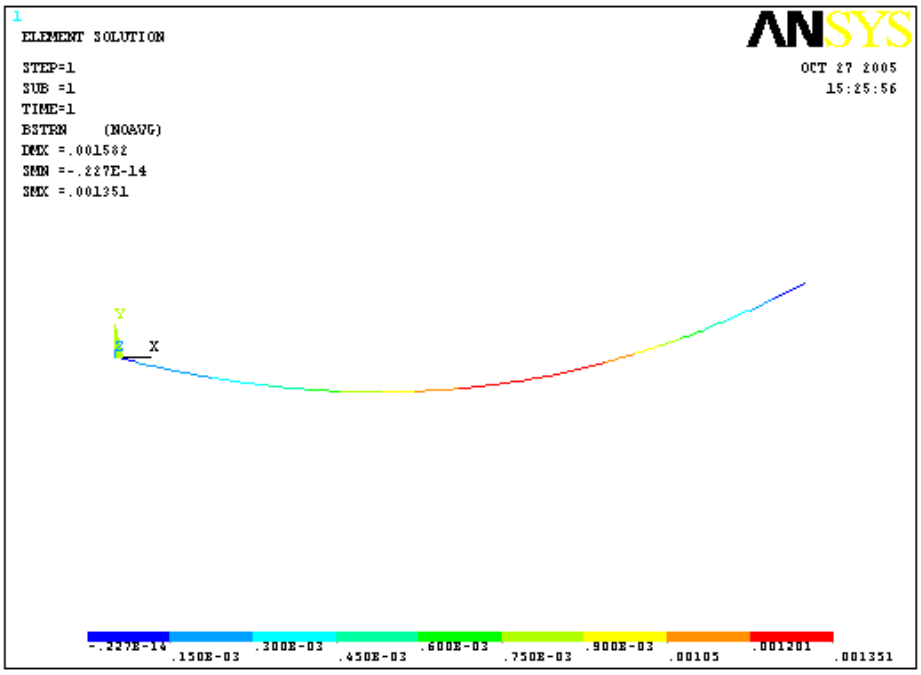

Figure 73. C5 knife - Bending strain

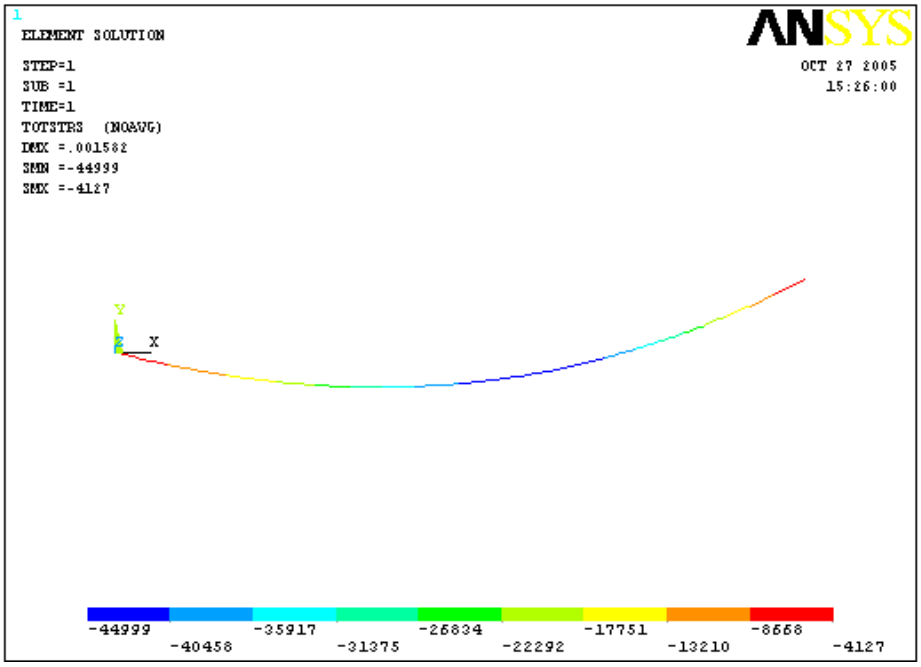

Figure 74. C5 knife - Total stress

Configuration CS1:

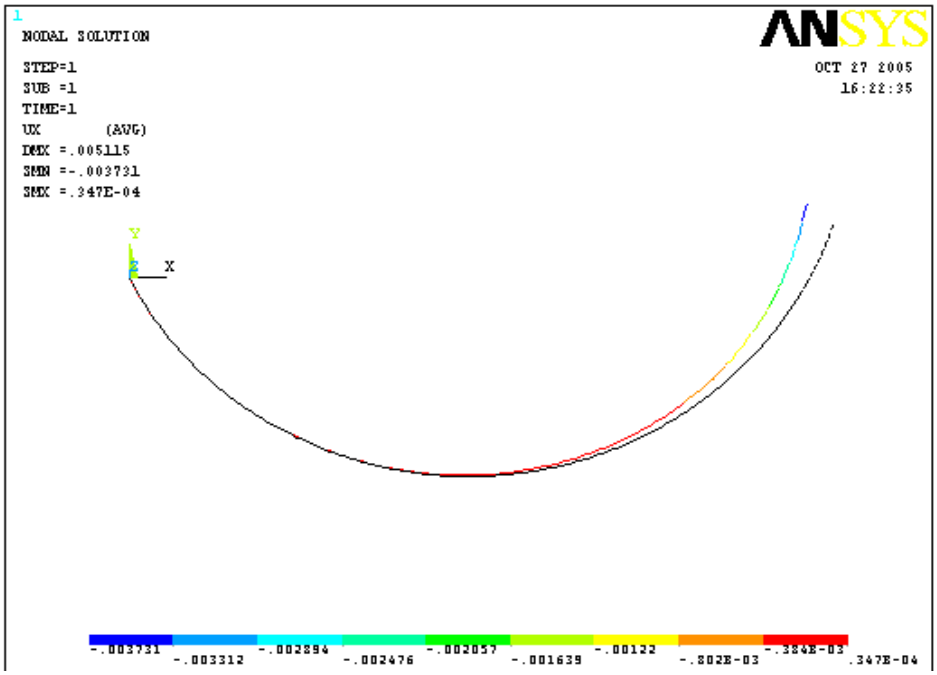

Figure 75. CS1 knife - Deformation along x-axis

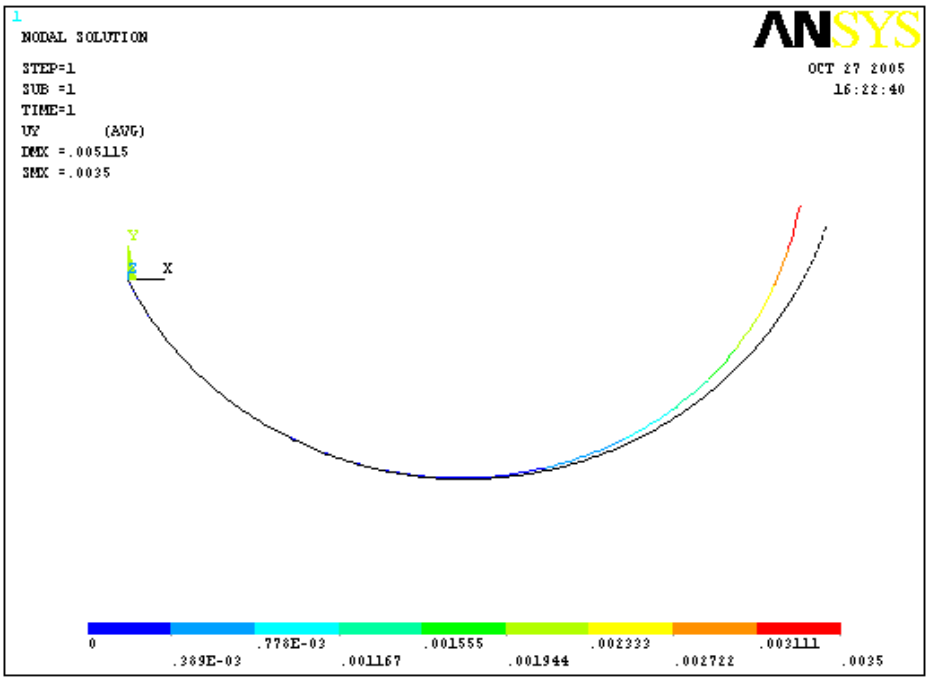

Figure 76. CS1 knife - Deformation along y-axis

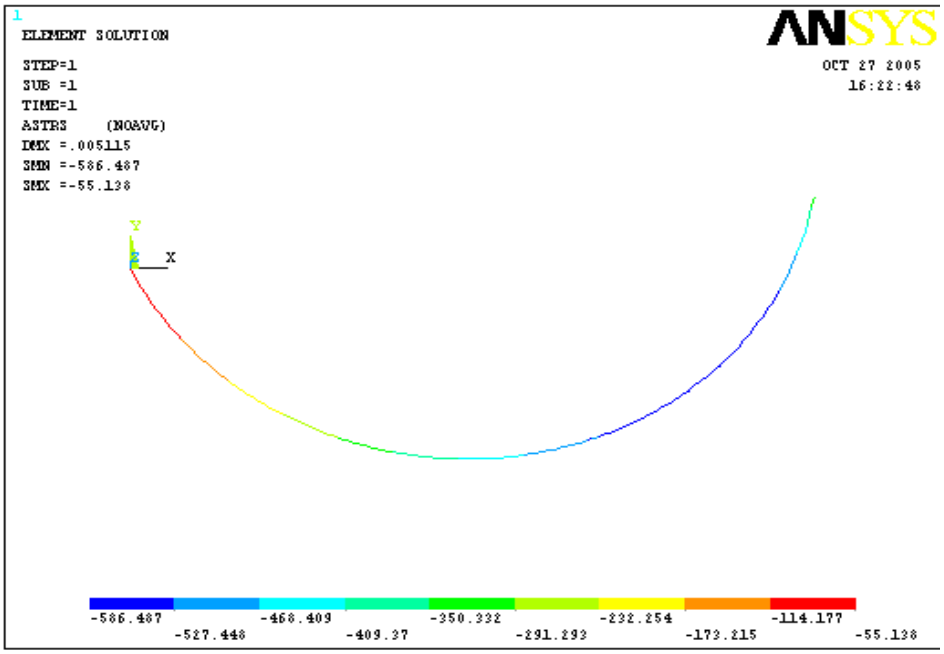

Figure 77. CS1 knife - Normal stress

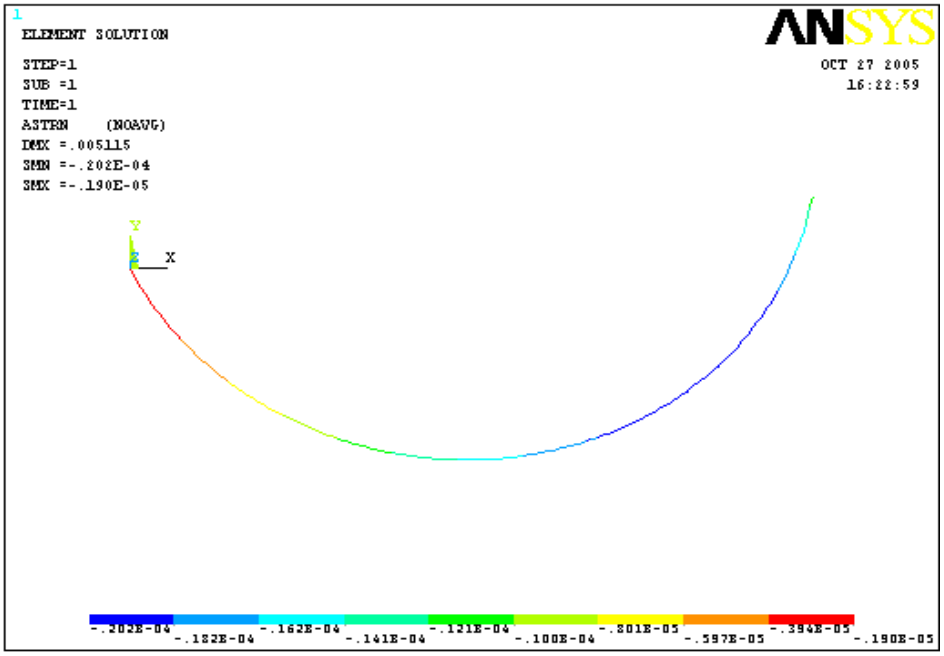

Figure 78. CS1 knife - Normal strain

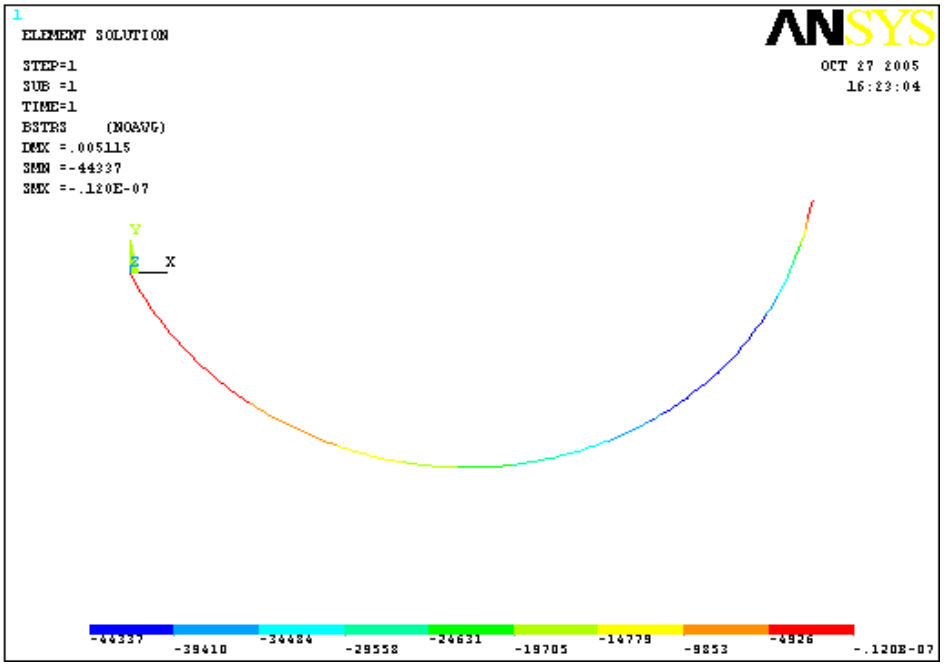

Figure 79. CS1 knife - Bending stress

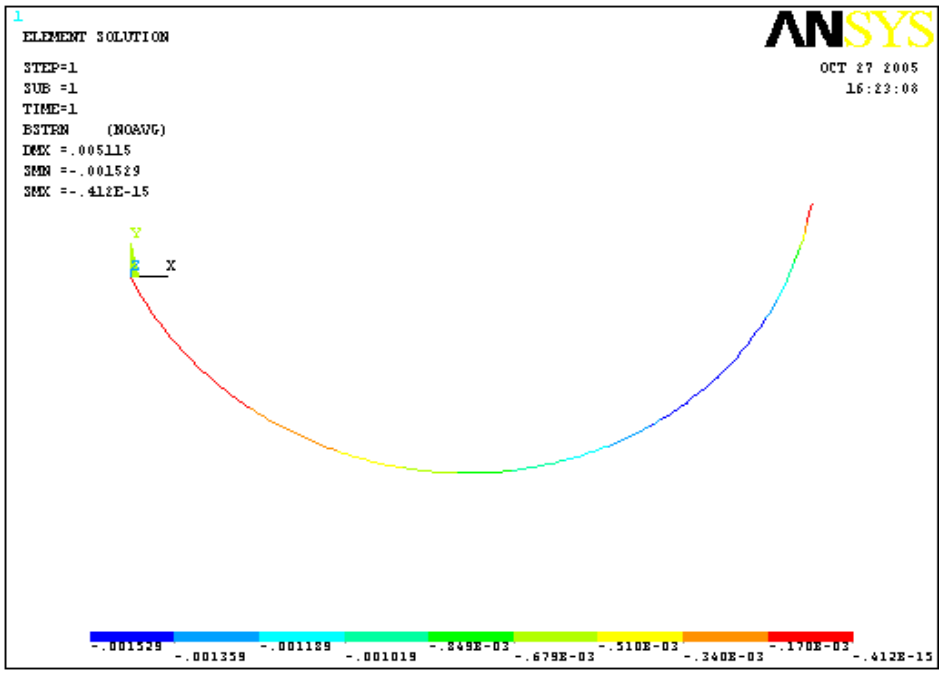

Figure 80. CS1 knife - Bending strain

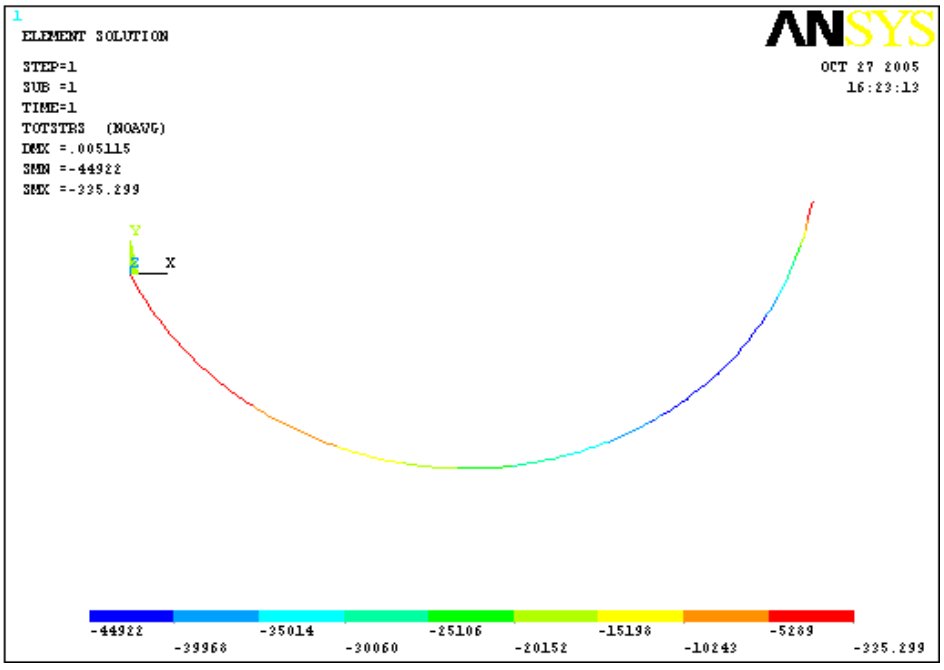

Figure 81. CS1 knife - Total stress

Configuration CS2:

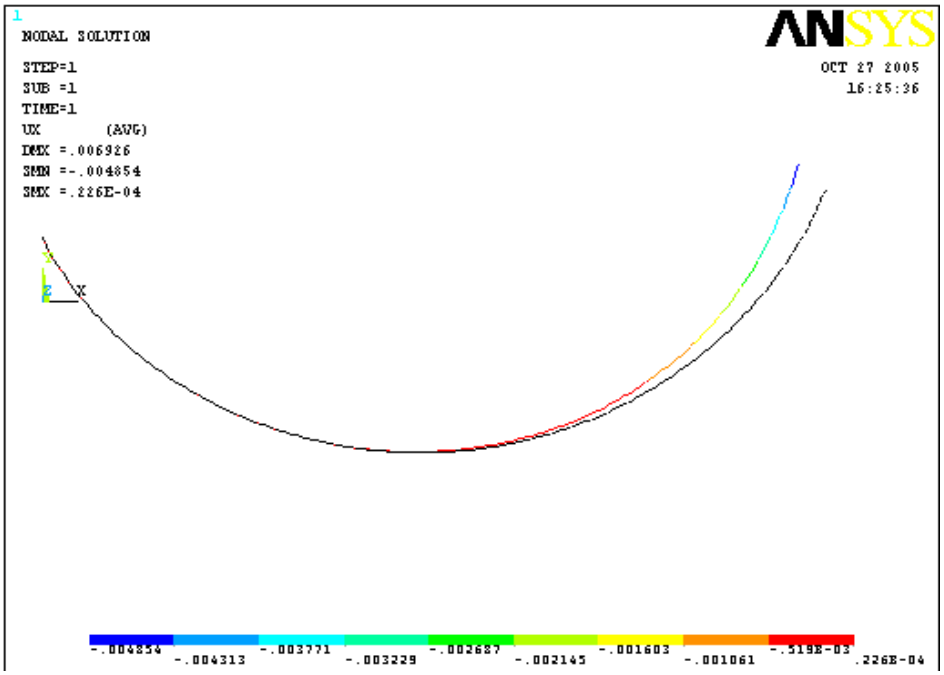

Figure 82. CS2 knife - Deformation along x-axis

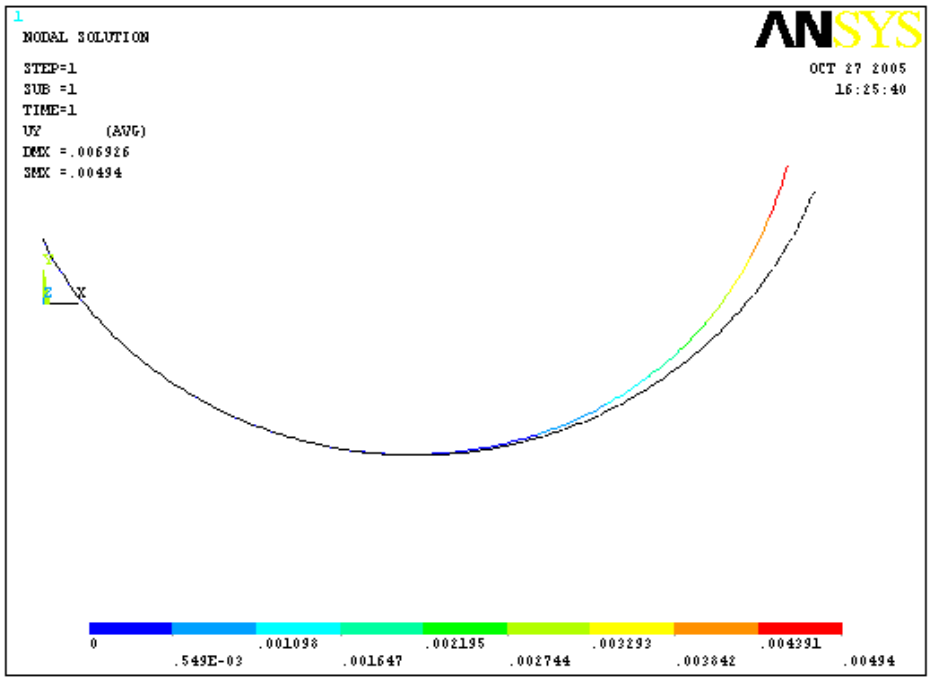

Figure 83. CS2 knife - Deformation along y-axis

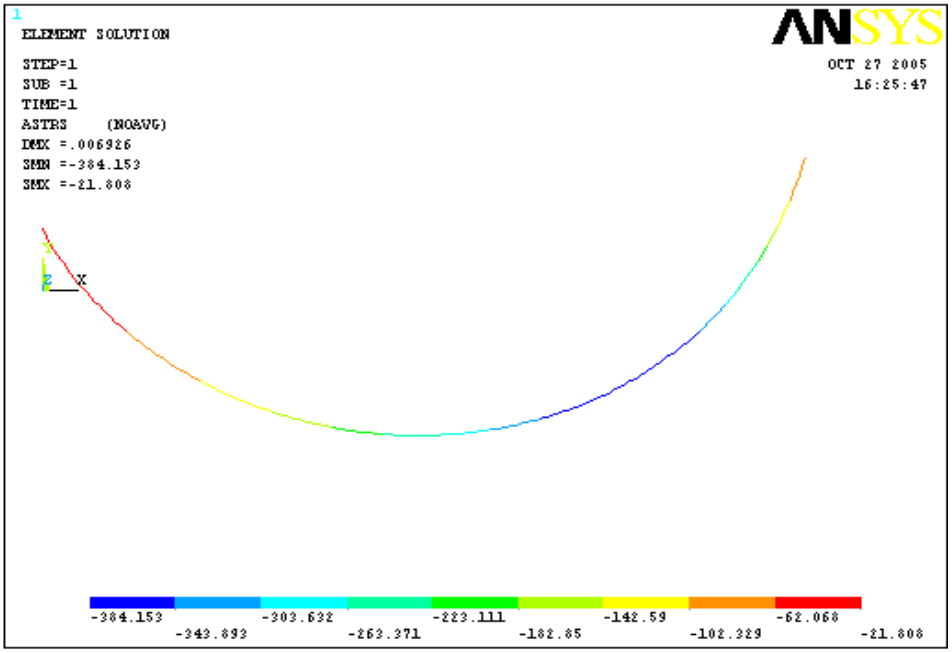

Figure 84. CS2 knife - Normal stress

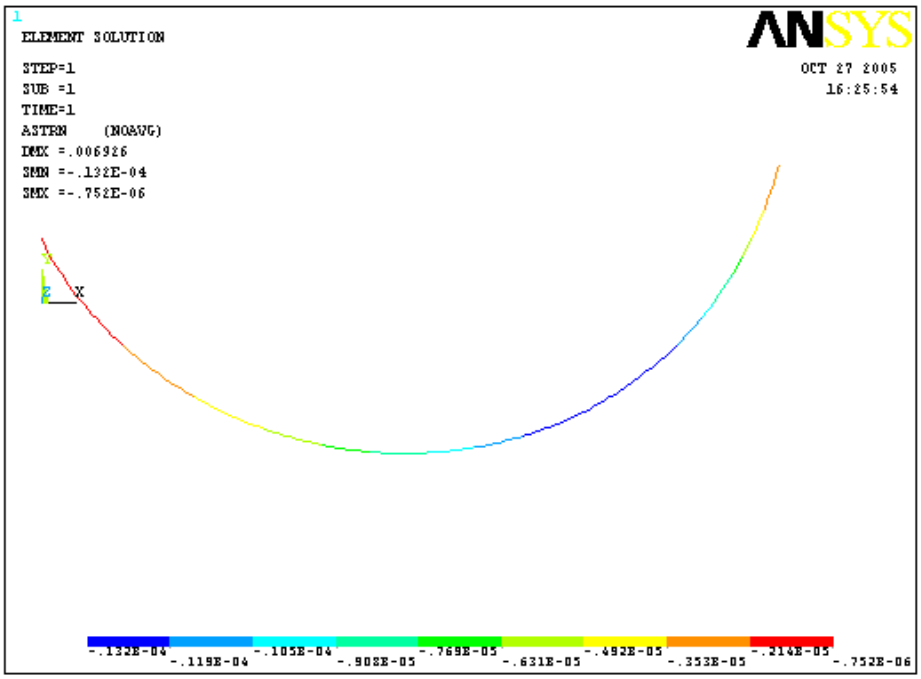

Figure 85. CS2 knife - Normal strain

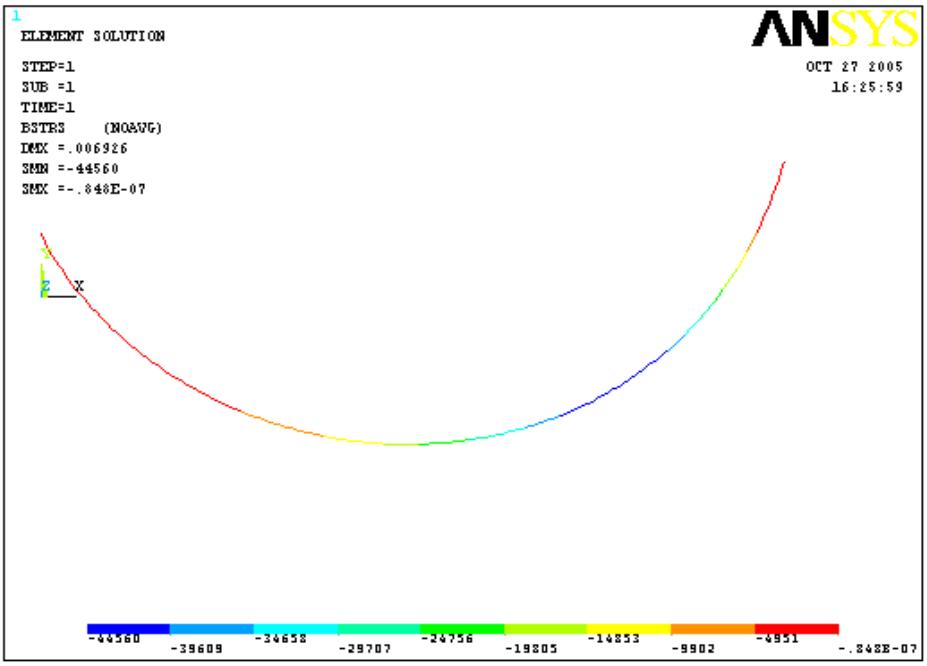

Figure 86. CS2 knife - Bending stress

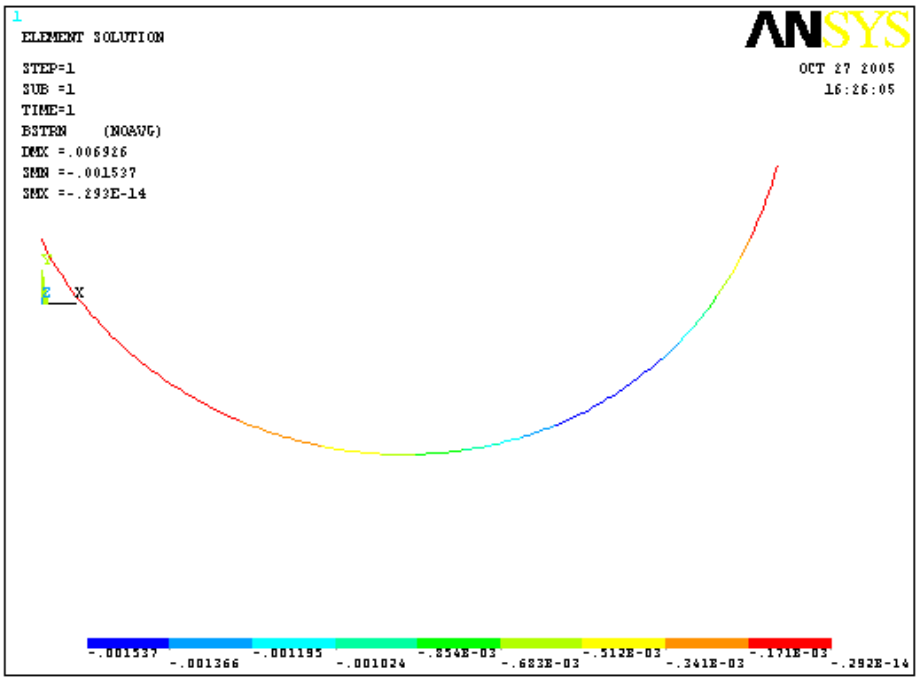

Figure 87. CS2 knife - Bending strain

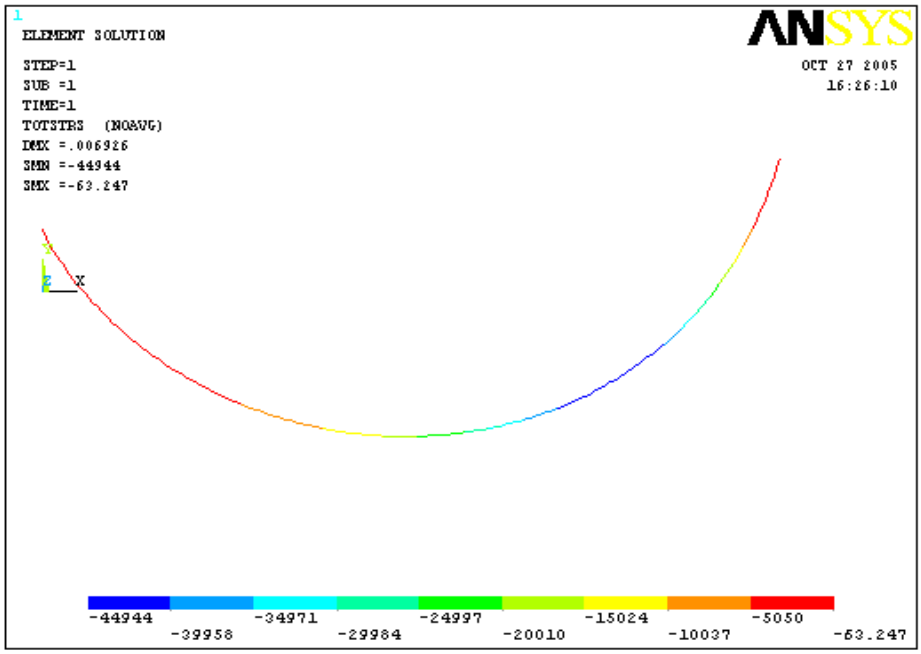

Figure 88. CS2 knife - Total stress

Vita

Sricharan Kishore Ayyalasomayajula comes from the colorful city of Hyderabad in south central India, where he was born on July 5, 1982. Born into a family where ethics and education are given the highest credence, he entered grade school at a very early age and completed college education even before turning nineteen. He was selected as a National Talent Search Scholar in 1997 by the National Council for Educational Research and Training, a Government of India organization overseeing the development of higher educational standards in India, an award given to students with high scholastic aptitude and mental ability. He received his Bachelor of Technology degree majoring in Mechanical Engineering from the Jawaharlal Nehru Technological University, Hyderabad, India in 2003. Having literally spent all his life till college in the same city, it was a major decision, backed by an unqualified support from family and friends, to travel overseas to the US for higher studies in engineering.

Sricharan is currently enrolled as a Graduate Research Assistant in the department of Mechanical, Aerospace and Biomedical Engineering at the University of Tennessee Space Institute, Tullahoma, TN and would be graduating during the fall semester of 2005 with a Master of Science degree in Mechanical Engineering. He plans to take up a PhD study in the US and continue his family's unqualified penchant for high quality education.